

**Effect of spatial resolution on erosion assessment in
Namchun watershed, Thailand**

Khatereh Polous

March, 2010

Effect of spatial resolution on erosion assessment in Namchun watershed, Thailand

by

Khatereh Polous

Thesis submitted to the International Institute for Geo-Information Science and Earth Observation in partial fulfilment of the requirements for the degree of Master of Science in Geo-Information Science and Earth Observation, Specialisation-Natural Resource Management

Thesis Assessment Board

Prof. Dr. V. G. Jetten	Chairman
Dr. E.A. Addink	External Examiner
Dr. Dhruba Pikha Shrestha	First Supervisor
Dr. Anton Vrieling	Second Supervisor



FACULTY OF GEO-INFORMATION SCIENCE AND EARTH OBSERVATION

UNIVERSITY OF TWENTE, ENSCHEDE, THE NETHERLANDS

Disclaimer

This document describes work undertaken as part of a programme of study at the International Institute for Geo-Information Science and Earth Observation. All views and opinions expressed therein remain the sole responsibility of the author, and do not necessarily represent those of the institute.

This page is intentionally blank.

Abstract

Water erosion is one of the most important environmental problems in Thailand. To control water erosion, assessing soil erosion at regional scale is important. Satellite imagery data and Digital Elevation Models are being used increasingly to assess erosion at different scales, but the main restrictions for these assessments are availability and quality of data. Therefore, it is necessary to analyse the reliability of erosion assessments at different spatial resolutions. To analyse the effect of spatial resolution of satellite images on erosion assessment independent of other sensor characteristics, several images with different spatial resolutions were simulated. Effects of spatial resolution was simulated by aggregating an ASTER image dataset (3 VNIR bands in 15m and 6 SWIR bands in 30m resolution) to three coarser spatial resolutions (30m, 90m, and 250m) through averaging function. In addition to analyse the effect of DEM resolution on erosion assessment, several DEMs in different resolutions (5m, 15m, 30m, 90m, and 250m) were created from digitized contour line map. In order to isolate the effect of spatial resolution, all simulated satellite images and DEMs in different resolutions were disaggregated to the finest resolution (5m). In this study, the RMMF model was applied to assess the effect of resolution on erosion.

As spatial resolution of satellite images became coarser, both overall accuracy and kappa coefficient of final erosion maps were significantly decreased, since the erosion classes were progressively converted to each other. Most conversions appeared between the classes that had completely different erosion rates. However, the general trend of conversions was from classes with lower erosion rate to the classes with higher erosion rate. The main reason behind these changes was the conversion of land use/cover classes with different erosion rates to each other. Firstly, as about 36% of the whole watershed was covered by agriculture as dominant class, the averaging caused a very high conversion of the other classes to agriculture in coarser resolutions. Secondly, by decreasing the spatial resolution, spectral details were progressively combined and the variation within satellite image reduced. Subsequently, classification results in coarser resolutions showed that bare and forest (with minimum and maximum spectral values in the near-IR band) disappeared and converted to the other classes.

By decreasing DEM resolution, both overall accuracy and kappa coefficient of final erosion maps were moderately decreased, since the erosion classes were converted to each other. Most conversions occurred between the classes that had almost the same erosion rates with general trend from classes with higher erosion rate to the classes with lower erosion rate, which proved the underestimation of erosion in coarser resolutions. Indeed, by changing DEM resolution, the slopes and the distribution of slopes have changed within watershed; the average slope, standard deviation, and maximum slope values reduced as DEM resolution became coarser, in other words the topographic features of the watershed were smoothed; which in turn affected the soil erosion prediction.

The results of this study showed, although by using satellite images in coarser resolutions soil erosion was slightly overestimated, but the RMMF model is not sensitive to the land use/cover factor; the spatial pattern of erosion maps in coarser resolutions even in 250m resolution approximately coincided with 5m resolution. Therefore, for stakeholders who want to assess erosion at regional scale, MODIS images at 250m resolution still can give reasonable results. Likewise, although more than 60% of the study area had steep slope ($>20^\circ$), but the spatial pattern of erosion maps in coarser resolutions even in 90m resolution conformed very well to the 5m resolution; thus SRTM could be an appropriate choice to assess erosion at regional scale with acceptable results. This implies that it may not be necessary to use costly, fine resolution remote sensing and DEMs data for the application of the erosion models at regional scale.

Keywords: Satellite imagery data resolution; DEMs resolution; SAM classification, RMMF model

Acknowledgments

I would like to express gratitude to Dr. Shrestha and Dr. Vrieling for their invaluable support and advice during the preparation of this thesis. Without their abundant insights and willingness to share knowledge, I would not have gained so much through my MSc thesis.

My sincere thanks go to Prof. Jetten for his invaluable guidance and support during my MSc thesis.

I would like to acknowledge Dr. Weir for his invaluable guidance and support during my MSc study and thesis.

I would also like to thank Dr. Farshad for his invaluable course and his advices and encouragements.

I would also like to express my sincere gratitude to European Union, Erasmus Mundus consortium and all ITC staffs and students for their support and helpfulness. I learned so much through the opportunities you provided.

I would like to thank my dear friend Dr. Saki for her friendship.

My special thanks to my lovely father and mother for their permanent support and love.

Finally, I would like to give my special thanks to my dear Amirhani for his understanding, love and support during my MSc study.

This page is intentionally blank.

Table of Contents

1	INTRODUCTION.....	1
1.1	BACKGROUND.....	1
1.2	PROBLEM STATEMENT.....	2
1.3	RESEARCH OBJECTIVES.....	3
1.3.1	General objective.....	3
1.3.2	Specific objectives.....	3
1.4	RESEARCH QUESTIONS AND HYPOTHESIS.....	3
1.5	ASSUMPTIONS.....	4
1.6	THESIS OUTLINE.....	4
2	LITERATURE REVIEW.....	5
2.1	SOIL EROSION.....	5
2.1.1	Controlling factors of soil erosion by water.....	5
2.1.2	Erosion Assessment Models.....	7
2.2	SPATIAL RESOLUTION EFFECT.....	8
3	STUDY AREA.....	10
3.1	LOCATION.....	10
3.2	CLIMATE.....	10
3.3	LAND USE/COVER.....	11
3.4	SOIL.....	12
3.5	GEOLOGY AND GEOMORPHOLOGY.....	12
4	MATERIALS AND METHODOLOGY.....	13
4.1	USED MATERIALS AND SOFTWARE.....	13
4.1.1	Materials.....	13
4.1.2	Software.....	13
4.2	METHODOLOGY.....	14
4.2.1	Aggregation of satellite imagery data to different resolutions.....	15
4.2.2	Image classification.....	17
4.2.3	Aggregation of land use/cover map.....	20
4.2.4	Digital Elevation Data in different resolution.....	21
4.2.5	Erosion assessment.....	21
4.2.6	Statistical analysis.....	28
5	RESULTS AND DISCUSSION.....	31
5.1	EFFECT OF SPATIAL RESOLUTION OF SATELLITE IMAGERY DATA ON CLASSIFICATION.....	31
5.1.1	Classification results.....	31
5.1.2	Accuracy assessment and statistical analysis.....	32
5.1.3	Analyse of results.....	34
5.2	EFFECT OF MAJORITY-BASE AGGREGATION ON CLASSIFICATION.....	36
5.2.1	Classification results.....	36
5.2.2	Accuracy assessment and statistical analysis.....	37
5.3	EFFECT OF SPATIAL RESOLUTION OF SATELLITE IMAGERY DATA ON SOIL EROSION.....	39
5.3.1	Soil erosion results.....	39
5.3.2	Accuracy assessment and statistical analysis.....	40
5.3.3	Analyse of results.....	42
5.4	EFFECT OF DEM RESOLUTION ON SLOPE MAP.....	42
5.4.1	Slope maps in different resolutions.....	42
5.4.2	Accuracy assessment and statistical analysis.....	43
5.4.3	DEM Cross section.....	44
5.5	EFFECT OF DEM RESOLUTION ON SOIL EROSION.....	46
5.5.1	Soil erosion results.....	46
5.5.2	Accuracy assessment and statistical analysis.....	47
5.5.3	Analyse of results.....	49
5.6	DISCUSSION.....	50
6	CONCLUSION AND RECOMMENDATION.....	52

6.1	CONCLUSION.....	52
6.2	LIMITATIONS.....	53
6.3	RECOMMENDATIONS.....	53
	REFERENCES.....	54
	APPENDIX I – MODEL INPUTS.....	59
	APPENDIX II – MATLAB CODES.....	61
	APPENDIX III – FIELD DATA VALIDATION POINTS.....	67
	APPENDIX IV – EFFECT OF SIMULATED SATELLITE DATA RESOLUTION ON CLASSIFICATION.....	71
	APPENDIX V – EFFECT OF MAJORITY-BASES AGGREGATION ON LAND USE/COVER..	73
	APPENDIX VI – EFFECT OF SIMULATED SATELLITE DATA RESOLUTION ON EROSION	75
	APPENDIX VII – EFFECT OF DEM RESOLUTION ON SLOPE MAP.....	77
	APPENDIX VIII – EFFECT OF DEM RESOLUTION ON EROSION.....	79

List of Figures

Figure 2-1: Erosion processes by water (Morgan, 1995).....	5
Figure 3-1: Nam Chun watershed in Thailand	10
Figure 3-2: Average monthly rainfall and temperature (1970-2006)	11
Figure 3-3: Effect of deforestation in study area (Sapkota, 2008) (a). Change in land use/cover from forest to orchard and cropland (Suriyaprasit, 2008) (b).....	12
Figure 4-1: Methodology Flow chart.....	15
Figure 4-2: The simulated satellite imagery data in 5m, 30m, 90m, and 250m resolutions in ENVI 4.3.....	16
Figure 4-3: Aggregation and disaggregation of satellite imagery data	17
Figure 4-4: Two-dimensional illustration on the concept of SAM algorithm (Margate and Shrestha 2001)	18
Figure 4-5: Derived spectral signatures for land use/cover classes	20
Figure 4-6: The relationship between annual rainfall and elevation.....	22
Figure 4-7: Schematic illustration of RMMF model at watershed scale	27
Figure 5-1: Land use/cover of the Namchun watershed derived from simulated satellite images	32
Figure 5-2: Covered area by different land use/cover classes in different resolutions (Appendix IV-9)	32
Figure 5-3: Overall accuracy and kappa coefficient of classification maps (Appendix IV).....	33
Figure 5-4: Kappa coefficients of individual classes in different resolutions (Appendix IV)	34
Figure 5-5: Producer's accuracy (Appendix IV-15).....	34
Figure 5-6: Conversion of different classes to dominant class	35
Figure 5-7: Conversion of different classes to a non-dominant class	35
Figure 5-8: Covered area by different land use/cover classes in different resolutions (Appendix V-16).....	36
Figure 5-9: Majority-base aggregation of land use/cover map in 5m resolution to 15m, 30m, 90m, and 250m ...	37
Figure 5-10: Overall accuracy and Kappa coefficient of classification maps (Appendix V)	38
Figure 5-11: Kappa coefficients of individual classes in different resolutions (Appendix V)	38
Figure 5-12: Producer's accuracy (Appendix V-23)	38
Figure 5-13: Erosion maps created from simulated satellite images	39
Figure 5-14: Fraction of erosion classes in different resolutions (Appendix VI-28).....	40
Figure 5-15: Overall accuracy and kappa coefficient of erosion maps (Appendix VI)	40
Figure 5-16: Kappa coefficients of individual classes in different resolutions (Appendix VI)	41
Figure 5-17: Producer's accuracy (Appendix VI-30).....	41
Figure 5-18: Effect of resolution on Slope (Appendix VII-35)	43
Figure 5-19: Overall accuracy and kappa coefficient of different slope maps (Appendix VII)	44
Figure 5-20: Kappa coefficients of individual classes in different slope maps (Appendix VII)	44
Figure 5-21: Cross section line (A-B)	45
Figure 5-22: DEM cross sections	45
Figure 5-23: DEM cross section in zoom view	46
Figure 5-24: Fraction of erosion classes in each resolution (Appendix VIII-41)	46
Figure 5-25: Erosion maps created from DEM in 15m, 30m, 90m, and 250m resolutions	47
Figure 5-26: Overall accuracy and kappa coefficient of erosion maps (Appendix VIII)	48
Figure 5-27: Kappa coefficients of individual classes in different resolutions (Appendix VIII).....	48
Figure 5-28: Producer's accuracy (Appendix VIII-44)	49

List of Tables

Table 3-1: Meteorological station records of 36 years period (1970 – 2006) (Suriyaprasit, 2008).....	11
Table 4-1: RMMF input parameters	13
Table 4-2: Meteorological records from eleven stations in Phetchabun province (1970-2006)	22
Table 4-3: Lay out of an error Matrix (Congalton, et al., 1991)	28
Table 5-1: Confusion matrix of 5m resolution land use/cover map based on validation points	33
Table 5-2: Statistical analysis of band 1-3 of satellite imagery data in different resolutions	35
Table 5-3: RMSE and RRMSE of erosion maps derived from simulated satellite images	42
Table 5-4: Namchun watershed Slope values for different resolutions	43
Table 5-5: RMSE and RRMSE of slope gradient maps	44
Table 5-6: RMSE and RRMSE of erosion maps derived from DEMs	49

List of Abbreviations

ASTER	Advanced Spaceborne Thermal Emission and Reflection Radiometer
AVHRR	Advanced Very High Resolution Radiometer
DEM	Digital elevation model
FAO	Food and Agriculture Organization
LDD	Land Development Department, Ministry of agriculture and cooperatives, Thailand
MODIS	Moderate Resolution Imaging Spectroradiometer
RMMF	Revised Morgan, Morgan and Finney Model
RMSE	Root Mean Square Error
RRMSE	Relative Root Mean Square Error
SAM	Spectral Angle Mapper
SRTM	Shuttle Radar Topography Mission
WEPP	Water Erosion Prediction Project

1 INTRODUCTION

1.1 Background

Land degradation is a process that decreases the capacity of land (FAO, 1994). It has been one of the major global issues during the last century and will continue to be important in the international agenda in the 21st century (Eswaran, et al., 2001). The importance of land degradation among other global issues is related to its impact on world food security and the quality of the environment (Allan, et al., 2007). Soil erosion by water is one of the most important land degradation problems in the world (Eswaran, et al., 2001), which has a negative impact on agricultural production, water quality and in general quality of life (Lal, 1998). Human activities such as unsustainable agriculture practices, deforestation, and over grazing accelerated the rate of soil erosion (Lal, 2001). Therefore, it is of vital importance to protect the land from further degradation.

The relationships between soil erosion and its driving factors are extremely complex and our knowledge from its processes often reflects only a part of the reality. However, in the last decades, different models have been developed to facilitate this problem. These are simplifications of the erosion processes, which can help us to structure our understanding of the reality. In general, the erosion models can be considered as predictive tools for assessing soil erosion (Lal, 1994). Depending on the purpose, availability and quality of data an appropriate model must be selected (Morgan, 1995). Traditional methods in collecting of data especially in inaccessible area are very time consuming and expensive. Nowadays Remote Sensing data effectively contribute to these assessments through providing the required input data (Siakeu and Oguchi 2000; Shanti, 2003).

To control water erosion, it is not enough to assess soil erosion only at the field, hill slope or watershed scale, so that an appropriate allocation of the conservation activities and development of new policies can be achieved through assessing soil erosion at regional scale (Vrieling, 2006). The main restrictions for these assessments are availability and quality of required data (Renschler and Harbor 2002; Van Rompaey and Govers 2002; Merritt, et al., 2003; de Vente and Poesen 2005; Vrieling, 2006).

An important characteristic of the satellite images is spatial resolution. In general, coarse spatial resolution data have less information as compared to that from the fine resolutions. Many studies are limited to relatively small areas, because high-resolution data for getting information on erosion factors such as land use/cover, topography, and soil are not available, while the spatial variation of these factors affects the assessment of soil losses (Rojas, et al., 2008). So several studies have been carried out to evaluate the effect of spatial resolution (cell size) on the accuracy of the soil loss prediction (Quinn, et al., 1991; Zhang and Montgomery 1994; Wolock and Price 1994; Beven, 1995;

De Roo, 1996; Yu, 1997; Wang, et al., 2000). Rojas, et al., (2008) reported that by increasing the spatial resolution (decreasing the cell size), the accuracy of the model can be increased.

One of the ways that spatial resolution of the satellite data can affect soil erosion assessment is the data used to derive a land use/cover map. Land use/cover classification at progressively coarser resolutions results in the increase of errors (Turner, et al., 1989; Moody and Woodcock 1994, 1995) that can rise by increasing the fragmentation and decreasing the patch size of land use/cover classes (Turner, et al., 1989). Such errors have significant effects on modelling and monitoring activities. Discovering the effect of spatial resolution on land use/covers is not only for assessing the reliability of land use/cover maps, but also to quantify the expected errors in model results to help potential users in applying these maps for their specific purposes.

Digital Elevation Models (DEMs) are used to extract topographic parameters in erosion modelling. The topographic features of the landscape have a great influence on amount of soil loss; therefore different DEMs with different resolution may produce different representations of topography that subsequently result in different erosion predictions. Zhang, et al., (2008) revealed that DEM in coarse resolution only can preserve major relief features; therefore it effects the soil erosion assessment especially in mountainous areas with large variation in slope. Considering the ever-increasing list of DEM uses in predictive models, it is important to explore the effect of spatial resolution on reliability of DEMs.

1.2 Problem Statement

Soil erosion is one of the most important environmental problems in Thailand. According to the report of Land Development Department of Thailand, increases in population and demands for food force people to cultivate on marginal land and steep slope (Sapkota, 2008). Deforestation has occurred either for timber or fuel wood collection therefore, forest has been converted into orchard and cropland (Patanakanog, et al., 2004). Indeed, human activities accelerate soil erosion rate in this country, which consequently decline crop yields and quality of environment. In order to protect the land from further degradation, conservation activities and development of new policies and regulations are necessary.

Many studies have been done in Thailand to predict soil erosion (e.g. Bamutaze, 2003; Saengthongpinit, 2004; Amare, 2007; Sapkota, 2008; Suriyaprasit, 2008), which most of them were at watershed scale and for small area. In erosion assessment, watershed analysis provides a framework for ecosystem management; it can be concerned as the best option for natural management and conservation activities (King, et al., 2005). However, to control water erosion, it is not enough to assess soil erosion at the field or watershed scale, but decision makers, policymakers, and environmental management agencies sometimes need to assess soil erosion at larger scales like regional or global level for their long-term planning.

Although several studies have been carried out to predict soil erosion in the previous years but, there is a lack of erosion assessment at large scale. The main restrictions for these assessments are availability and quality of required data. Using available low-resolution data instead of detailed data, can affect the results of soil erosion models (Renschler and Harbor 2002). Therefore, to find out the reliability of erosion assessment at different spatial resolutions; it is important to analyze the effect of using remote sensing and DEM data at various spatial resolutions on deriving land use/cover and topographic factors, and subsequently on the prediction of soil loss. This study intends to analyse the aforementioned effects, so that may better address the issues of spatial resolution when selecting remote sensing and DEM data for erosion assessment.

1.3 Research Objectives

1.3.1 General objective

The main objective of this study is to analyse the effect of using remote sensing imagery and DEM at various spatial resolutions for the assessment of soil erosion.

1.3.2 Specific objectives

- To analyze the effect of spatial resolution of satellite imagery data on land use/cover mapping.
- To evaluate the impact of satellite imagery data resolution on erosion assessment.
- To assess the effect of DEM resolution on soil erosion.

1.4 Research Questions and Hypothesis

1. How the resolution of satellite imagery data affect land use/cover mapping?

H₀: Spatial resolution of the satellite imagery data has no effect on land use/cover classification.

H₁: Spatial resolution of remote sensing data has an impact on land use/cover classification.

2. What is the impact of satellite imagery data resolution on assessment of soil erosion using the RMMF model within a watershed?

H₀: Satellite imagery data does not affect soil loss prediction.

H₁: Satellite imagery data affects the predicted soil loss.

3. What is the effect of majority-based aggregation on land use/cover maps?

H₀: Aggregation has no impact on the land use/cover maps.

H₁: Aggregation influences the land use/cover maps.

4. What is the effect of DEM resolution on extraction of topographic parameters?

H₀: DEM resolution does not affect slope map.

H₁: DEM resolution has an impact on slope map.

5. What is the effect of DEM resolution on soil erosion prediction?

H₀: The predicted soil loss is not affected by DEM resolution.

H₁: DEM resolution affects the result of the RMMF model.

1.5 Assumptions

The study was carried out without any fieldwork. Therefore, all required data and maps were provided by previous MSc thesis carried out in the same watershed (Sapkota, 2008; Suriyaprasit, 2008). In addition, the accuracy assessment of land use/cover classification was accomplished based on the collected ground truth points from field by previous MSc students.

1.6 Thesis Outline

The thesis is organized as follows in six chapters: Chapter 1 introduces the research problem and the research context; describing the research objectives and questions.

Chapter 2 describes and summarizes the literature with respect to the soil erosion process, erosion controlling factors, soil erosion modelling and finally gives an introduction to the scale problem.

Chapter 3 briefly describes the study area.

Chapter 4 is devoted to explain the used materials and applied methods in analysing the data to achieve the research objectives.

In chapter 5 the results obtained from chapter 4 were discussed regarding with the research objectives and research questions.

Finally, chapter 6 presents the conclusions of the research, developed in the thesis and some recommendation and possibility for future studies.

2 LITERATURE REVIEW

2.1 Soil Erosion

Soil erosion as one of the land degradation components, has a negative impact on agricultural production, water quality and in general quality of life. Soil erosion is the process of detaching and transporting of soil particles, which is caused by wind or water or both of them (Morgan, 1995). Factors, which cause soil erosion, can be divided into natural parameters such as climate or topography and anthropogenic parameters such as improper land management and deforestation activities. Figure 2-1 clearly shows the basic processes of soil erosion.

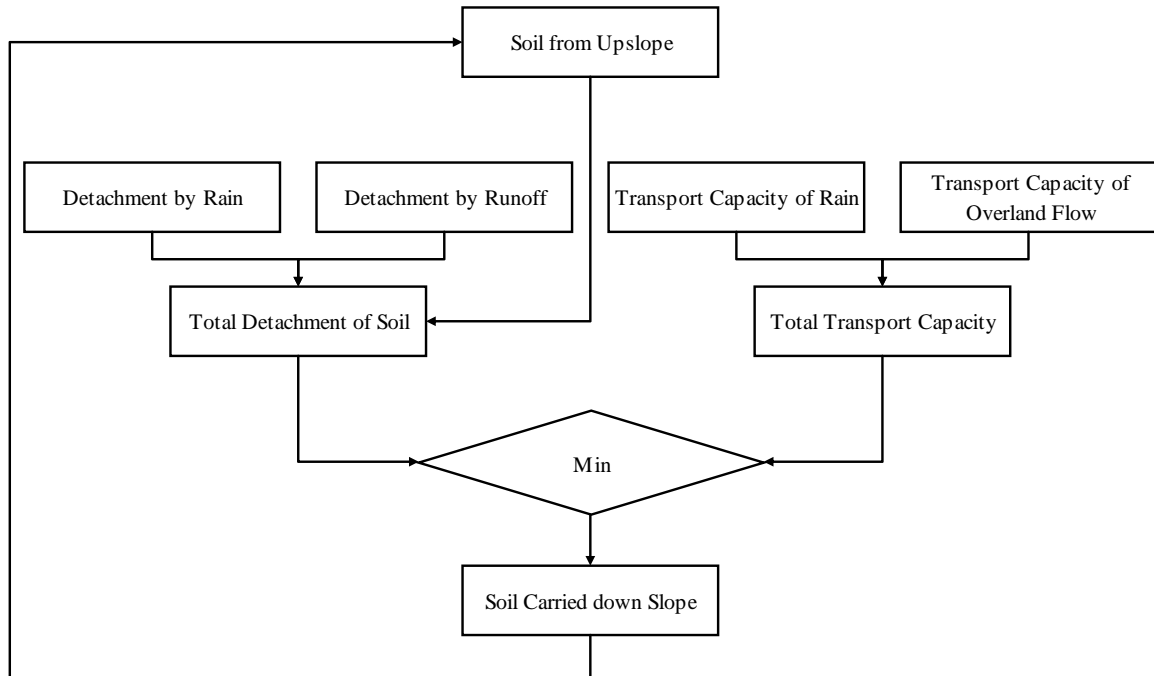


Figure 2-1: Erosion processes by water (Morgan, 1995)

2.1.1 Controlling factors of soil erosion by water

As mentioned, many factors cause soil erosion. For an effective modelling of erosion, these factors need to be considered in the model. Among all these parameters, climate, soil erodibility, topography, and vegetation cover are the most important factors (Morgan, 1995). These terms are explained briefly in the following.

2.1.1.1 CLIMATE

Rainfall intensity is the most important climatic factor, which can directly influence erosion, but amount and frequency of the rainfall as well as the size of raindrop are other effective parameters of rainfall that can significantly influence the soil erosion (Lal, 1994). The kinetic energy of rain drops and also overland runoff can detach soil particles, which is transported down the slope by runoff. The effect of rainfall on erosion can vary with different soil types, vegetation types, and slope steepness. Rainfall, which is not absorbed into the soil or trapped in a pit on a slope, creates the surface runoff. Soil compaction, crusting or freezing can reduce the infiltration of the soil, and consequently increase the amount of runoff.

2.1.1.2 SOIL

Soil erodibility is a function of several soil properties such as the soil particle size distribution, organic matter content, aggregate stability, soil structure, bulk density, top soil shear strength, crust thickness, penetration resistance, and infiltration capacity (Lal, 1994). The size of particles is an important erodibility factor; clay sized particles cannot be detached easily but they can be easily transported, while sand particles are vice versa. Very fine sand and silt sized particles are most susceptible to erosion, whereas clay or sand-sized particles are more resistance to erosion. (Lal, 1994; Morgan, 1995). Soils with high infiltration rates, high organic matter or clay content and developed structures are less prone to erosion.

2.1.1.3 TOPOGRAPHY

A very critical factor in soil erosion is slope. Slope steepness and slope length have crucial effect on amount of soil loss by water. By increasing the slope steepness, the velocity of runoff increases which in turn increases the kinetic energy of the flow. In the same way by increasing the slope length, the volume of overland flow increases. Steep slopes with a short slope length may cause less soil loss in comparison with long gentle slopes (Morgan, 1995; Wischmeier and Smith 1978).

2.1.1.4 VEGETATION COVER

Vegetation cover is an important protective factor against soil erosion. It affects soil detachment and transport capacity of run off significantly. It can be divided into two categories; above ground cover (Canopy Cover) and ground cover. The above ground cover minimizes the impact of raindrop on the soil surface, and the ground cover reduces the energy of the runoff. In addition, the roots of the plants increase the mechanical strength of the soil and also infiltration rate (Morgan, 2005). Dead leaves by increasing the organic matter of the soil can affect soil erosion. Results of a study in Queensland,

Australia showed that by increasing the vegetation cover from 0% to 47%, the erosion rate reduces from 30-35ton/h to 0.5ton/h (Loch, 2000).

2.1.2 Erosion Assessment Models

Different erosion models try to represent the underlying principles and process of soil erosion but no model can describe the complexity of the erosion process like reality. These models try to take into account the essential factors relating to the soil erosion according to obtained field observation, measurement, experiment, and finally the statistical analysis (Morgan, 1995). With increasing computation power of computers, many erosion models have been developed, and still new developments are in progress, as it is not possible to apply a model, which is developed under a certain condition and specific scale, for other locations and scales, without modifications or changes (Jetten, et al. 1999, 2003).

There are many different erosion models with different grade of simplification, from very simple to very complex, but they can be categorized into three main groups: empirical, conceptual and physically based models (Lal, 1994). Among all three model types, empirical models are the simplest one and their computational and data requirements are usually less than the other two model types. Empirical models are mainly based on the statistical analysis of experiments and observations, and trying to characterise a response from these data (Wheater, et al., 1993). Conceptual models lie between physically based and empirical models, they include a general description of catchment processes, without considering process interaction details, which need detailed information about catchment (Bowles and O'Connell 1991). Physically based models are based on the solution of fundamental physical equations that describe the erosion process, tending to represent the essential mechanisms of erosion such as the equations of conservation of mass and momentum for flow and the equations of conservation of mass for sediment (Bennett, 1974). The most important character of the Physically based models is their ability to represent a synthesis of the individual erosion components, including the complex interactions, which occur between various components and their spatial and temporal variations (Lal, 1994).

The differences of these models are relating to complexity, considered processes, and the required data. There is no 'best' model that can be used everywhere, however with regard to; data requirements of the model, the accuracy and validity of the model, model capabilities, the objectives of the user(s), and hardware requirements for the model, the most appropriate model could be selected (Merritt, et al., 2003). Input data is one of the most important factors among them; the main reason that the more complex physically based erosion models cannot predict better than lumped regression-based models is probably the input data (Jetten, et al., 2003).

2.2 Spatial resolution effect

Spatial resolution as one of the most important characteristics of the satellite imagery data is defined as the smallest object that can be identified on the ground. In a digital image the pixel size limits the spatial resolution. Although the terms 'spatial resolution' and 'pixel size' are often used synonymously, they are not equivalent; an image with small pixel size does not necessarily have a high resolution (Justice, 1989). In the proposed study the terms 'fine' resolution and 'coarse' resolution are used relatively not numerically, it means smaller pixels are labelled as finer spatial resolution whereas larger pixels are referred as coarser spatial resolution (Forshaw, et al., 1983). The term 'spatial aggregation' is also used to degrade satellite image data from finer spatial resolution to coarser spatial resolution for simulating the data from different sensor resolutions (Justice, et al., 1989).

Satellite imagery data can be implemented in erosion assessment directly through visual interpretation of erosion features large enough to be seen by the sensor. Several studies have used direct erosion detection techniques (e.g. Langran, 1983; Bocco, et al., 1991, 93; Kumar, et al., 1996). Meanwhile, the erosion modelling can be affected by satellite images indirectly through derived attribute maps as controlling factors. One of the ways that spatial resolution of the satellite data can affect soil erosion assessment is the data used to derive a land use/cover map.

Marceau, et al., (1994a,b) reported that by decreasing the spatial resolution, the spectral details of satellite images are combined, therefore the variance in the image reduces. Atkinson and Curran (1995) obtained an important relationship between the spatial resolution of satellite data and the precision of mean percentage of vegetation cover. Mayaux and Lambin (1995) proved that the land cover maps derived from the satellite data in coarse resolutions like MODIS and AVHRR show the underestimation of covered area by forest where forest is more fragmented, and overestimation in the areas with less fragmentation. Similarly, Pax-Lenny and Woodcock (1997) revealed that in coarser resolutions agricultural fields, which are in small size patches, cause lower accuracy in the maps while agricultural fields in large size patches cause higher accuracy in the classification maps.

Different works indicates that the proportion of the classes after aggregation is affected by the spatial resolution (level of aggregation), initial covered area by each land use/cover class, and the spatial variation within the landscape (Turner, et al., 1989; Moody and Woodcock 1994). In fact, the classes that are smaller with more inter-patch distances, are decreased while the classes, which are larger and more clustered, are increased.

Digital elevation models (DEMs) are the most common representation form of the topography in a geographic information system (GIS). From DEM various topographical and hydrological parameters can be derived. Several studies (Jenson and Domingue 1988; Chang and Tsai 1991; Florinsky, 1998; Gao, 1998; Usery, et al., 2004) show that the quality and resolution of the DEM has a considerable effect on the accuracy of generated topographic and hydrological attributes. Generally, coarser DEMs

generalize the terrain and show only main relief features, it means in the coarser resolutions local slope and aspect results can be changed (Gerrard and Robinson 1971, Fahsi, 1989), which in turn results in less accurate slope maps (Chang and Tsai 1991, Gao, 1998, Kienzle, 2004). Decrease in the DEM resolution, decreases the slope gradient, especially in steeper slope areas (Chang and Tsai 1991; Wolock and Price 1994; Thielen, et al., 1999). The slope distribution of the derived slope maps from coarser DEM resolutions is different from those in finer resolutions (Molnar and Julien 2000). By increasing the cell size, average slope, maximum slope, and standard deviation decrease (Molnar and Julien 2000). In fact, the maximum error occurs on steepest slopes while the minimum error takes place in the smoother areas (Sasowski, et al., 1992; Bolstad and Stowe 1994).

Wilson and Gallant (2000) showed that due to spatial resolution micro topographic features, and steep slopes decrease, while the length of flow paths and in turn the size of catchment areas may increase. In the other word, as DEM became coarser, total flow lengths and drainage density (total channels length per area of watershed) decrease (Thielen, et al., 1999). By decreasing the spatial resolution, the peak discharge predicted in hydrological models increases (Zhang and Montgomery 1994; Thielen, et al., 1999), as a result runoff volume increases and time to reach at peak flow decreases (Thielen, et al., 1999). Wolock and Price (1994) reported that in a topographically based hydrologic model, by increasing the cell size the predicted ratio of overland flow to total flow and the maximum daily flow increases. In spite of the aforementioned works, Rojas, et al., (2008) observed that in greater cell sizes the portion of the infiltrated water increased, therefore the runoff volume and as a result discharge volume decreased. These changes substantially change the soil loss estimation.

Although created drainage networks from DEM in coarser resolutions are not fully integrated, a fine resolution DEM can sometimes exaggerate the topographical details, so that through unrealistic barriers the natural stream flows can be changed (MacMillan, et al., 2003). Therefore, it is not true that in all cases the topographic and hydrological attributes of a finer resolution DEM are more accurate.

Although, there is no unique spatial resolution which can be considered appropriate for the detection and discrimination of all geographical entities composing a complex natural scene, there is an appropriate spatial resolution for each entity accords with its spatial and spectral characteristics (Marceau, et al., 1994a).

To fully understand the effects of spatial resolution of remote sensing and topographic data on erosion assessment it is necessary to analyse the effect of input parameter resolutions on erosion modelling, so that the most adequate resolution can be selected to obtain high reliability of the predictions.

3 STUDY AREA

3.1 Location

The study area is located in Namchun watershed, Petchabun province in northern Thailand. The watershed is situated 400 kilometers north of Bangkok and 40 kilometers far from Petchabun. It is around 67km²; located between the latitudes 16° 40' and 16° 50' North and between the longitudes 101° 02' and 101° 15' East (Figure 3-1). The elevation of the watershed varies from 186 to 1490 meter above sea level.

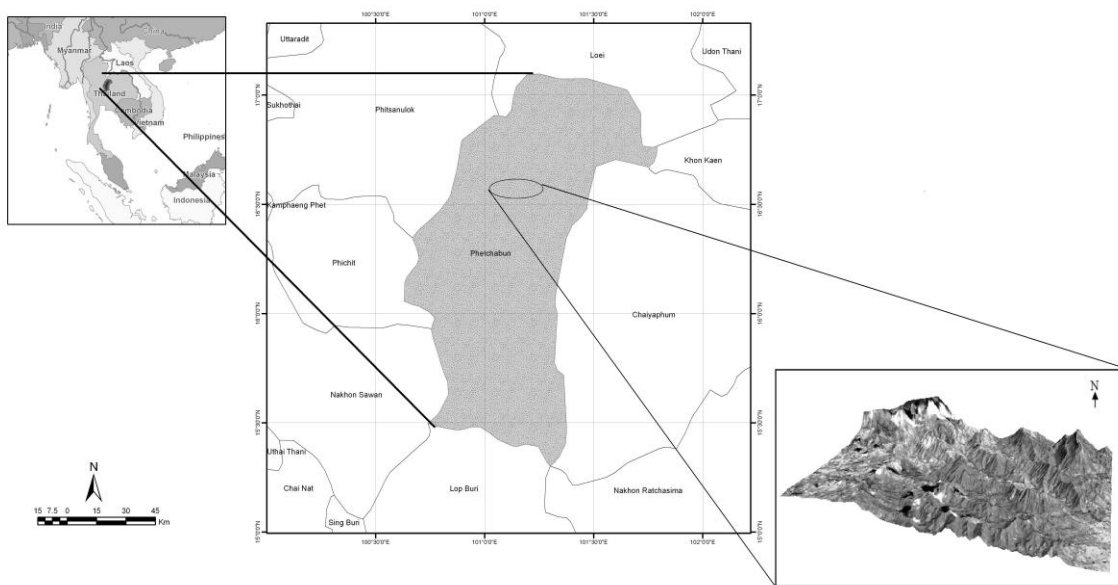


Figure 3-1: Nam Chun watershed in Thailand

3.2 Climate

The climate in the study area is humid tropical affected by annual monsoon, which is characterized by having distinct climate, dry and wet seasons. The rainy season starts from May to September and the rest of the year is dry. According to the detailed climate data from Lom sak meteorological station for a period of 36 years from 1970 to 2006, average annual rainfall in the study area is around 1075 mm with 120 rainy days, and 28 °C average annual temperatures (Table 3-1). Figure 3-2 illustrates that most of rainfalls are in the duration of May to September.

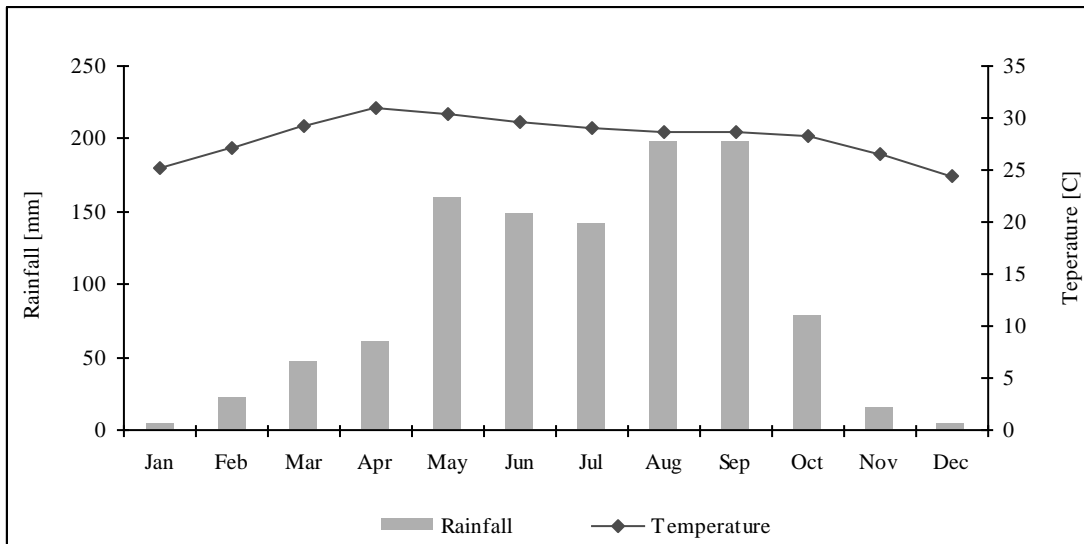


Figure 3-2: Average monthly rainfall and temperature (1970-2006)

Table 3-1: Meteorological station records of 36 years period (1970 – 2006) (Suriyaprasit, 2008)

Month	Rainfall (mm)	Rainy Day	Max Temp. (°C)	Min Temp. (°C)	Mean Temp. (°C)
Jan	4.5	1	32.8	17.5	25.2
Feb	22.2	2	34.8	19.5	27.2
Mar	46.4	5	36.6	22.0	29.3
Apr	59.9	8	37.5	24.3	30.9
May	159.1	16	35.8	25.0	30.4
Jun	148.1	17	34.0	25.1	29.6
Jul	141.4	18	33.2	24.8	29.0
Aug	197.4	21	32.5	24.7	28.6
Sep	198.3	19	32.9	24.5	28.7
Oct	78.1	10	33.2	23.3	28.3
Nov	15.3	2	32.5	20.4	26.5
Dec	4.8	1	31.6	17.4	24.5
Total	1074.6	120	34.0	22.4	28.2

3.3 Land use/cover

Five different types of land use/cover can be observed in the study area; forest, degraded forest, cropland, grassland and orchard. Rice and maize are the main agriculture crops (Shrestha, et al., 2001). Maize and beans are farmed in the hill slope area, while rice and vegetables are grown in the low land (Suriyaprasit, 2008). There are different orchard types, such as tamarind, mango, papaya, and banana in the area but tamarind is the major type (Sapkota, 2008).

It has been reported by Land Development Department of Thailand (LDD, 2001), increases in population and demands for food force people to cultivate on marginal land. Deforestation has occurred either for timber or fuel wood collection (Figure 3-3a) therefore, forest has been converted into orchard and cropland (Figure 3-3b). Agriculture practices in steep slope cause soil erosion in the study area. Recently reforestation programme has started with planting tree species like teak, eucalyptus, gliricidia and leucaena.



Figure 3-3: Effect of deforestation in study area (Sapkota, 2008) (a). Change in land use/cover from forest to orchard and cropland (Suriyaprasit, 2008) (b)

3.4 Soil

The clay content of soil in the study area is high and their textures categorized in silty loam to silty clay loam (Prachansri, 2007). Soil in the study area is classified into five classes according to USDA soil taxonomy; Entisols, Mollisols, Inceptisols, Alfisols and Ultisols. Entisols are mainly found in mountains and plateau hills whereas the Mollisols are distributed over the mountains, piedmont and plateau hills. Inceptisols can be found in all type of landscape (Sapkota, 2008; Suriyaprasit, 2008).

3.5 Geology and Geomorphology

High plateaus, the mountainous area and the low-lying narrow valley are the main landforms in the study area. Based on the reports from Mineral Resources Department, Thailand (2006), Upper catchments in the study area consist of uplifted sedimentary rocks of the Korat group. The oldest Huai Hin Lat formation is made up of conglomerate, sand stone and shale formed during the Triassic period. The youngest formation is Pha Wihan which is composed of white and pink, cross-bedded sand stone with pebbly layers in the upper beds and some interstratifications of the reddish-brown and gray shale. Phu Kradung formation consists of silt stone, shale and sandstone, was formed along the scarp in the study area. In lower part colluvial and alluvial terraces were formed during the Quaternary (Suriyaprasit, 2008).

4 MATERIALS AND METHODOLOGY

4.1 Used Materials and Software

4.1.1 Materials

Materials used in this study can be listed as follows:

- Digitized contour line with 10 meters interval from Land Development Department (LDD) Thailand.
- Geo-Pedological map with the scale of 1:100,000 from ITC (Solomon, 2005).
- Satellite imagery data: nine bands of ASTER images obtained on December 8, 2007.
- Rainfall records from meteorological stations between 1970 and 2006.
- Ground control point for land use/cover from previous field work.

Some of the RMMF inputs such as soil properties and land use/cover parameters were obtained from Land Development Department (LDD) and the previous MSc thesis respectively (Sapkota, 2008; Suriyaprasit, 2008). Table 4-1 presents these input parameters.

Table 4-1: RMMF input parameters

Soil Parameters	Land use/cover
Bulk Density	Rainfall Intercepted by The Crop Cover, A
Soil Cohesion, COH	E_t/E_o
Effective Hydrological Depth, EHD	Cover Management, C-factor
Soil Moisture Content at Field Capacity, MS	Canopy Cover, CC
Soil Detachability Index, K	Ration of Vegetation Ground Cover, GC
	Plant Height, PH

4.1.2 Software

Used software to accomplish this research is:

- MATLAB 7.8.0 (R2009a)
- ENVI 4.7
- ILWIS 3.6
- ERDAS 9.3

- ArcGIS 9.3.1
- OpenEV

4.2 Methodology

To achieve the objectives of the study, the methodology of this research includes three main parts; Data preparation, erosion modelling and statistical analysis. Data preparation consists of different steps such as converting formats, geo-referencing, geo-coding, and creating satellite imagery data and DEMs in different resolutions. For erosion modelling, the Revised Morgan-Morgan-Finney model (RMMF) was used. This model was selected for two reasons; first, this study was carried out without any fieldwork and the input data for the RMMF model were available from a cooperative project between ITC and Land Development Department (LDD) from previous year fieldwork. Second, the objective of the study is to analyse the effect of spatial resolution on erosion assessment, so it is necessary to use a raster-based model; the RMMF model can be easily used in raster-based geographic information systems (Shrestha, 1997).

By using input data with different spatial resolutions it is possible to assess the effect of spatial resolution on soil loss estimation. The study evaluated the effect of spatial resolution in five different resolutions, namely 5m, 15m, 30m, 90m, and 250m. The choice of these resolutions was made to simulate the effect of spatial resolution of commonly used resolutions; ASTER (15m), Landsat (30m), and MODIS (250m) satellite images and SRTM (90m) Digital Elevation Model (DEM). Regarding to the resolution of the used DEM in the study, 5m resolution also was considered. The effect of spatial resolution of satellite imagery data on estimation of soil loss was simulated by aggregation of ASTER image (15m) to coarser resolutions (30m, 90m, and 250m), independent of other sensor characteristics. However, the aggregation from ASTER image (15m) to coarser spatial resolution likely creates an image with much better characteristics than the originally coarser spatial resolution image (Townshend and Justice 1988). In this study, only spatial resolution of satellite imagery data and DEM is evaluated; the effects of other model inputs are held constant. In order to isolate the effect of spatial resolution on model output, all simulated satellite images and DEM in coarser resolutions were disaggregated to 5m resolution. Comparison of the results from different resolution was done using statistical methods. The overall methodology is illustrated in Figure 4-1.

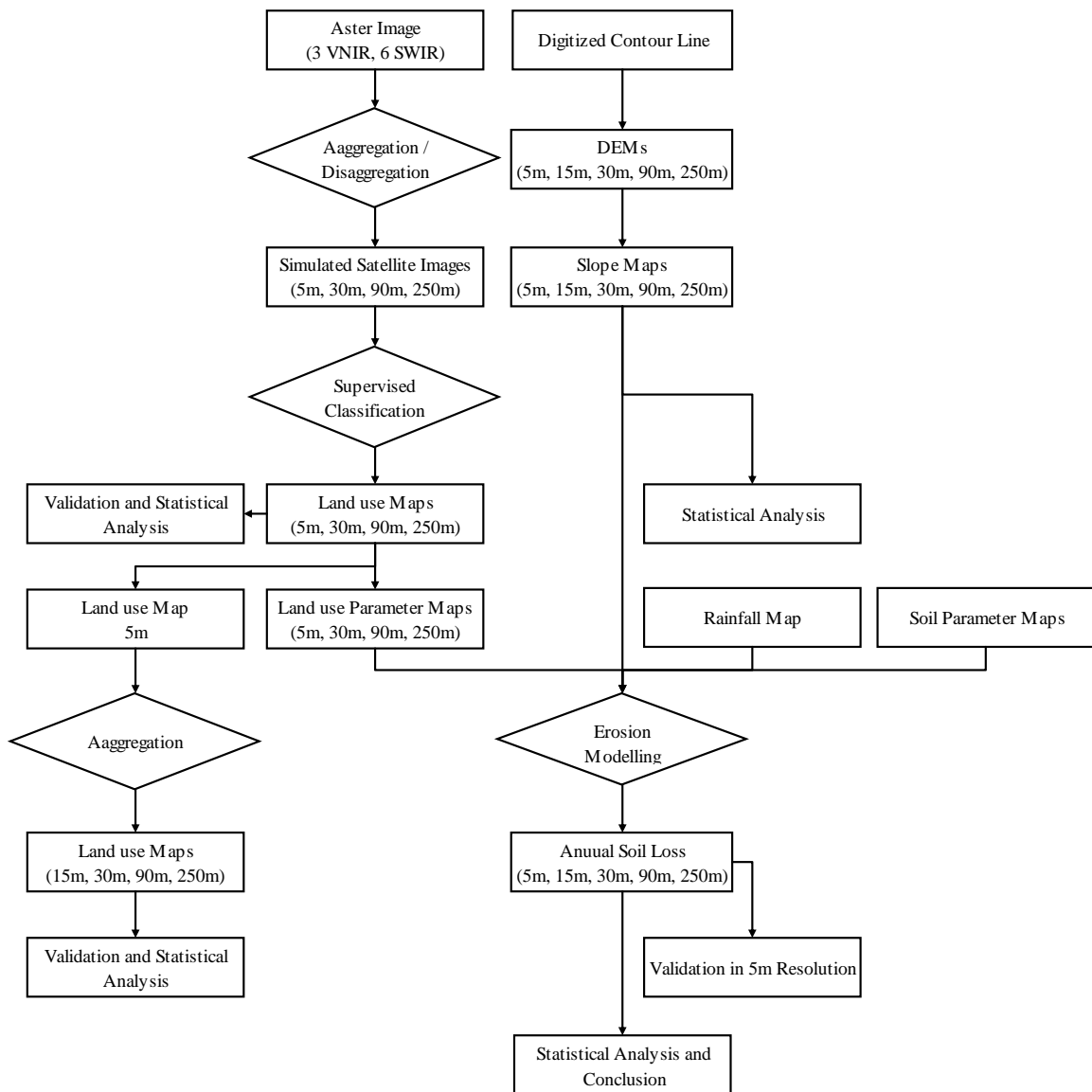


Figure 4-1: Methodology Flow chart

4.2.1 Aggregation of satellite imagery data to different resolutions

To create the satellite images in coarser resolutions, all nine bands of the ASTER HDF file were imported into ERDAS for geo-referencing, geo-coding and converting the DN value into radiance. They were geo-referenced in UTM map projection with WGS84 datum. Geo-coding step was accomplished by using the nearest neighbour interpolation and the first order of the polynomial transformation. The Nearest Neighbour re-sampling method was selected, as the original values have to be remained for classification (Qu, et al., 2006). For reducing the computing time, the ASTER image was sub mapped for covering only the study area. The nine ASTER bands were individually disaggregated from the original resolution (3 VNIR bands with 15m resolution and 6 SWIR bands with 30m resolution) to 5m resolution. For disaggregation, exactly the same value from the coarser

resolution was considered for 5m resolution. It means the value of 36 pixels in 5m resolution is the same with the value of corresponding pixel in 30m resolution. Since, the disaggregation process has no effect on the quality of data (Kuriakose, et al., 2009) and the disaggregated image in 5m resolution can be considered as the original ASTER image. From the 5m resolution disaggregated data, nine bands in 30m, 90m, and 250m resolution were generated. All aggregation and disaggregation processes have been done automatically in MATLAB environment (Appendix II).

Aggregation was done for nine bands of the ASTER image individually by using the average function (Ju, et al., 2005). The ratio between coarse resolution and fine resolution defines the number of pixels that have to be aggregated. For instance, the average value of 36 pixels in 5m resolution is the value of one pixel in 30m resolution. In the study, the term “average-based aggregation” refers to aggregation of satellite imagery data with average function. Finally, to make the simulated satellite images compatible with other data sets, all nine bands should be individually disaggregated to 5m resolution. At the end, nine bands in 30m, 90m, 250m, which also have been disaggregated in 5m resolution, were saved in ASCII format in MATLAB. In the last step, OpenEv software was used to convert all these generated bands from ASCII format to ENVI format. Figure 4-2 represents the simulated satellite imagery data in coarser resolutions. Figure 4-3 explains the procedure of aggregation and disaggregation of nine ASTER bands in MATLAB.

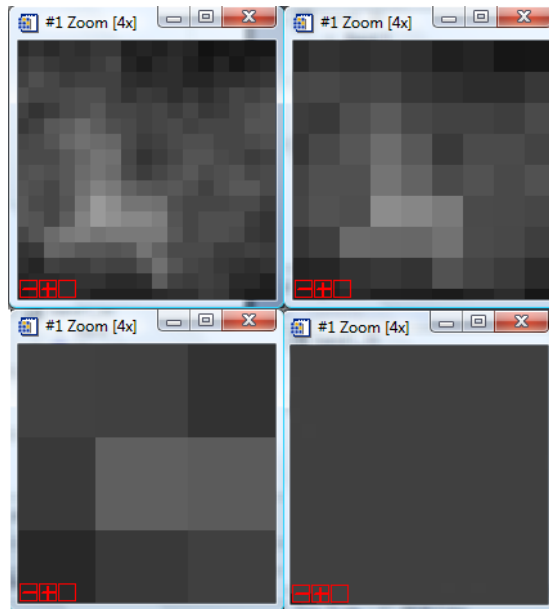


Figure 4-2: The simulated satellite imagery data in 5m, 30m, 90m, and 250m resolutions in ENVI 4.3

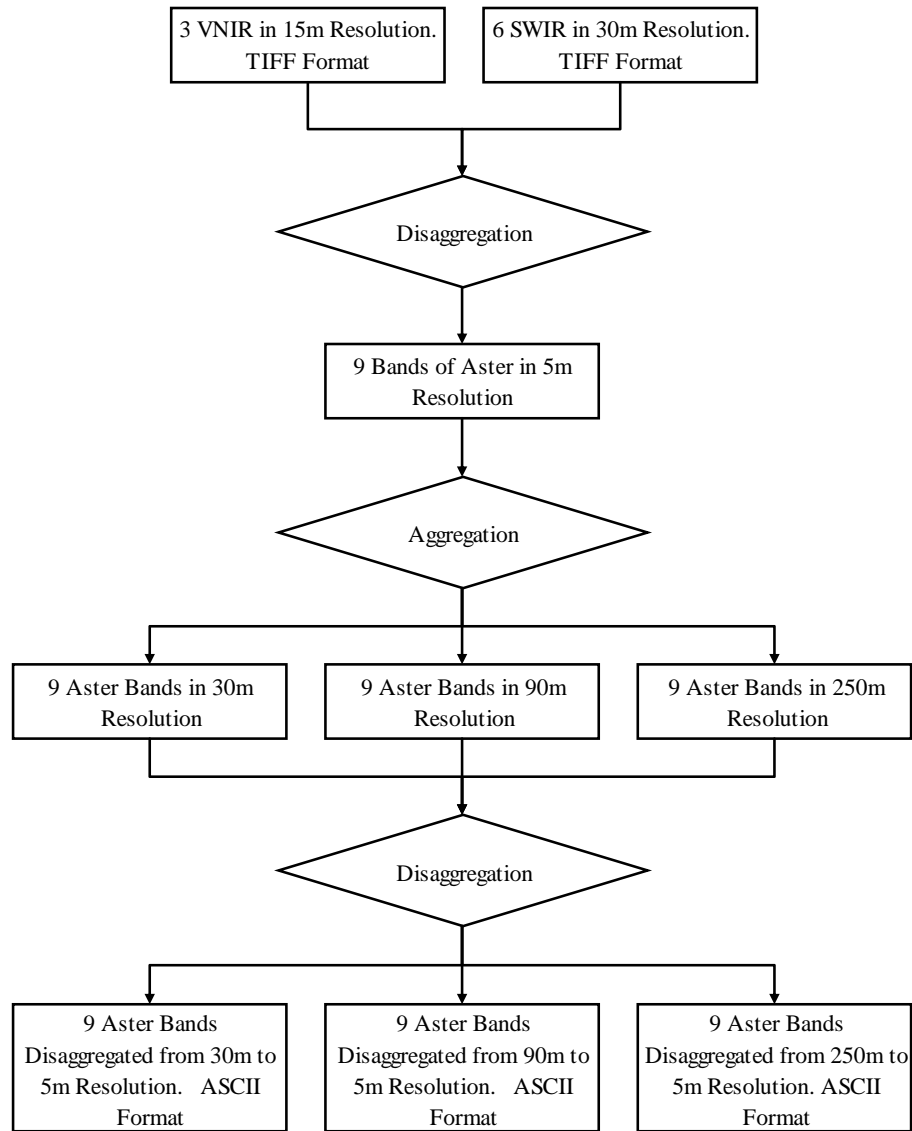


Figure 4-3: Aggregation and disaggregation of satellite imagery data

4.2.2 Image classification

For evaluating the effect of spatial resolution of satellite imagery data on classification and consequently on erosion assessment, it is necessary to classify satellite imagery data in different resolutions. For classification, supervised classification with the Spectral Angle Mapper (SAM) algorithm was applied in ENVI 4.3 on satellite imagery data with different resolutions to obtain corresponding land use/cover maps.

The SAM algorithm was chosen in the study; first, it can be considered as a scale independent method, which avoids the problem of training points in the coarser resolutions. Second, Namchun watershed is a mountainous area that is affected by illumination variation, while SAM algorithm is comparatively insensitive to this factor (Kruse, et al., 1993).

4.2.2.1 SPECTRAL ANGLE MAPPER (SAM) ALGORITHM

Spectral Angle Mapper (SAM) is a spectral classification that uses an n-D angle to specify the spectral similarity between two spectra; the unknown spectra and the reference spectra (end members or spectral libraries) (Kruse, et al., 1993; Boardman, 1992). Figure 4-4 illustrates the concept of the SAM algorithm in two-dimensional.

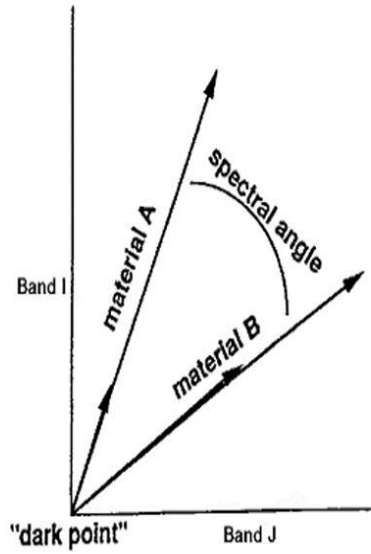


Figure 4-4: Two-dimensional illustration on the concept of SAM algorithm (Margate and Shrestha 2001)

The mathematical formulation of SAM calculates the angle between an unknown spectrum (t) from image and a reference spectrum (r) by treating them as vectors in a space with dimensionality equal to the number of bands (Kruse, et al., 1993; Boardman, 1992).

$$\Theta = \cos^{-1} \left[\frac{\sum_{i=1}^n t_i r_i}{\sqrt{\sum_{i=1}^n t_i^2 \sum_{i=1}^n r_i^2}} \right] \quad (4-1)$$

where:

Θ = Angle between a reference spectrum and an unknown spectrum in radian.

t = Unknown spectrum

r = Reference spectrum

n = number of bands

A low angle represents more similarity between unknown spectra and reference spectra. Although, SAM algorithm assumes reflectance data as input, but by using radiance data that is the case in this study, the error is generally not significant (Kruse, et al., 1993).

In the study to classify the satellite imagery data two steps were implemented; collecting the end members from disaggregated original ASTER image with 9 bands in the 5m resolution, and creating the spectral signatures for each land use/cover type to apply them as spectral library in the coarser resolution.

The end members were selected through the regions of interest tool from the original ASTER image. Field data, collected during September 2007, along with existing land use/cover from the study area were used to train the ASTER data. These training points were categorized into five land use/cover classes including forest, degraded forest, agriculture, grassland and orchard with a minimum of 30 pixels per each class to represent the characteristics of classes statistically (Swain and Davis 1978). The bare soil class was also considered because the used ASTER image in the study was on December, while the fieldwork was carried out on September; according to the crop calendar on December, some crops are at the beginning of the plantation period and some of them were already harvested (Appendix III-8). The spectral characteristic of the bare soil is significantly different from vegetation cover; it is easy to separate this class from the others. The bare soil was extracted from the image by interpreting the False Color Composite.

Certain characteristics of each land use/cover enable us to distinguish different land use/cover types from each other according to their response in the given wavelengths. Spectral signatures can be created by plotting these responses against wavelengths. Spectral signatures were created in nine bands for defined classes in 5m resolution.

The separability between two signatures can be evaluated statistically through measuring the spectral distance between them. If the distance between two signatures is statistically significant, the satisfied classification can be obtained.

Transformed Divergence (TD) and Jeffries-Matusita algorithms were used to compute the spectral separability between two spectral signatures in ENVI 4.3 (Appendix IV-13). These values vary between 0 and 2 that indicate the selected ROIs pairs are separated enough to produce a successful classification. The closer value to two, the more separability between classes (Richards, 1999).

The spectral values of the training points for each class in nine bands were used to create their spectral signatures. The derived signatures from training points were saved as spectral library to classify the satellite images in coarser resolutions, thus the same training spectra were used for classifying satellite images in all resolutions. Figure 4-5 presents the derived signatures for different land use/cover classes.

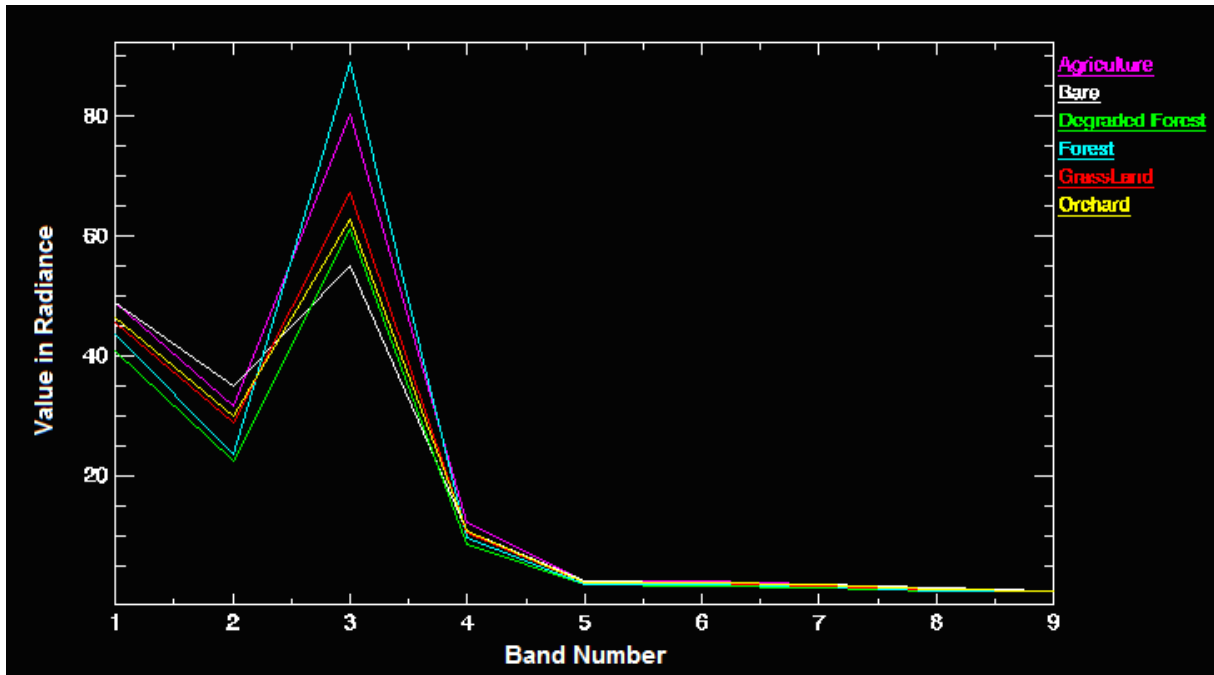


Figure 4-5: Derived spectral signatures for land use/cover classes

To assess the accuracy of the produced land use/cover map in 5m resolution, the validation points that were collected from the previous fieldwork (appendix III) were imported to ENVI in ASCII format. The accuracy of the land use/covers in coarser resolutions was evaluated by considering the created land use/cover map from original ASTER image as ground truth image. The accuracy was assessed through the confusion matrix in all resolutions. Overall accuracy, kappa coefficient, user and procedure accuracy were computed respectively. All these parameters will be explained extensively in the section of statistical analysis. Finally, all the land use/cover maps were converted to ILWIS format through OpenEV for further uses.

4.2.3 Aggregation of land use/cover map

In addition of studying the effect of aggregation of satellite data in land use/cover classification, the other objective of the study is to assess the effect of the aggregation of classified land use/cover map at 5m resolution to 15m, 30m, 90m, and 250m resolution. In the study, the term “majority-based aggregation” refers to aggregation of land use/cover map with Predominant function (Ju, et al., 2005). All these aggregated land use/cover maps were disaggregated with nearest neighbour method to 5m resolution (Quattrochi and Goodchild 1997). The accuracy assessment of the land use/cover maps in the coarser resolutions was compiled in an error matrix by considering 5m resolution map as ground truth image. In addition, the changes in the proportion of land use/cover classes along with statistical analyse were computed.

4.2.4 Digital Elevation Data in different resolution

To investigate the effect of DEM resolution on erosion assessment; DEMs in 5m, 15m, 30m, 90m, and 250m resolution were created from digitized contour map with 10m interval. It was achieved through contour interpolation in ILWIS 3.6. The slope maps in 5m, 15m, 30m, 90m, and 250m were subsequently derived from DEMs. To evaluate the effect of DEM resolution on erosion prediction with the RMMF model, all slope maps were disaggregated to 5m resolution. It was carried out by using the re sampling operation with the nearest neighbour method. In addition, fill sink operation was accomplished to improve the DEM quality.

4.2.5 Erosion assessment

As mentioned, the RMMF model was selected to assess the annual soil loss in different spatial resolutions. As the objective of the study is to analysis the effect of spatial resolution, all input parameters for running the model are in the raster format. Therefore, it is easy to handle the RMMF model in ILWIS 3.6 software.

In following, the RMMF model and its input parameters will be briefly described. The input parameters of the RMMF model at field scale can be categorized into slope map, rainfall map, geo pedological attribute maps, and land use/cover attribute maps. The slope map was derived from Digital Elevation Model (DEM) and the rainfall map was created from the meteorological records. To create the geo pedological and land use/cover attribute maps the input parameters, which are listed in Table 4-1, were added to their attribute tables (Appendix 4-1).

Revised Morgan-Morgan-Finney model (RMMF) divides the process of soil erosion into two phases: water phase and sediment phase. In water phase, the kinetic energy of rainfall to detach soil particles from the soil mass is determined. Sediment phase indicates the total soil particle detachment by runoff and raindrop along with the transport capacity of runoff (Morgan, 2001).

4.2.5.1 ESTIMATION OF RAINFALL KINETIC ENERGY

Rainfall map is needed to compute the kinetic energy of rainfall. In order to create rainfall map meteorological records from different stations are necessary. Due to the lake of rainfall data for generating rainfall map, rainfall records from 11 meteorological stations in Phetchabun province was used (Table 4-2). The annual rainfall and elevation of meteorological stations were correlated to find the relationship between rainfall and elevation. A regression technique was applied to obtain the equation for creating the rainfall map (Suriyaprasit, 2008; Shrestha, 1997) (Figure 4-6).

Table 4-2: Meteorological records from eleven stations in Phetchabun province (1970-2006)

Station	Annual Rainfall	Elevation	X-Coordinate	Y-Coordinate
Lom Sak	1089.6	140	740000	1857000
Lom Kao	1050.5	160	738000	1868000
Khao Kao sta.	1556.1	720	715000	1854000
Na Sum	972.0	180	737200	1880900
Hin Hao	837.0	170	736300	1873700
Nam Ko	1108.0	170	732400	1857700
Lao Ya	1742.0	720	716700	1854600
Dong Khwang	843.0	150	732500	1848400
Khao Kho	1595.0	920	713500	1840400
Om Kong	1045.0	140	730000	1837000
Na Ngua	946.0	140	729000	1827700

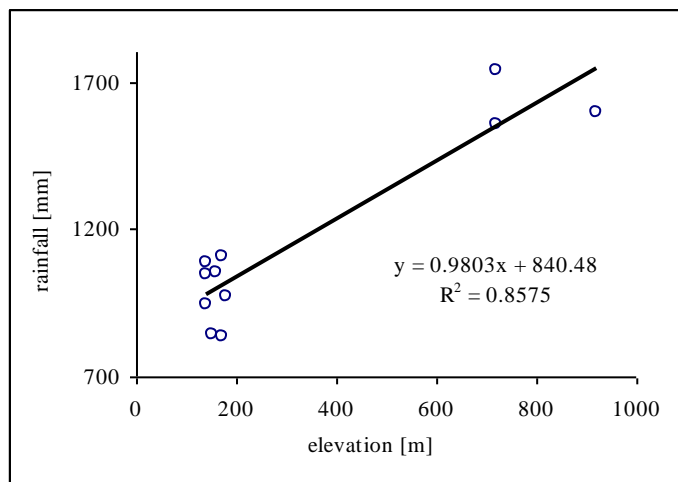


Figure 4-6: The relationship between annual rainfall and elevation

The regression equation for prediction of rainfall map within watershed is:

$$Rainfall = 0.9803 \times (elevation) + 840.48 \quad (4-2)$$

After preparing the rainfall map, Effective Rainfall (ER) is calculated as below:

$$ER = R \times (1-A) \quad (4-3)$$

where:

ER = effective rainfall (mm)

R = annual rainfall (mm)

A = rainfall interception (0-1)

Effective Rainfall is a function of annual rainfall and rainfall intercepted by canopy cover, i.e. the proportion of the rainfall that is not intercepted by canopy cover.

The effective rainfall is divided into leaf drainage, which reaches to soil after being intercepted by canopy cover and direct through fall, which is the differences between effective rainfall and leaf drainage.

Leaf drainage is obtained by using following equation:

$$LD = ER \times CC \quad (4-4)$$

where:

LD = leaf drainage (mm)

CC = plant canopy (%)

After it, by subtracting leaf drainage from effective rainfall, direct through fall is computed:

$$DT = ER - LD \quad (4-5)$$

where:

DT = direct through fall (mm)

The kinetic energy of the direct through fall depends on intensity of rainfall while kinetic energy of leaf drainage is a function of plant height. Finally, the total rainfall kinetic energy is obtained by the sum of the two components.

Kinetic energy of leaf drainage is calculated as follows:

$$KE(LD) = LD \times (1.58 \times PH^{0.5}) - 5.87 \quad (4-6)$$

where:

KE(LD) = leaf drainage kinetic energy (j/ m²)

PH = plant height (m)

Kinetic energy of direct through fall is defined by using equation as below:

$$KE(DT) = DT \times (11.9 + 8.7 \log I) \quad (4-7)$$

where:

KE(DT) = kinetic energy of direct through fall (j/ m²)

I = rainfall intensity (mm/hr)

The value 25 is considered as a reasonable value for rainfall intensity in tropical countries like Thailand (Morgan, 2001).

Finally, the total kinetic energy is:

$$KE = KE (DT) + KE (LD) \quad (4-8)$$

where:

KE(DT) = kinetic energy of direct through fall (j/ m²)

KE(LD) = leaf drainage kinetic energy (j/ m²)

The splash detachment rate is determined by rainfall kinetic energy, which is obtained as:

$$F = 10^{-3} \times K \times KE \quad (4-9)$$

where:

F = soil particle detachment by raindrop impact (kg/ m²)

K = soil detachability index (g/j)

4.2.5.2 ESTIMATION OF RUNOFF

The volume of annual runoff is a function of soil properties and the mean rainy days. Soil properties is introduced in equation as soil moisture capacity which is in turn calculated by equation including bulk density, effective hydrological depth, ratio of actual to potential evapotranspiration and soil moisture content at field capacity.

Following equation was used to calculate soil moisture storage capacity:

$$R_C = 1000 \times MS \times BD \times EHD \times (ET_o/ET_p)^{0.5} \quad (4-10)$$

where:

R_c= soil moisture storage capacity (mm)

MS = soil moisture content at field capacity (%ww)

BD = bulk density (g/cm³)

EHD = effective hydrological depth (m)

ET_o/ET_p = ratio of actual to potential evapotranspiration

For mean rainy days, following equation is used:

$$R_o = R/R_n \quad (4-11)$$

where:

R_o = mean rainy days

R = annual rainfall (mm)

R_n = number of rainy days in a year.

According to the meteorological stations records, the number of rainy days in a year was 120 rainy days in the period of 36 years from 1970 to 2006.

In general, surface run off is generated when the amount of daily rainfall is over the soil moisture storage capacity. In the RMMF model at field scale the following equation is applied to compute the volume of runoff.

$$Q = R \exp(-R_c/R_o) \quad (4-12)$$

where:

Q = volume of annual runoff (mm)

R = annual rainfall (mm)

The RMMF model has been originally designed to predict annual soil loss at field scale. In order to apply this model at larger scale, additional mechanisms should be taken in to account. In this case, a new introduced component is the accumulation of runoff along the slope within watershed. In fact, total surface runoff of each pixel is equal to sum of the generated surface runoff in each pixel, and generated surface runoff from the immediate upslope area. To consider upslope area contribution, weighted factor along flow accumulation should be defined.

This step was done by using spatial analyst tool in ArcGIS software. DEMs were used to obtain flow directions and subsequently flow accumulations by providing the run off maps as weighted factor in different resolution. The total run off was used to calculate the soil particle detachment rate by runoff.

Using total runoff as input for estimation of soil detachment causes an overestimation problem along the stream lines (Vigiak, 2005). To solve this problem the stream lines were masked out from the flow accumulation map.

Soil detachment by runoff was estimated by following equation:

$$H = Z \times Q^{1.5} \times \sin\beta \times (1 - GC) \times 10^{-3} \quad (4-13)$$

where:

H = soil particle detachment by runoff (kg/ m²)

β = slope steepness (°)

GC = ground cover (%)

Z = soil resistance

Soil resistance is defined as:

$$Z = 1 / (0.5COH) \quad (4-14)$$

where:

COH = surface cohesion (kpa)

4.2.5.3 ESTIMATION OF TRANSPORT CAPACITY OF RUNOFF

The transport capacity is a function of total runoff, cover management factor and slope steepness. The transport capacity is equal to

$$TC = C \times Q^2 \times \sin\beta \times 10^{-3} \quad (4-15)$$

where:

TC = transport capacity (kg/ m²)

C = cover management (C-factor)

β = slope steepness (°)

4.2.5.4 ESTIMATION OF ANNUAL SOIL LOSS

Soil erosion rate was obtained by comparing the total soil particle detachment (sum of detachment by runoff and raindrop) and transport capacity of runoff. Indeed, the average annual soil loss was estimated as the minimum value of the total soil particle detachment and transport capacity:

$$E = \text{MIN} [(F + H), TC] \quad (4-16)$$

Where:

E = annual soil loss rate (kg/m²)

All these procedure are summarized in Figure 4-7.

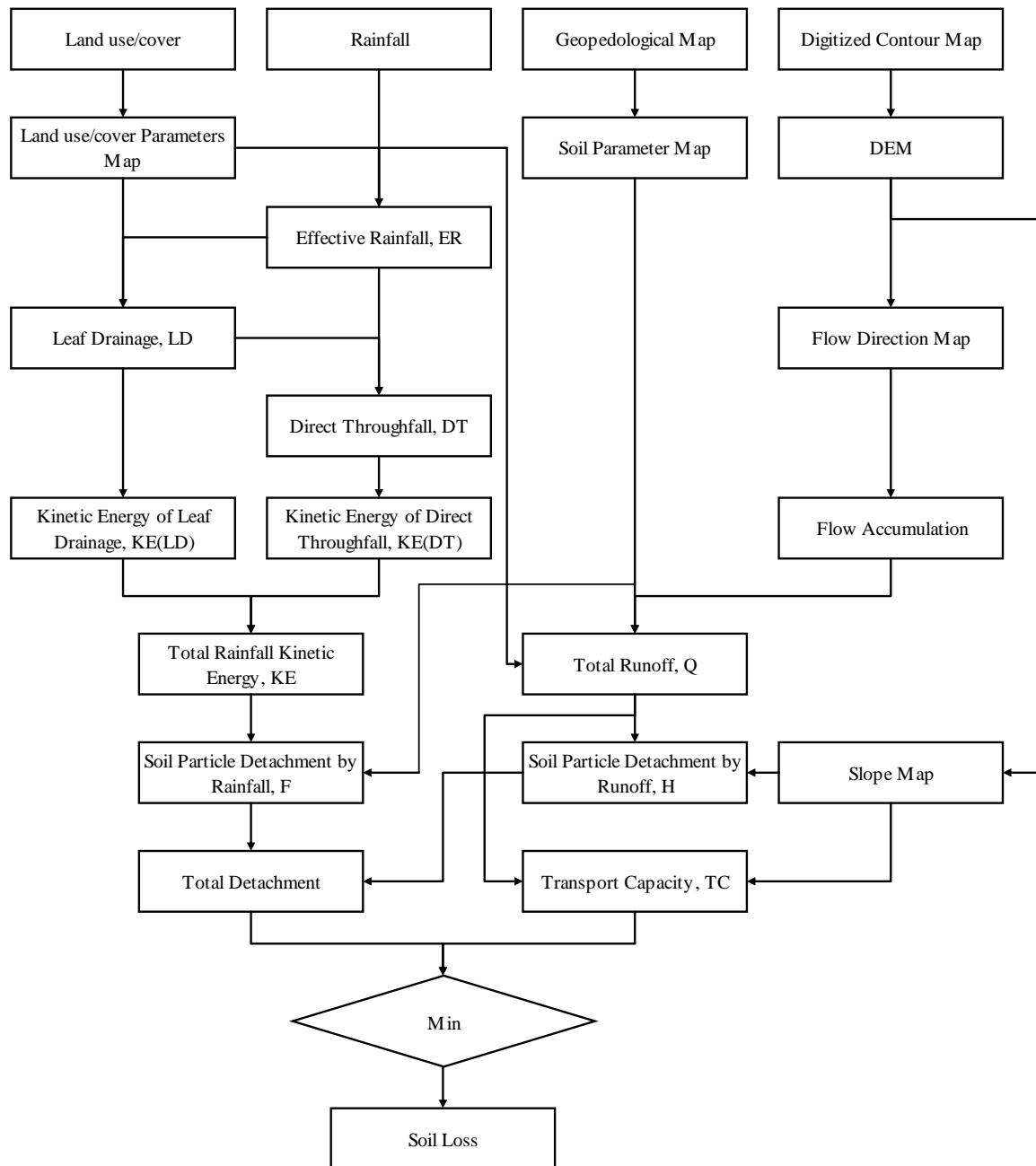


Figure 4-7: Schematic illustration of RMMF model at watershed scale

4.2.5.5 ANALYSIS OF MODEL RESULTS

In general, to find out the effect of spatial resolution on erosion assessment, all obtained erosion maps from different spatial resolutions have to be compared with the real amount of erosion in the field. In this study, due to non-availability of field erosion measurements, the finest resolution was taken as a reference for evaluating the results in coarser resolutions. To handle these comparisons, final erosion maps were classified to five classes; very slight (1-4.99 tons/hectare/year), slight (5-9 tons/hectare/year), moderate (10-24 tons/hectare/year), severe (25-44.99 tons/hectare/year) and very severe (> 45 tons/hectare/year) (Morgan, 1995; Singh and Phadke 2006). Then the other coarser

erosion maps in 15m, 30m, 90m, and 250m were crossed to original 5m resolution to obtain different confusion matrixes.

Before evaluating the results, model validation has to be carried out. There is no erosion data available from the field in the study area but it is possible to validate the results of the model based on the ratio between the predicted discharge value and measured value in the field (Sapkota, 2008). The ratio between 0.5 and 2 can be considered as an acceptable performance for the model (Morgan, 2005). Sapkota (2008) proved that the RMMF model can predict the soil erosion in an acceptable range in the study area.

4.2.6 Statistical analysis

This section briefly describes confusion matrix, overall accuracy, kappa coefficient, producer and user's accuracy, RMSE, RRMSE and their calculation formulas.

4.2.6.1 ERROR MATRIX

Error matrix also known as confusion matrix is a widespread method for assessing the classification accuracy (Table 4-3). The error matrix is calculated by comparing of the classification map with the ground truth map or sample field results. From an error matrix different statistical analysis such as; overall accuracy, user and producer's accuracy, kappa coefficient and a lot more can be derived. The main diagonal of the matrix shows the number of pixels which has been correctly classified. This matrix is for not only accuracy assessing of classification maps, but also through it all types of maps like erosion map, or slope map can be evaluated. The overall accuracy, kappa coefficient, and user and producer's accuracy are described in next subsections.

Table 4-3: Lay out of an error Matrix (Congalton, et al., 1991)

		Ground Truth				
		Class	I	II	III	Total
Created Map	I	X_{ii}			X_{i+}	
	II					
	III					
	Total	X_{+i}				N

4.2.6.2 OVERALL ACCURACY AND KAPPA COEFFICIENT

By summing the main diagonal of the matrix (correctly classified pixels) and dividing by the total number of pixels, the overall accuracy is achieved:

$$OA = \sum_{i=1}^n \frac{X_{ii}}{N} \quad (4-17)$$

In contrast to the overall accuracy, kappa coefficient is a measure, which considers also non-diagonal elements (Rosenfield and Fitzpatrick 1986). The Kappa coefficient measures the conformity of classification after removing the chance agreements. Kappa is between one and minus one. A kappa of zero means the classification map has an agreement equal to chance (Fenstermaker, 1991). Formula 4-18 shows the calculation method of the kappa (Bishop, et al., 1975). Individual kappa for each class is calculating with help of Formula 4-19.

$$\hat{K} = \frac{N \sum_{i=1}^n X_{ii} - \sum_{i=1}^n X_{i+} X_{+i}}{N^2 - \sum_{i=1}^n X_{i+} X_{+i}} \quad (4-18)$$

$$\hat{K}_{\text{individual}} = \frac{N(X_{ii}) - (X_{i+} X_{+i})}{N(X_{i+}) - (X_{i+} X_{+i})} \quad (4-19)$$

where;

n = number of rows and columns in error matrix,

N = total number of observations,

X_{ii} = observation in row i and column i,

X_{i+} = total of row i, and

X_{+i} = total of column i.

4.2.6.3 PRODUCER AND USER'S ACCURACY

Two approaches for assessing the accuracy of individual classes are producer and user's accuracy. Producer's accuracy indicates the probability that a pixel in the class is correct classified; it reduces when number of pixels left out of the class increase. The user's accuracy shows the reliability of the map; it reduces when number of extra pixels in the class increases (Jensen, 1986).

$$Pacc = \sum_{i=1}^n \frac{X_{ii}}{X_{+i}} \quad (4-20)$$

$$Uacc = \sum_{i=1}^n \frac{X_{ii}}{X_{i+}} \quad (4-21)$$

4.2.6.4 RMSE

The root mean square error (RMSE) and the relative root mean square error (RRMSE) are two useful tools for the accuracy assessment of created maps in different resolutions. They can be calculated as:

$$RMSE = \sqrt{\frac{1}{N} \sum_{k=1}^N (MAP_k^{\text{Reference}} - MAP_k^{\text{Calculated}})^2} \quad (4-22)$$

$$RRMSE = \frac{\sqrt{\frac{1}{N} \sum_{k=1}^N (MAP_k^{\text{Reference}} - MAP_k^{\text{Calculated}})^2}}{\frac{1}{N} \sum_{k=1}^N MAP_k^{\text{Reference}}} \quad (4-23)$$

where:

N = total number of pixels

$MAP_k^{\text{Reference}}$ = reference map

$MAP_k^{\text{Calculated}}$ = calculated map

Here, the reference map is the ground truth and calculated map is a map that is comparing with ground truth for accuracy assessment. The RMSE represents the error in the map with unit, for example degree, kg or etc, but RRMSE is free of units. Higher RMSE and RRMSE indicate more inaccurate calculated map in comparison with the reference map (DeGroot, 1980).

5 RESULTS AND DISCUSSION

The fifth chapter of the thesis focuses on the analysis of the results and discussion.

This chapter is organized as follows. Section 5-1 shows the effect of spatial resolution of satellite imagery data on classification (Average-base aggregation), and section 5-2 shows the effect of Majority-base aggregation on classification. In section 5-3, the effect of spatial resolution of remote sensing data (Average based aggregation) on erosion assessment is outlined. Sections 5-4 and 5-5 are devoted to show the effect of DEM resolution on slope map and respectively soil loss prediction. Finally, in section 5.6 the acquired results are discussed.

5.1 Effect of Spatial Resolution of Satellite Imagery Data on Classification

The erosion assessment can be affected by spatial resolution of satellite images through derived land use/cover map as input parameters. In the following, the effect of spatial resolution on land use/cover is analysed.

5.1.1 Classification results

Land use/cover classification was done by using supervised classification with the Spectral Angle Mapper (SAM) algorithm in ENVI 4.3 software. The land use/cover maps were classified in six classes; agriculture, bare, degraded forest, forest, grassland, and orchard. Figure 5- 1 show created land use/cover classification maps from simulated satellite images in 5m, 30m, 90m, and 250m resolution.

According to Figure 5-2, land use/cover map in 5m resolution was covered by agriculture (36%) followed by degraded forest (26%), forest and orchard (11%), Grassland (10%) and bare (6%) respectively. In 30m resolution, the area covered by different classes remains almost constant (maximum 1% change). In 90m resolution the area covered by agriculture increases to 42%, degraded forest, grassland, and orchard remained without any change, meanwhile bare and forest areas decreased to 4% and 7% respectively. The land use/cover in 250m resolution showed agriculture area continue increasing to 47%, followed by grassland 14%, while bare and forest decreased significantly to 2% and 4%, orchard reduced moderately to 8%, whereas degraded forest had almost no change.

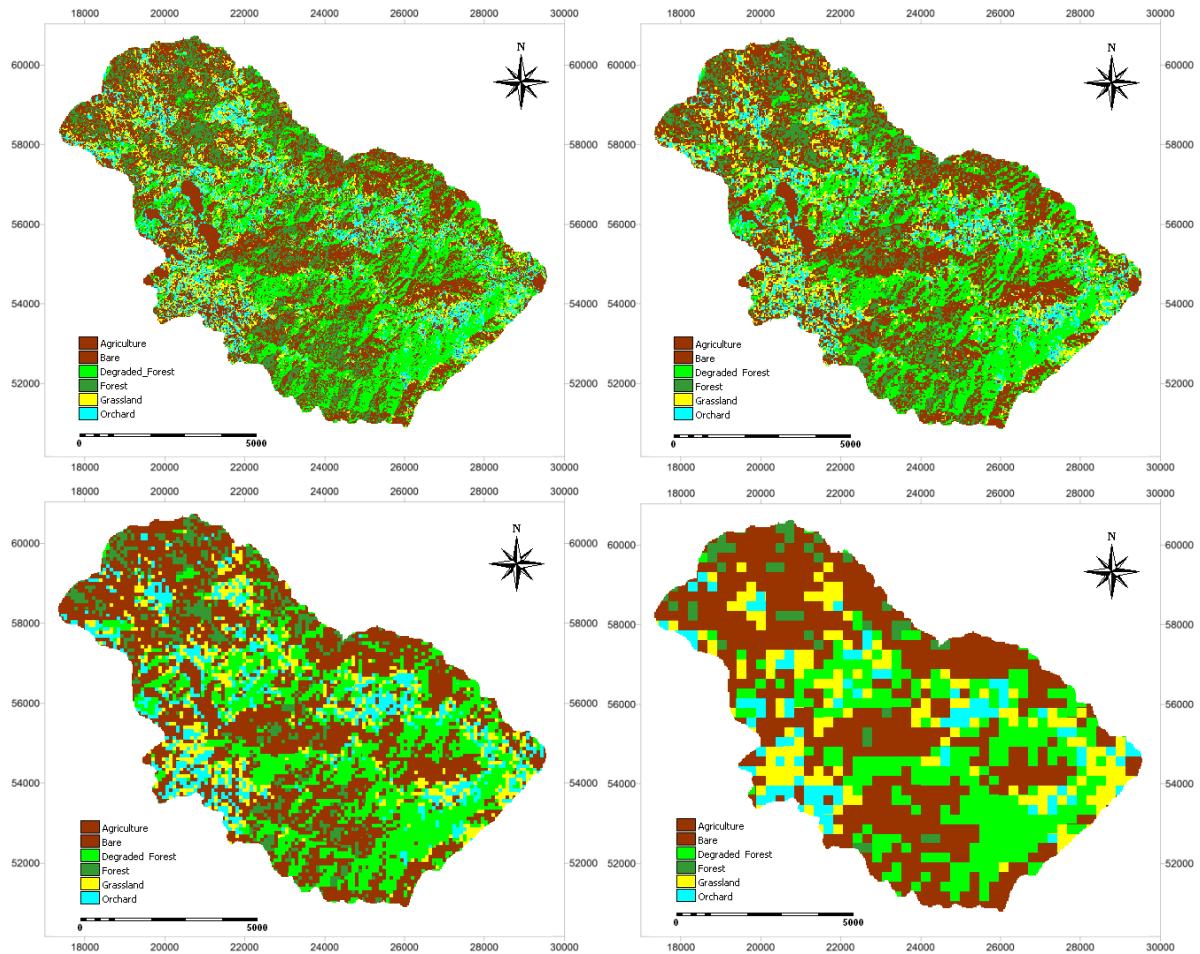


Figure 5-1: Land use/cover of the Namchun watershed derived from simulated satellite images

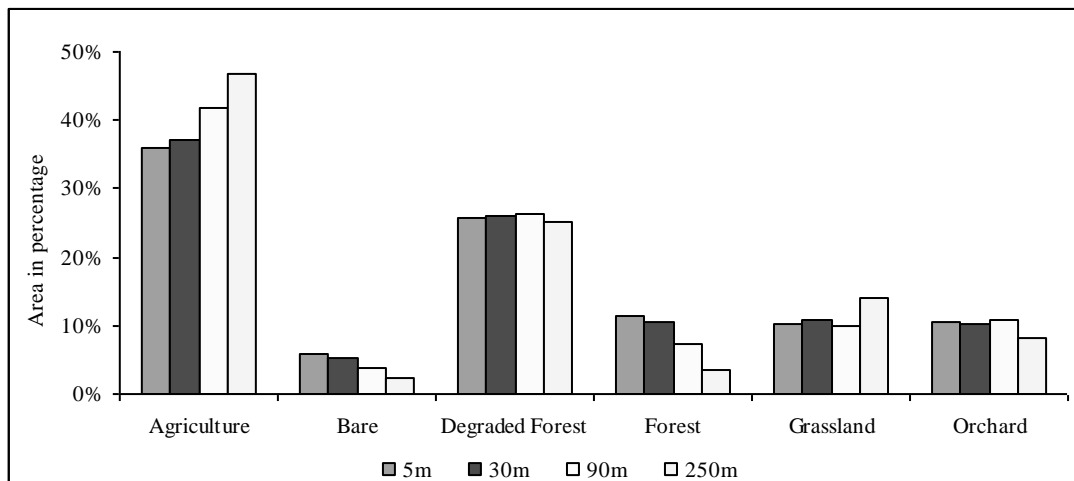


Figure 5-2: Covered area by different land use/cover classes in different resolutions (Appendix IV-9)

5.1.2 Accuracy assessment and statistical analysis

Based on the collected ground truth data from previous fieldworks, the accuracy of land use/cover map in 5m resolution through confusion matrix was assessed (Table 5-1). Beside from overall accuracy and

kappa coefficient, the matrix indicates the kappa coefficients of the individual classes. The overall accuracy of land use/cover map in 5m resolution was 78% and the kappa coefficient was 0.74.

Table 5-1: Confusion matrix of 5m resolution land use/cover map based on validation points

Class	Agriculture	Bare	Deg. Forest	Forest	Grassland	Orchard	Total
Unclassified	0	0	0	0	0	0	0
Agriculture	23	0	3	16	1	0	43
Bare Soil	0	37	0	0	0	0	37
Degraded Forest	1	0	35	2	5	2	45
Forest	0	0	0	20	0	0	20
Grassland	6	0	0	0	24	2	32
Orchard	0	5	2	0	4	35	46
Total	30	42	40	38	34	39	223
Kappa Coefficient	0.46	1.00	0.73	1.00	0.71	0.71	0.74
Overall Accuracy							78.03%

By assuming the created land use/cover map in 5m resolution as ground truth image, other classification results in coarser resolutions (30m, 90m, and 250m) were assessed. The overall accuracy, kappa coefficient and producer’s accuracy were computed to analyse the results. There was a downward trend in overall accuracy and kappa coefficient in coarser resolutions. The overall accuracy of the maps reduced from almost 73% in 30m resolution to 46% in 250m resolution; accordingly, the Kappa coefficient decreased from 0.68 in 30m resolution to 0.28 in 250m resolution (Figure 5-3).

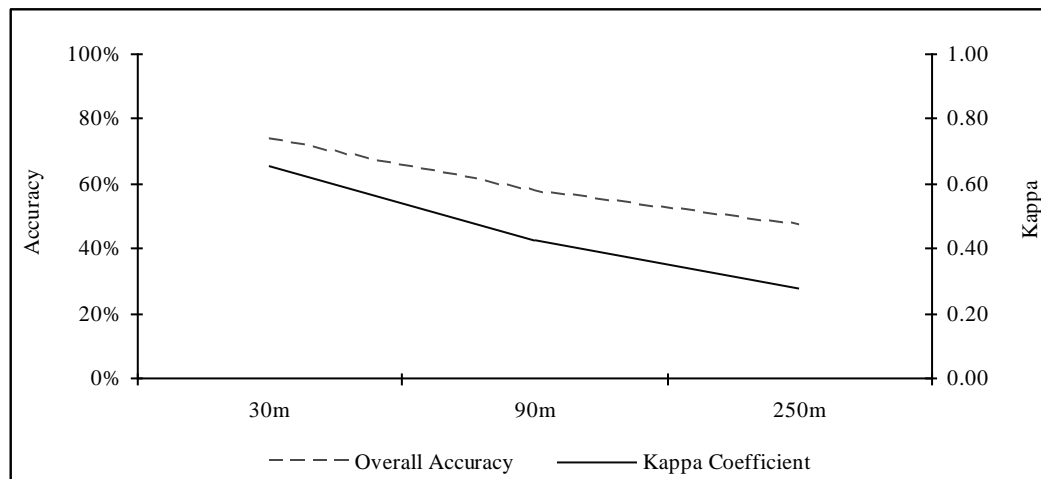


Figure 5-3: Overall accuracy and kappa coefficient of classification maps (Appendix IV)

The Kappa coefficient of individual classes also reduced in coarser resolutions (Figure 5-4). The results showed that the individual kappa coefficient of bare soil in all resolutions was considerably higher than the other classes; meanwhile the kappa coefficient of agriculture and grassland were substantially lower than the others. High kappa coefficients for bare in all resolutions indicated high reliability of this class; low conversion of the other classes to bare. Whereas, the low producer’s accuracy of this class disclosed the high conversion of bare to other classes. This trend also was followed by forest. Conversely, agriculture showed low kappa coefficients and high producer’s

accuracies. The low kappa coefficient along with high producer's accuracy for agriculture proved a great conversion of the other classes to agriculture and low changing of agriculture to other classes.

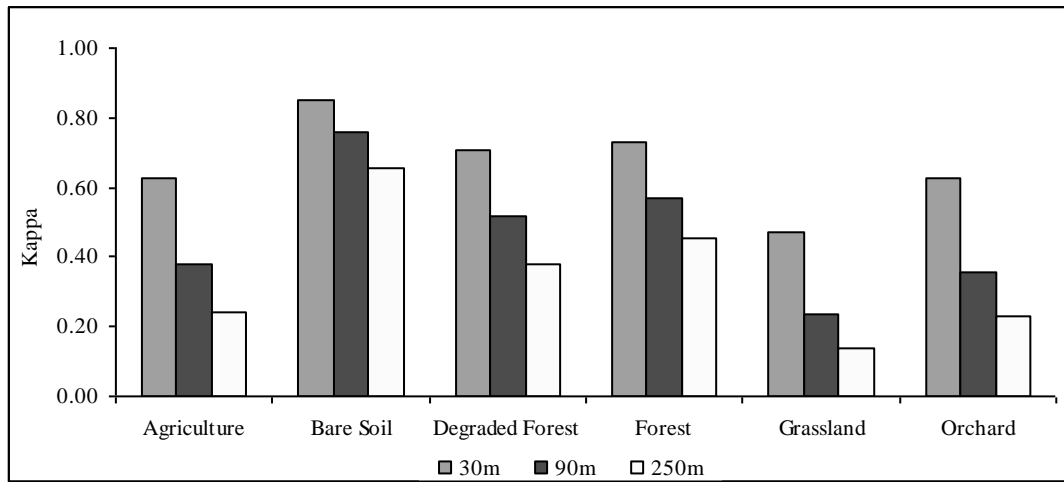


Figure 5-4: Kappa coefficients of individual classes in different resolutions (Appendix IV)

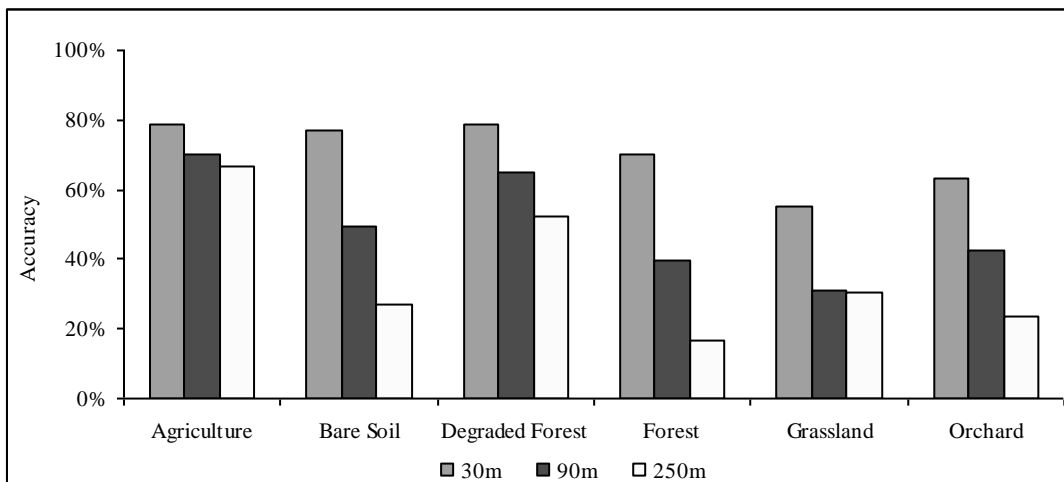


Figure 5-5: Producer's accuracy (Appendix IV-15)

5.1.3 Analyse of results

According to the obtained results, by decreasing the spatial resolution, covered area by bare and forest decreased considerably conversely, covered area by agriculture significantly increased. The main reasons for these trends can be derived from Figure 4-5 and Table 5-2. Figure 4-5 discloses that the signature of forest had minimum values in bands one and two, and maximum value in band three. Whereas bare signature was maximum in bands one and two, and minimum in band three. Table 5-2 shows the mean value and standard deviation of the first three bands of the satellite images in different resolutions; it indicates almost constant mean spectral values and decreasing standard deviation of image bands, due to spatial averaging to coarser resolutions. Indeed, by decreasing the spatial resolution, spectral details were combined, so obviously the standard deviation was reduced.

Table 5-2: Statistical analysis of band 1-3 of satellite imagery data in different resolutions

Resolution	Band1		Band2		Band3	
	Mean	Std. Dev.	Mean	Std. Dev.	Mean	Std. Dev.
5m	44.81	9.78	26.48	9.70	71.66	12.62
30m	44.81	9.59	26.47	9.43	71.66	12.00
90m	44.76	8.55	26.46	8.53	71.65	10.52
250m	44.78	7.40	26.38	6.72	71.61	8.62

The simulated satellite imagery data were affected by average-based aggregation in two forms; first, value of a pixel in coarser resolution was average of all corresponding pixels in finer resolution. Therefore, mean value of a pixel in coarser resolution was likely close to the spectral value that frequently occurred. As about 36% of the whole watershed was covered with agriculture and 64% was covered with other five land use/cover classes, the averaging caused a very high conversion of other classes to agriculture in coarser resolutions. Figure 5-6 pictorially sums up the aforementioned discussions; obviously can be seen that in 250m resolution all classes were changed to agriculture. This conversion was occurred because agriculture was the dominant class in 5m resolution; therefore, average value of the pixel in 250m resolution was close to spectral value of agriculture.



Figure 5-6: Conversion of different classes to dominant class

Second, pixels with a very high (or very low) spectral value in different bands were disappeared in the coarser resolutions. It means the range of values in the entire map reduced and became closer to the average value. By disappearing pixels with very high or very low spectral values, consequently forest and bare that had maximum and minimum spectral values disappeared and converted to the other classes. Therefore, area covered by bare and forest reduced about 50% and respectively 75% in 250m resolution.



Figure 5-7: Conversion of different classes to a non-dominant class

The average-based aggregation did not only affect pixels with very high or very low values, but due to averaging a new class could be generated that did not exist in fine resolution any more. Figure 5-7 clearly illustrates this effect.

Two important factors can intensify these two effects; first, the patch size and fragmentation of land use/cover classes, second, spectral characteristics of dominant class. Patch size and fragmentation influence mainly the first effect; the smaller patch size and more fragmentation, the higher conversion of land use/cover classes to each other. Whereas spectral characteristic of the dominant class refers primarily to the second effect; a dominant class with minimum and maximum spectral values would not show the same response to changes of spatial resolution like a class with spectral values close to mean. For instance, average base aggregation of a dominant class like forest does not show significant changes like agriculture (Nelson, et al., 2009).

5.2 Effect of Majority-Base Aggregation on Classification

This section is devoted to analyse the effect of majority-based aggregation on classification.

5.2.1 Classification results

Figure 5-9 presents the effect of majority-based aggregation on land use/cover map in 5m resolution. It clearly shows a considerable increase of agricultural area by decreasing the resolution. Figure 5-8 shows that covered area by agriculture increased from 36% in 5m resolution to 53% in 250m resolution, area of degraded forest also increased slightly from 26% in 5m resolution to 31% in 250m resolution. By increasing the aggregation rate, forest and grassland converted to other classes widely; up to 50% of covered area by forest and 70% of covered area by grassland, whereas the bare and orchard remained with only 1% change approximately constant at 6% and respectively 11%.

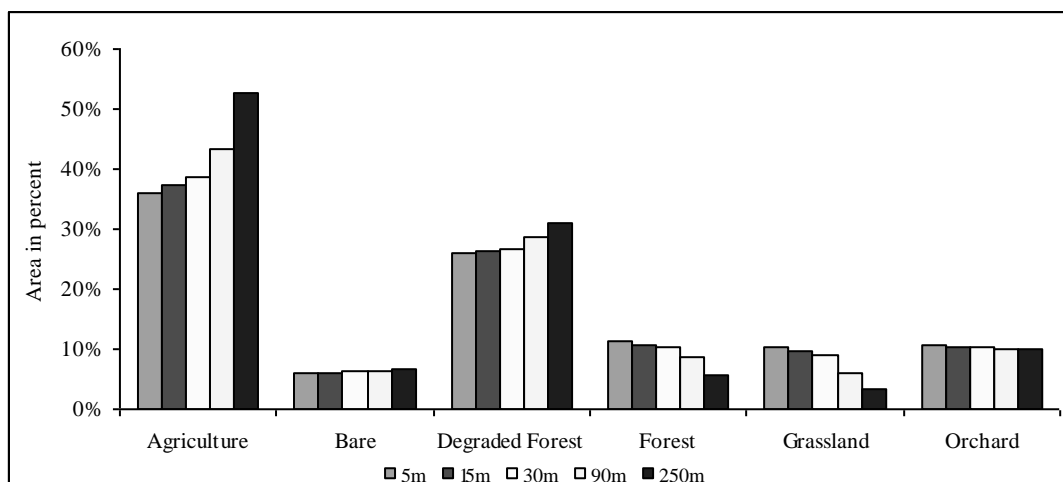


Figure 5-8: Covered area by different land use/cover classes in different resolutions (Appendix V-16)

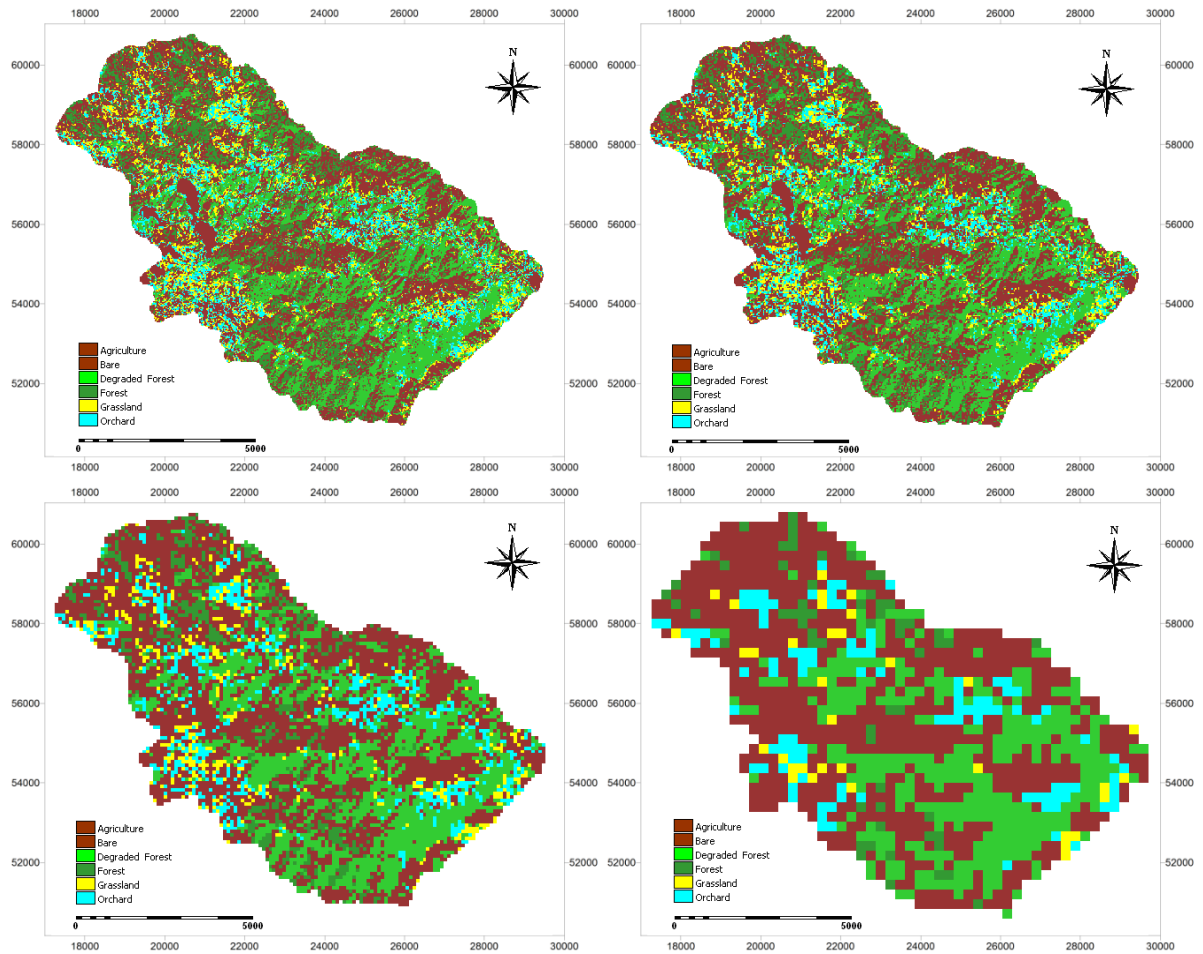


Figure 5-9: Majority-base aggregation of land use/cover map in 5m resolution to 15m, 30m, 90m, and 250m

High conversion of other classes to agriculture was because of its dominance in the study area, degraded forest increased approximately 5% as well, because it was also second dominant class. Fragmentation and patch size of land use/cover classes are the only factors that affect the result of majority-based aggregation; it can aggravate the effect of dominant class in aggregation. In areas with low fragmentation of land use/cover classes, aggregation has slight effect, conversely in areas with high fragmentation and small patch size of land use/cove classes, aggregation can cause significant changes. In the study, forest and especially grassland were fragmented a lot, therefore by aggregating to coarser resolutions they converted increasingly to the other classes.

5.2.2 Accuracy assessment and statistical analysis

As illustrated in Figure 5-10, the accuracy of maps reduced from 80% in 15m resolution to fewer than 50% in 250m, also the Kappa coefficient reduced from over 0.70 to 0.30.

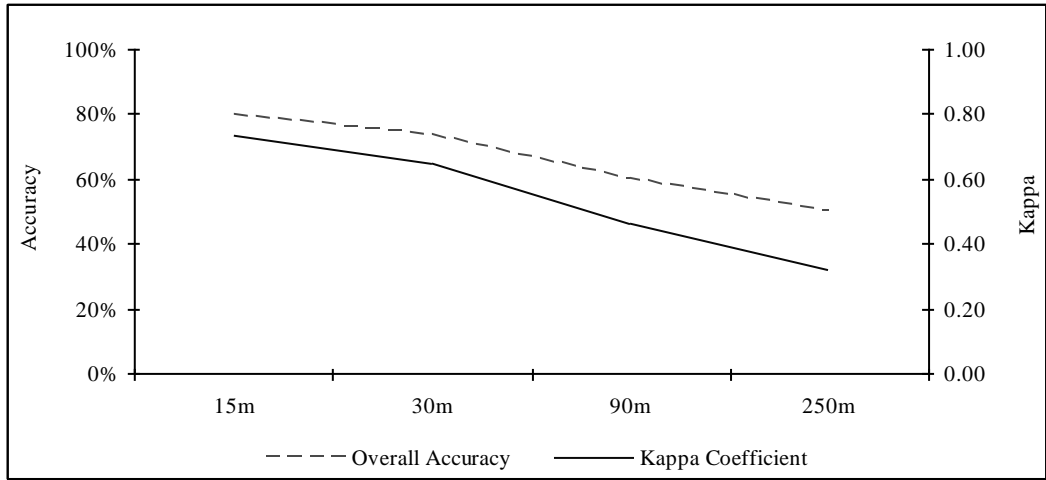


Figure 5-10: Overall accuracy and Kappa coefficient of classification maps (Appendix V)

Agriculture had the minimum Kappa while the bare had the maximum kappa (Figure 5-11). Low reliability of agriculture by increasing the cell size, was because of the high conversion of other classes to agriculture. Higher producer's accuracy of agriculture and degraded forest show the high classification quality of agriculture and degraded forest (Figure 5-12).

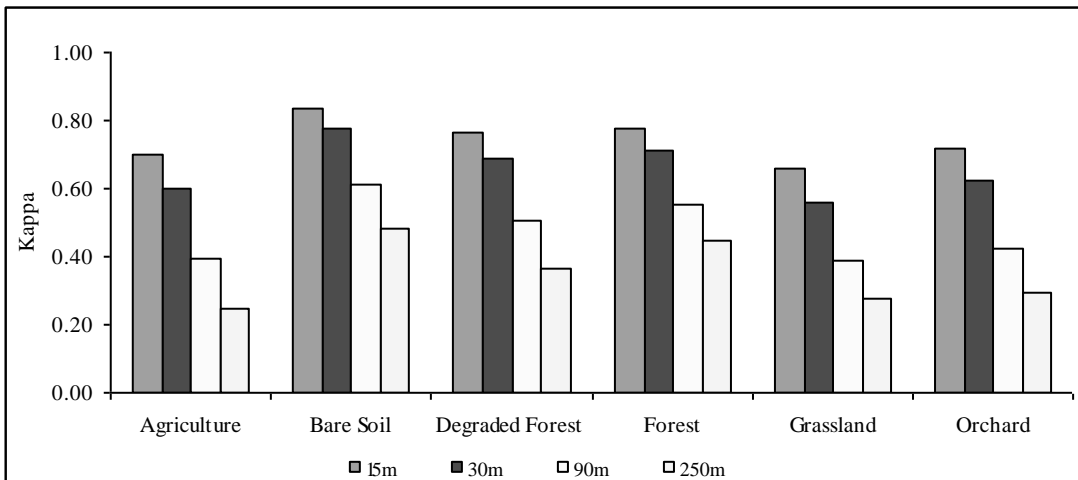


Figure 5-11: Kappa coefficients of individual classes in different resolutions (Appendix V)

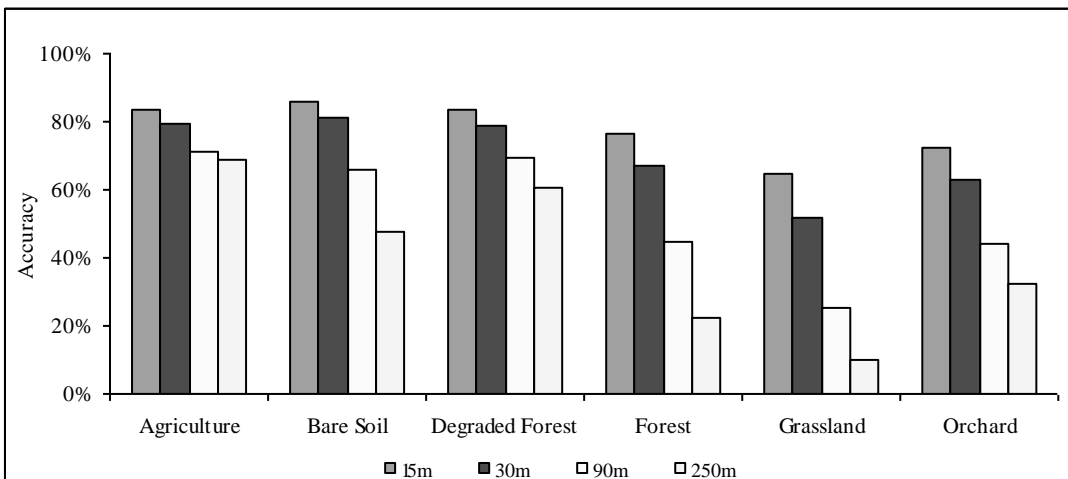


Figure 5-12: Producer's accuracy (Appendix V-23)

5.3 Effect of Spatial Resolution of Satellite Imagery Data on soil Erosion

In erosion assessment, land use/cover maps play an important role while different land use/cover classes have different erosion rates. Indeed, the spatial resolution of satellite imagery data affects the erosion assessment indirectly through land use/cover maps. In this section, by using the land use/cover maps derived from simulated satellite images in different resolutions, the effect of spatial resolution on erosion assessment was evaluated.

5.3.1 Soil erosion results

Figure 5-13 presents the erosion maps, which have been derived from simulated satellite images in different spatial resolutions (5m, 30m, 90m, and 250m). To assess the accuracy of erosion maps in 30m, 90m, and 250m resolutions, the created map in 5m resolution was regarded as ground truth (Section 4.2.5.5).

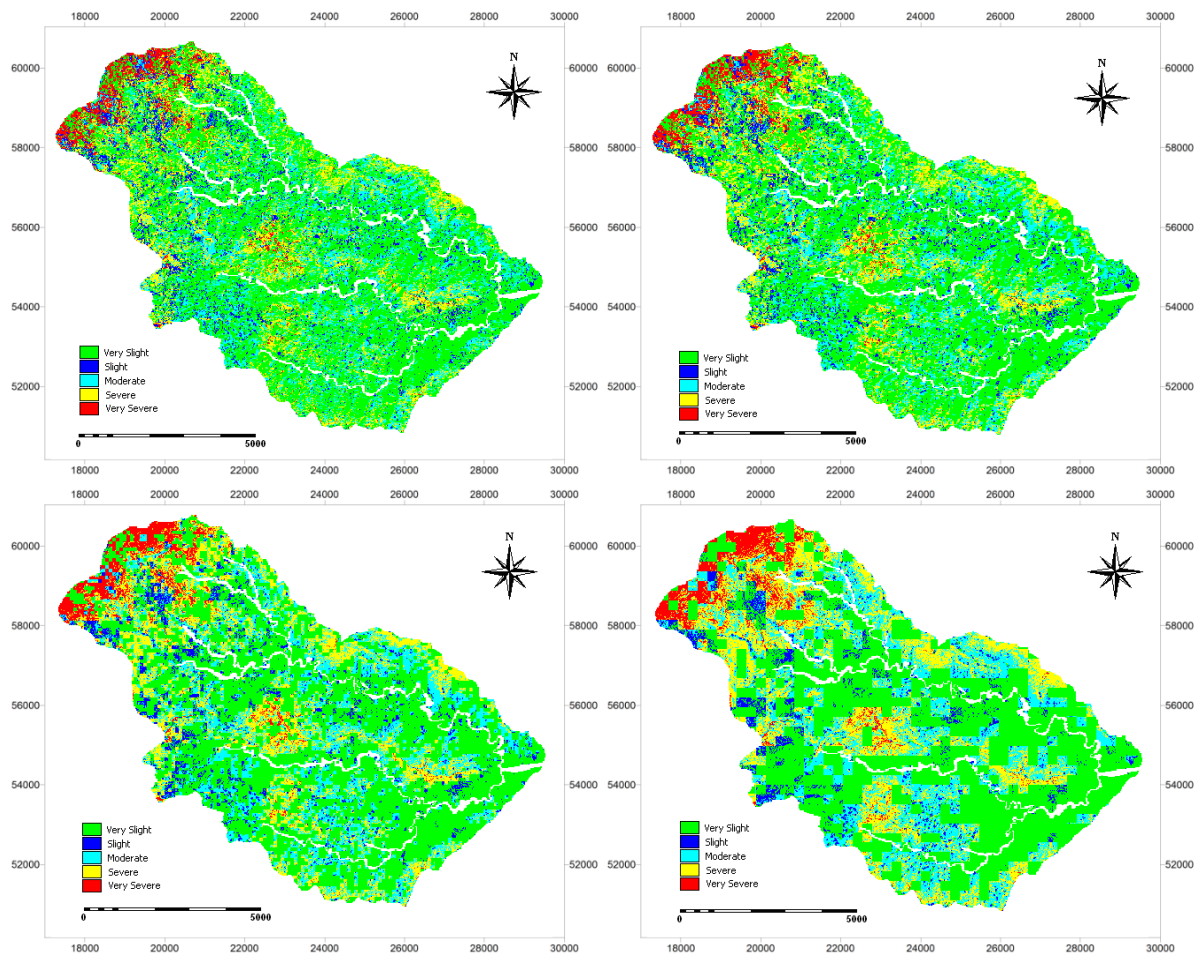


Figure 5-13: Erosion maps created from simulated satellite images

By increasing the resolution, the average annual soil loss of different land use/cover classes remained almost constant. Agriculture had the highest erosion rate with 2.47 kg/m^2 per year while the lowest erosion rate was for the forest with 0.04 kg/m^2 per year in 5m resolution (Appendix VI-27).

Figure 5-14 also shows that by decreasing the spatial resolution of satellite images, areas categorized into very slight and slight erosion classes, to some deal decreased; respectively areas with very severe and severe erosion rate increased. Altogether in coarser resolutions of satellite imagery data, the erosion is to some extent overestimated.

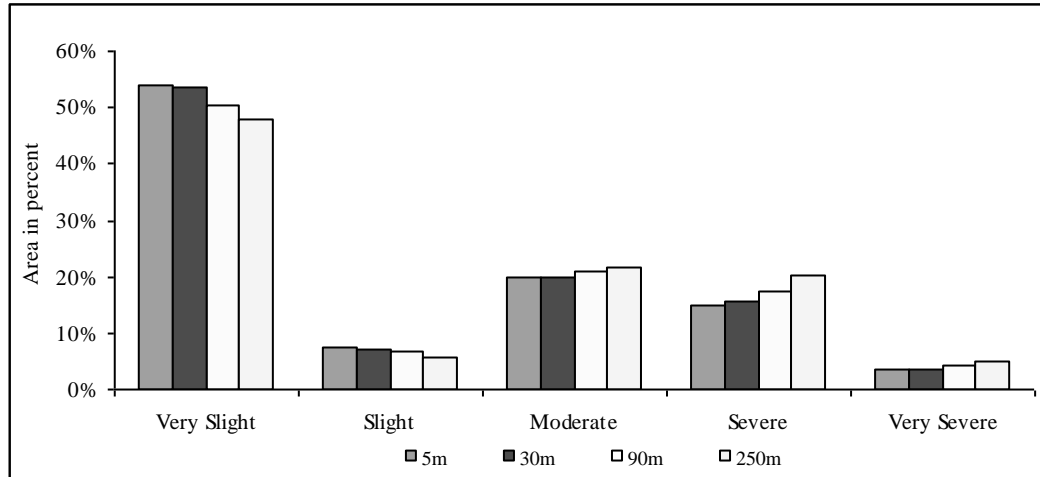


Figure 5-14: Fraction of erosion classes in different resolutions (Appendix VI-28)

5.3.2 Accuracy assessment and statistical analysis

Figure 5-15 figures out the overall accuracy and kappa coefficient of created erosion maps. The accuracy of maps reduced from 80% in 30m resolution to 60% in 250m, consequently kappa coefficient reduced from 0.70 to 0.40.

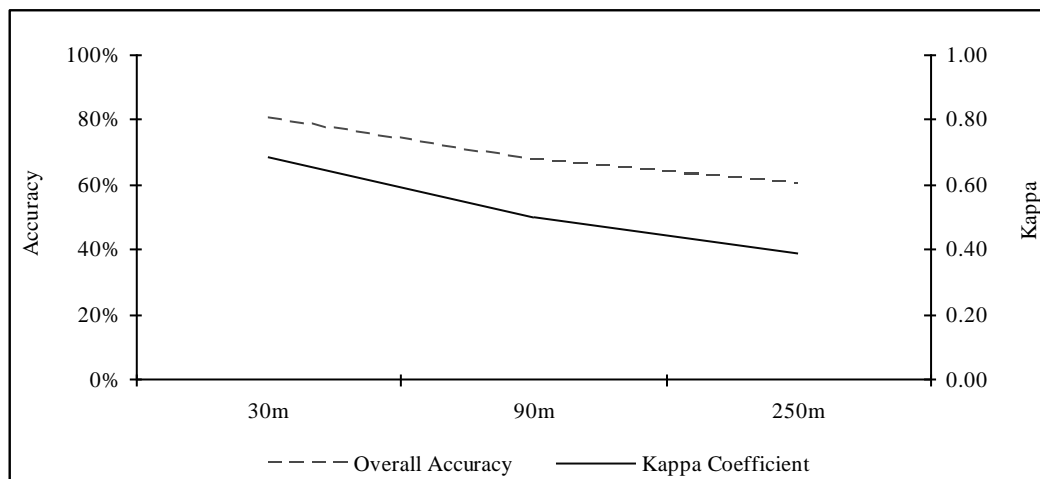


Figure 5-15: Overall accuracy and kappa coefficient of erosion maps (Appendix VI)

The individual kappa coefficients in Figure 5-16 followed the same trend like the overall accuracy and kappa coefficient. Figure 5-16 and 5-17 show the effect of spatial resolution of satellite images on the conversion of the erosion classes. According to the Figures 5-16 and 5-17 and confusion matrix of erosion maps in different resolutions (Appendix VI), as the spatial resolution became coarser, the erosion classes were progressively converted to each other. Most conversions appeared between the

classes that had completely different erosion rates, for instance from very slight to very severe or from severe to very slight. However, the general trend of conversions was from classes with lower erosion rate to the classes with higher erosion rate. The main reason behind these changes was the conversion of land use/cover classes with different erosion rates to each other; for instance from forest (very low erosion rate) to agriculture (very high erosion rate). Regarding to the high conversion of land use/cover classes to agriculture in coarser resolutions (Section 5.1.1), the general trend in overestimation of erosion could be justified. It means depends on changes in land use/cover map due to resolution, the predicted erosion results could be overestimated, underestimated, or remained constant.

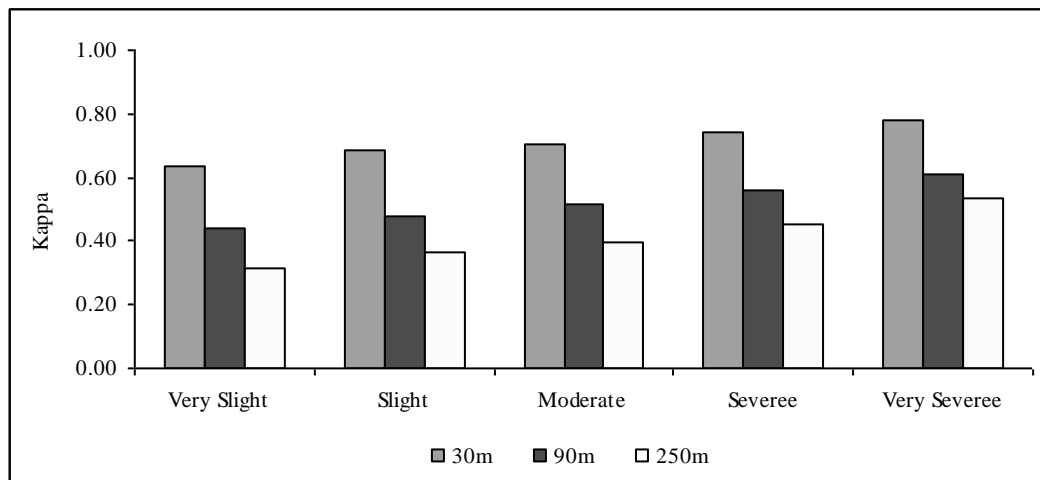


Figure 5-16: Kappa coefficients of individual classes in different resolutions (Appendix VI)

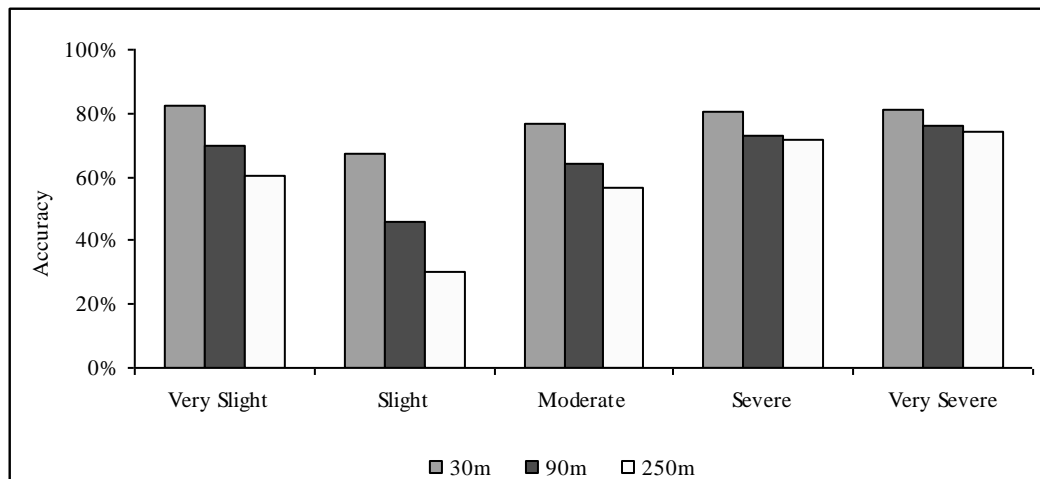


Figure 5-17: Producer's accuracy (Appendix VI-30)

Results of the RMSE and RRMSE calculation of the erosion maps derived from satellite images in different resolutions are listed in Table 5-3. The smaller RMSE and RRMSE value, the more accurate is the erosion map. According to the Table 5-3, there was an upward trend in RMSE and RRMSE in coarser resolutions.

Table 5-3: RMSE and RRMSE of erosion maps derived from simulated satellite images

Resolution	RMSE (kg/m ² /y)	RRMSE
30m	1.09	0.94
90m	1.40	1.21
250m	1.59	1.37

5.3.3 Analyse of results

Results showed that the RMMF model is not very sensitive to the land use/cover map; although the predicted erosion was slightly overestimated, but Figure 5-13 demonstrates, that the spatial pattern of erosion maps in coarser resolutions even in 250m resolution coincided with the 5m resolution. It means for decision makers who want to assess erosion at regional or global scale, images with even 250m resolution can still give reasonable results. However, in some cases (e.g. at field scale) that detailed erosion assessment results are needed, the conversion of erosion classes to each other, which occur mostly between completely different erosion rates, should be taken into account. Since it can make the soil conservation activities ineffective; areas that have a high erosion problem might be shown as problem-free and areas that do not have any serious erosion problem might be categorized as very severe erosion. In these cases, choosing satellite images 30m spatial resolution or finer are more reasonable. However, a very important factor that has direct effect on accuracy of the predictions is fragmentation and patch size of land use/cover classes in the study area; the smaller patch size and more fragmentation, the less accurate erosion map. In addition, the erosion rate of land use/cover classes can aggravate or improve accuracy of spatial resolution on erosion assessments, the more similar erosion rate of land use/cover classes, the more accurate soil loss predictions.

5.4 Effect of DEM Resolution on slope map

Slope is a topographic feature that can affect soil erosion significantly. In general, areas with high degree of slope have more erosion than areas that are flat. Slope map derives from DEM, therefore an adequate selection of DEM resolution is an important factor for success of soil erosion assessment. To achieve a general accepted view about the effect of DEM resolution on erosion assessment, in this section it is tried to find out the effect of DEM resolution on slope map.

5.4.1 Slope maps in different resolutions

The created slope maps from DEMs in different resolutions were categorized into five slope classes (Sapkota, 2008). Figure 5-18 shows that classified area in different slope classes in 5m, 15m and 30m resolutions remained almost constant (less than 5% change), whereas in 90m and 250m resolutions the classes categorized in higher slope degrees, significantly converted to the classes with lower slope degrees.

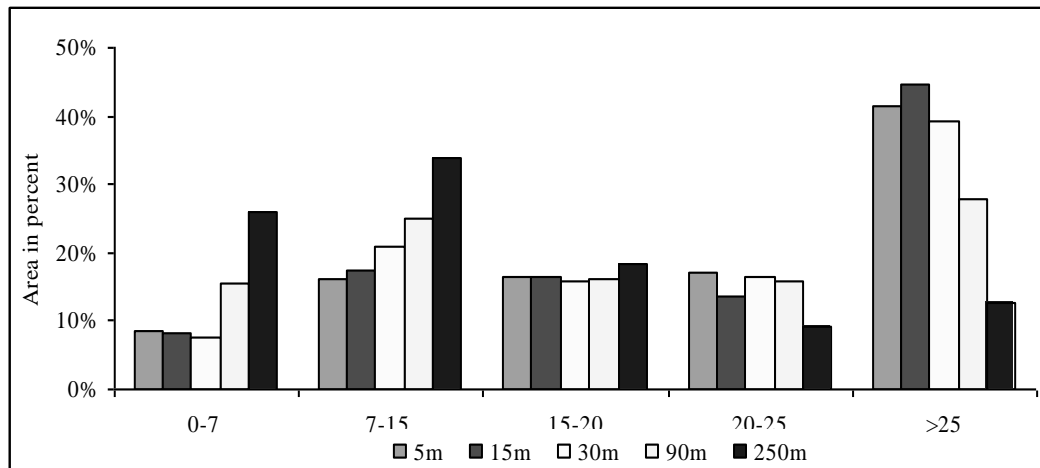


Figure 5-18: Effect of resolution on Slope (Appendix VII-35)

In Table 5-4, some descriptive statistical calculations are listed; as the DEM resolution became coarser, the average slope and maximum slope values reduced substantially, while, the standard deviation slightly increased in 30m resolution and then decreased significantly in coarser resolutions. Indeed, by changing the DEM resolution, the slopes and the distribution of slopes will change. In other words, when DEM is coarser, the topographic features of the watershed are smoother.

Table 5-4: Namchun watershed Slope values for different resolutions

	5m	15m	30m	90m	250m
Average slope	48.67	32.87	26.24	26.12	15.24
Standard deviation	15.13	15.14	16.23	11.79	9.52
Minimum slope	0	0	0	0	0
Maximum slope	74.37	69.88	70.01	59.94	45.32

5.4.2 Accuracy assessment and statistical analysis

As illustrated in Figure 5-19 the overall accuracy and Kappa coefficient of slope maps are very sensitive to the resolution, hence the accuracy reduced from 60% in 15m resolution to 20% in 250m resolution. In addition, kappa coefficient reduced from 0.40 in 15m resolution to under 0.10 in 250m resolution. The kappa coefficient of individual classes followed the same trend (Figure 5-20). The results showed that the individual kappa coefficient of the steepest slope class (>25) in 90m and 250m resolutions was considerably higher than the other classes. These values indicated high reliability of this class; low conversion of the other classes to steepest slope class in coarser resolutions, whereas Figure 5-18 shows substantial conversion of steepest class to the smoother classes.

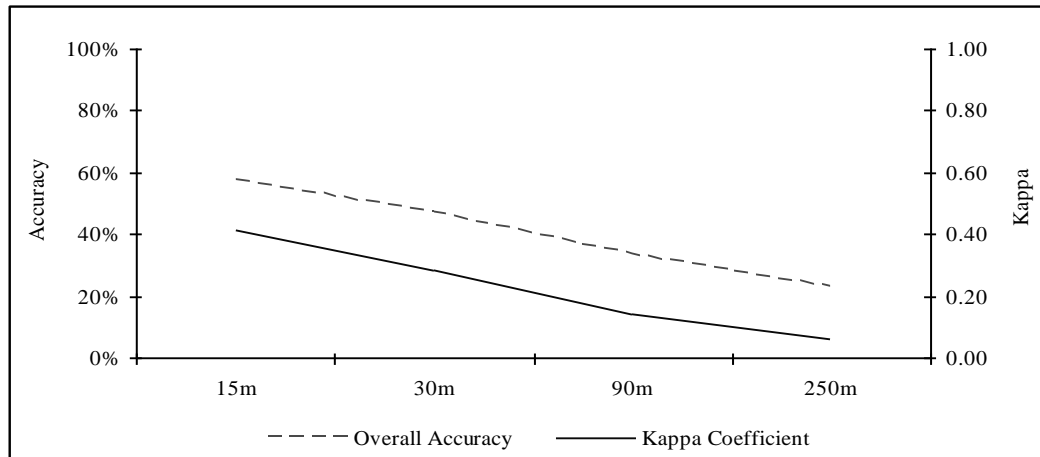


Figure 5-19: Overall accuracy and kappa coefficient of different slope maps (Appendix VII)

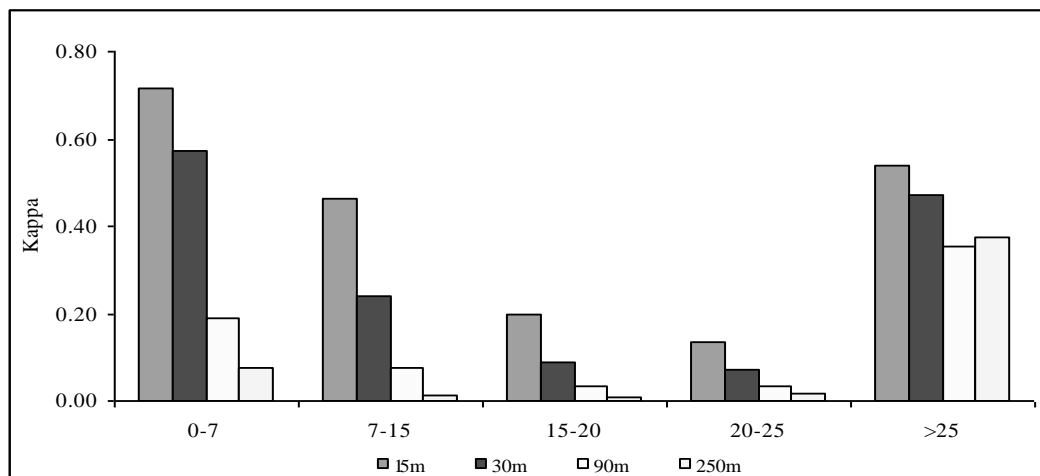


Figure 5-20: Kappa coefficients of individual classes in different slope maps (Appendix VII)

Results of the RMSE and RRMSE assessment of the slope gradient maps are presented in Table 5-5. The smaller RMSE and RRMSE value, the more accurate is the slope map. According to the Table 5-5, there was an upward trend in RMSE and RRMSE in coarser resolutions.

Table 5-5: RMSE and RRMSE of slope gradient maps

Resolution	RMSE (°)	RRMSE
Slope 15m	7.70	0.34
Slope 30m	9.45	0.41
Slope 90m	12.52	0.55
Slope 250m	15.30	0.67

5.4.3 DEM Cross section

DEMs in coarser resolutions represent changes of the elevation less than reality. In very coarse resolutions like 250m, it might happen that small hills disappear. In mountainous areas, where in a rather short distance elevation changes very sharp, the problem is worse. To visualize the changes of DEM in different spatial resolutions, along A-B line (from (720490.22, 1853590.5) to (720490.22,

1860755.5)) the variation of elevation was illustrated. A-B line was selected, as along this line, the elevation varies between 400m and 1000m in a rather short distance (Figure 5-21).

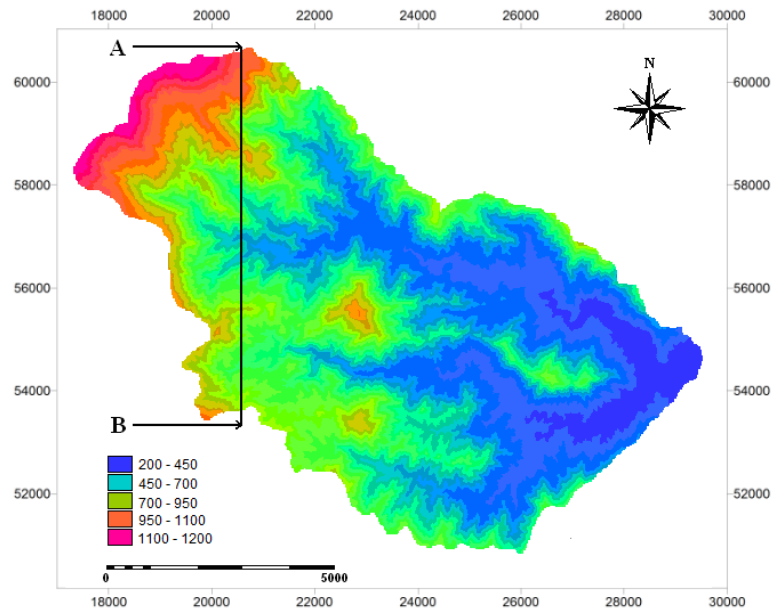


Figure 5-21: Cross section line (A-B)

Figures 5-22 and 5-23 clearly display the changes of DEM in different spatial resolutions. Especially in 90m and 250m resolutions, the changes were very tangible.

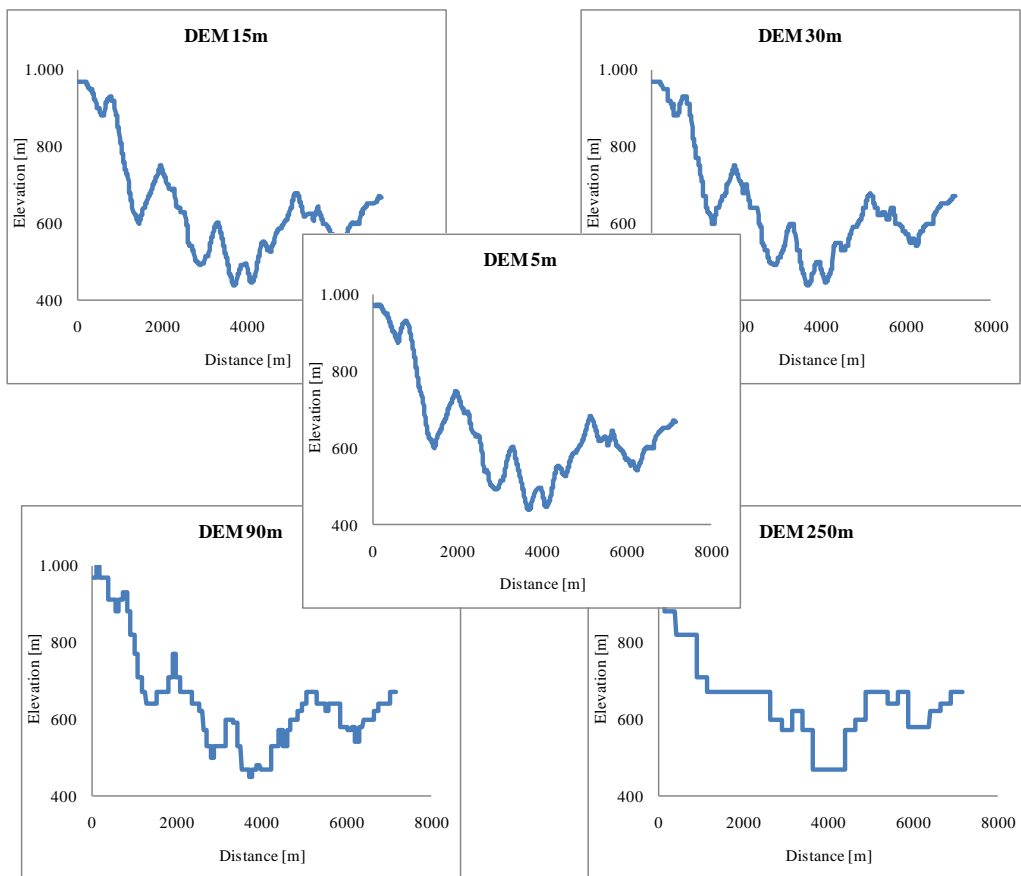


Figure 5-22: DEM cross sections

A detailed cross section of DEMs in different resolutions from (720490.22, 1859770.5) to (720490.22, 1859320.5) is demonstrated in Figure 5-23; the figure proves the resolution effects on DEM.

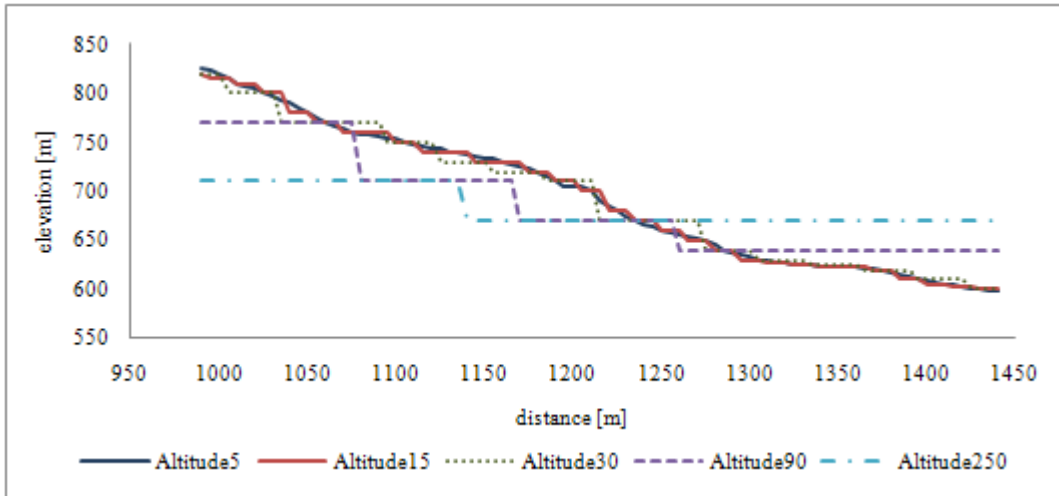


Figure 5-23: DEM cross section in zoom view

5.5 Effect of DEM Resolution on soil Erosion

According to the research objectives, in this section, it is tried to analyse the effect of DEM resolution on erosion assessment.

5.5.1 Soil erosion results

The created erosion maps from DEMs in 15m, 30m, 90m, and 250m resolutions are illustrated in Figure 5-25. In general, by decreasing the DEM resolution, areas categorized as very slight and slight erosion slightly increased, whereas areas categorized as very severe and severe erosion moderately decreased; which proved the underestimation of erosion in coarser resolutions (Figure 5-24).

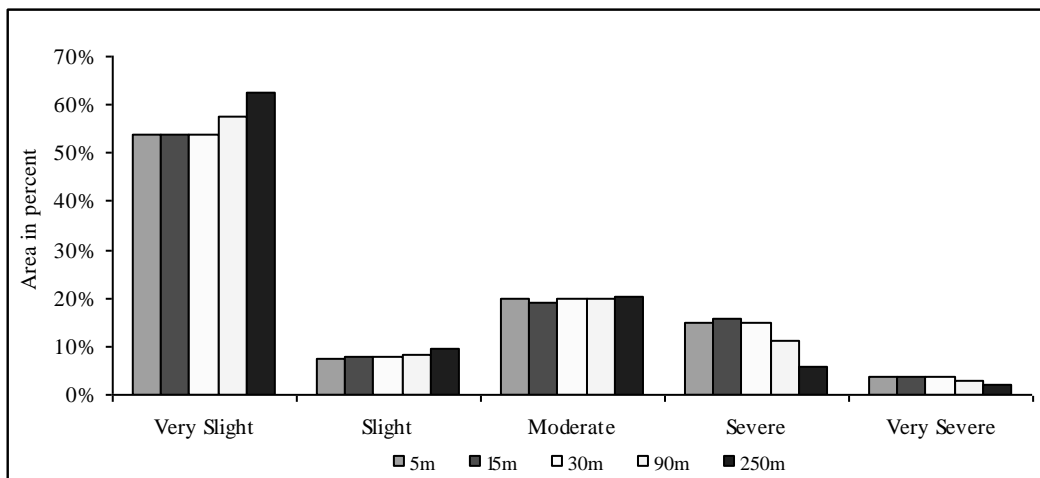


Figure 5-24: Fraction of erosion classes in each resolution (Appendix VIII-41)

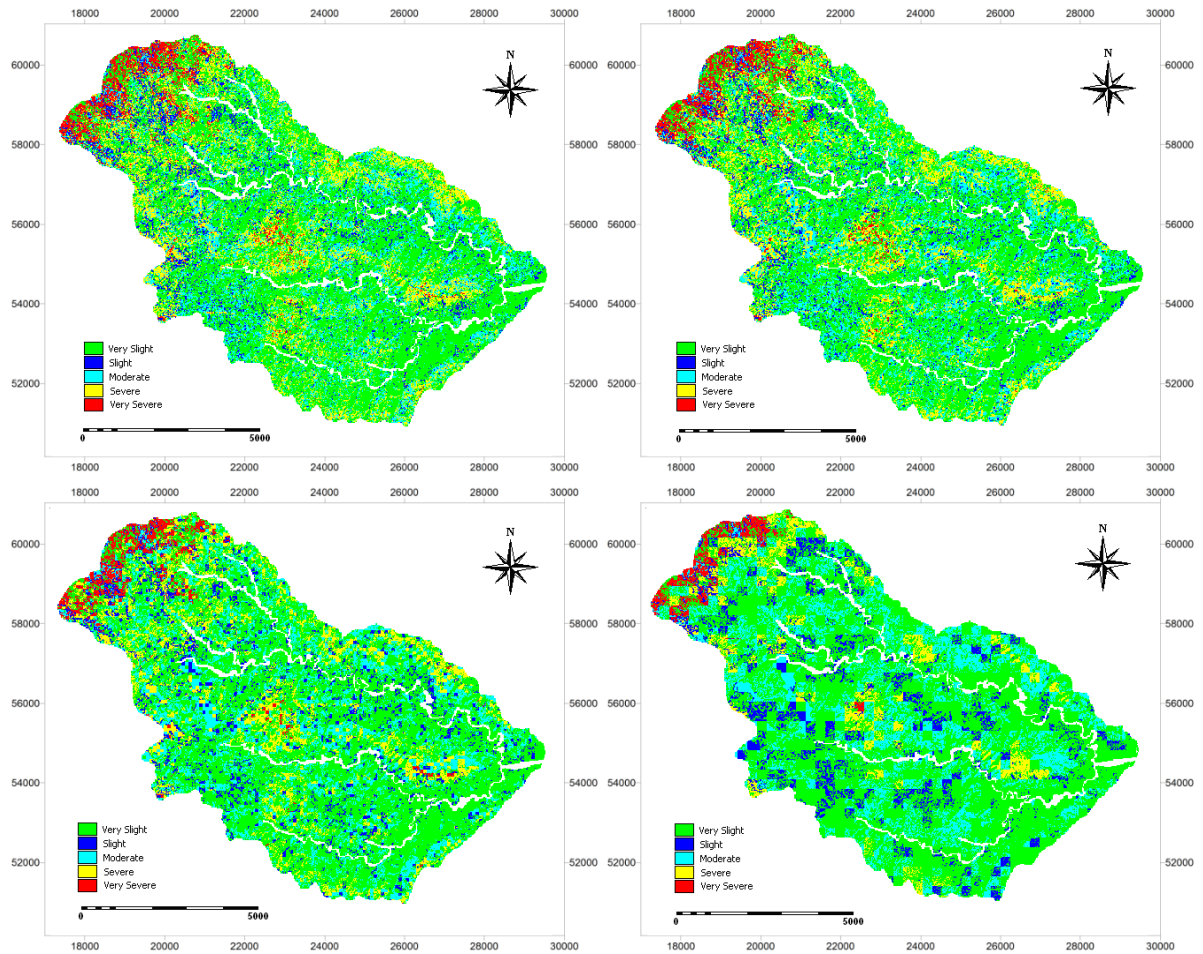


Figure 5-25: Erosion maps created from DEM in 15m, 30m, 90m, and 250m resolutions

By decreasing the DEM resolution, the average annual soil loss of different land use/cover classes also decreased in 90m and 250m resolutions; in 90m resolution the underestimation was 15% and in 250m resolution 35% (Appendix VIII-42).

5.5.2 Accuracy assessment and statistical analysis

By comparing the erosion maps in 15m, 30m, 90m, and 250m resolution -which were categorized into five erosion classes- with the erosion map in 5m resolution, following results were achieved; the overall accuracy reduced from 85% in 15m resolution to approximately 70% in 250m resolution. The kappa coefficient followed the same trend; it decreased subsequently from 0.80 in 15m resolution to under 0.50 in 250m resolution (Figure 5-26).

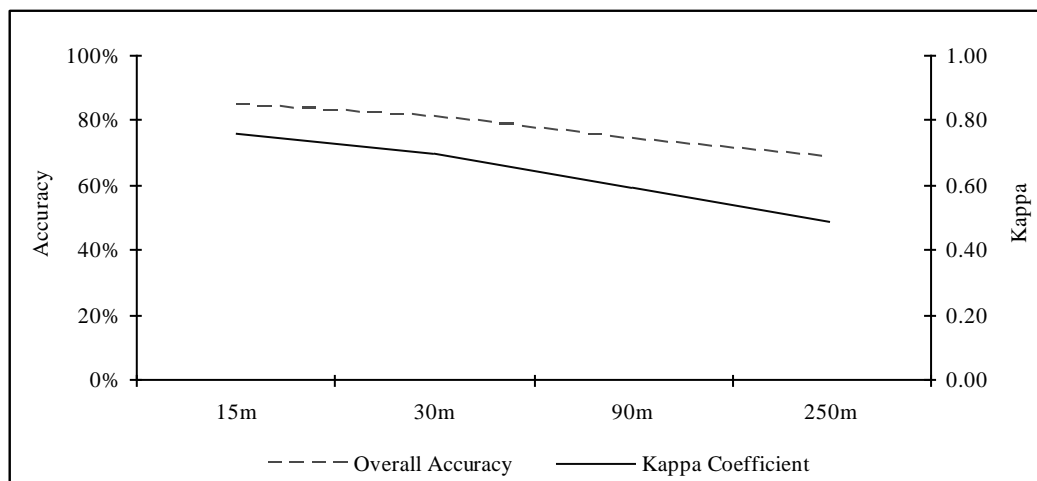


Figure 5-26: Overall accuracy and kappa coefficient of erosion maps (Appendix VIII)

Figure 5-27 and Figure 5-28 make it apparent that very slight class had the highest individual kappa and producer’s accuracy while slight had the lowest individual kappa and producer’s accuracy among all classes. The producer’s accuracy of the very slight class indicates that less than 5% of this class was converted to the other classes in all resolutions. However, the reliability of the very slight reduced gradually to under 70% in 250m resolution, which shows the conversion of other erosion classes to very slight. The effect of DEM resolution on severe and very severe classes was very different; especially in 90m and 250m resolution, they changed substantially to lower rate erosion classes. According to the results; most of the conversions in erosion classes occurred between classes that had almost the same erosion rate, for example from very severe to severe, or from moderate to slight. The underlying cause of these conversions was the smoothing of the slope map in coarser resolutions, which the steeper slope classes were converted to the smoother slope classes.

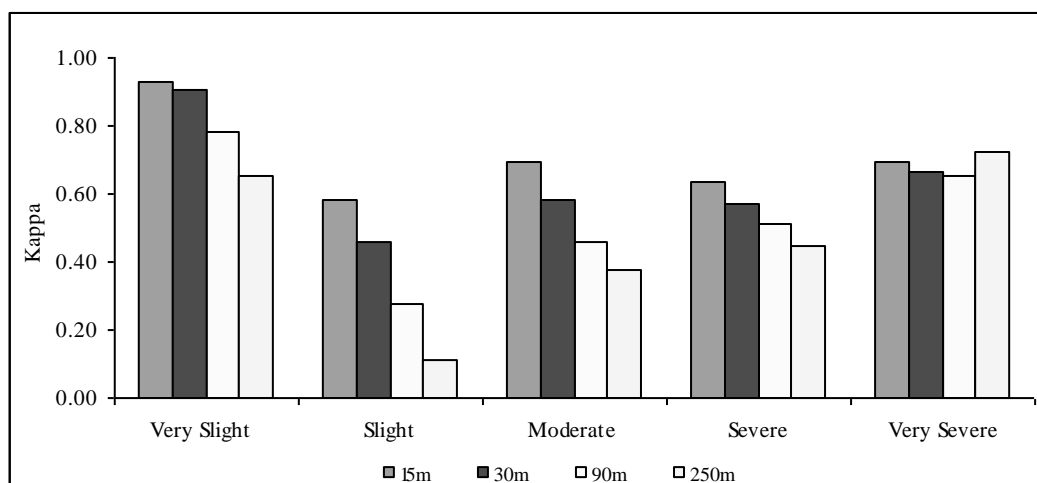


Figure 5-27: Kappa coefficients of individual classes in different resolutions (Appendix VIII)

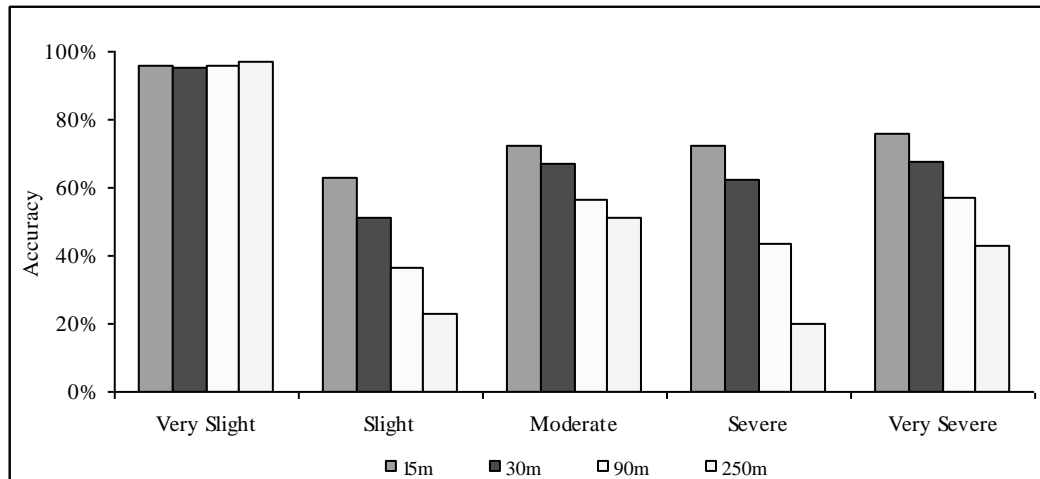


Figure 5-28: Producer's accuracy (Appendix VIII-44)

Results of the RMSE and RRMSE assessment of erosion maps derived from different DEMs are listed in Table 5-6. The results of RMSE and RRMSE show also the same trend in decreasing accuracy of the erosion maps by decreasing the resolution of DEM.

Table 5-6: RMSE and RRMSE of erosion maps derived from DEMs

Resolution	RMSE (kg/m ² /y)	RRMSE
15m	0.49	0.42
30m	0.59	0.51
90m	0.76	0.66
250m	0.97	0.84

By comparing the results of Table 5-6 with the results of Table 5-3, can be observed that the RMSE and RRMSE of derived erosion maps from satellite imagery data in different resolutions are relatively higher than derived erosion maps from DEMs in different resolutions. The main reason was; by decreasing the spatial resolution of satellite imagery data, most conversions appeared between the classes that had completely different erosion rates, while as DEM became coarser, most conversions occurred between the classes that had almost the same erosion rates.

5.5.3 Analyse of results

According to Figure 5-18 and Table 5-4, interpretation of results is possible; Figure 5-18 shows that in 90m and 250m resolutions the portion of slope, which had a range between 0° and 15° increased dramatically, accordingly the portion of slopes higher than 20° decreased significantly. Table 5-4 also shows that the average slope reduced from 49° in 5m resolution to 15° in 250m resolution. Indeed, by changing the DEM resolution, the slopes and the distribution of slopes will change. In other words, when DEM is coarser, the topographic features of the watershed are smoother, which in turn affect the soil erosion prediction.

Although more than 60% of the study area has a slope more than 20°, but Figure 5-25 demonstrates, that the spatial pattern of erosion maps in coarser resolutions even in 250m resolution conforms very well to the 5m resolution. It means for decision makers who want to assess erosion at regional or global scale, DEMs with coarser resolutions such as SRTM DEM can still give reasonable results.

5.6 Discussion

Finally, this section is devoted to have an overall view on all acquired results.

By decreasing the spatial resolution through spatial averaging, the spectral details of satellite images were combined, therefore the variance in the image reduced. Similarly, Henderson-Sellers and Pitman (1992), Marceau, et al., (1994a, b), and Nelson, et al., (2009) reported that as spatial resolution became coarser, mean spectral values remains almost constant and variances decrease.

According to the results, progressive conversion of land use/cover classes to each other in coarser resolution of satellite data reduced the accuracy of the classification results. Most of the conversions were from non-dominant classes to the dominant class (agriculture). Two important factors intensified these conversions; first, spectral characteristics of dominant class, second, the patch size and fragmentation of land use/cover classes in the study area. The high heterogeneously of land use/cover classes along with small patch sizes caused a significant increase in covered area by agriculture. The results coincide with the works of Mayaux and Lambin (1995), and Marceau (1994a). Moody and Woodcock (1994,1995) and Turner, et al., (1989) found that the classes that are smaller with more inter-patch distances are decreased while the classes, which are larger and more clustered, are increased. Similarly, Pax-Lenny and Woodcock (1997) revealed that in coarser resolutions agricultural fields, which are in smaller size patches cause lower accuracy in the land use/cover classification while agricultural fields in larger size patches cause higher accuracy in the classification maps. The results of this study showed, although by using satellite images in coarser resolutions soil erosion was slightly overestimated, but the RMMF model is not sensitive to the land use/cover factor; the spatial pattern of erosion maps in coarser resolutions even in 250m resolution approximately coincided with 5m resolution. Therefore, for stakeholders who want to assess erosion at regional scale, MODIS images at 250m resolution still can give reasonable results.

By increasing the cell size, average slope, maximum slope, and standard deviation decreased. This is also reported by Gerrard and Robinson (1971), Fahsi (1989), Chang and Tsai (1991), Wolock and Price (1994), Zhang and Montgomery (1994), Thielen, et al., (1999), Molnar and Julien (2000), and Zhang, et al., (2008). Coarser DEMs resulted in less accurate slope maps. This is in agreement with the findings of Chang and Tsai (1991), Gao (1998), and Kienzle (2004). In addition, the distribution of slope maps derived from coarser DEM resolutions was different from those in finer resolutions. This finding is consistent with the observation of Molnar and Julien (2000). Although, using DEM data in different resolutions affected the output of the erosion model, the large-scale patterns of predicted soil

erosion in coarser resolutions were similar to those with fine resolution DEM. This result is in agreement with the findings of Renschler and Harbor (2002) that used WEPP model to predict soil erosion and sediment yield and Vente, et al., (2009), which compared the quality and performance of remote sensing data for soil erosion and sediment yield modelling at regional scale with the WATEMSEDEM model in South East Spain. The results of the study implies that it may not be necessary to produce costly, fine resolution DEMs data for application of erosion models at regional scale; but freely available SRTM data could be an appropriate choice to assess erosion with acceptable results, which is also recommended by Vente, et al., (2009).

Fragmentation and patch size of land use/cover classes are the only factors that affect the result of majority-based aggregation; it can aggravate the effect of dominant class in aggregation. In areas with low fragmentation of land use/cover classes, aggregation has slight effect, conversely in areas with high fragmentation and small patch size of land use/cove classes, aggregation can cause significant changes. In the study, forest and especially grassland were fragmented a lot, therefore by aggregating to coarser resolutions they converted increasingly to the other classes. Similarly, Nelson (2009) reported that majority-based aggregation, resulted in overestimation of forest proportion in a heavily forested area and underestimation of forest proportion in a sparsely forested area.

Although in this study it was tried to analyse the effect of DEM and satellite imagery data resolution on erosion assessment separately, but interaction between topographic features and Land use/cover factor is another term that can affect soil erosion assessment significantly. So it is strongly recommended to analyse the effect of DEM and satellite imagery data resolution on erosion assessment simultaneously, so that it can provide a framework to disclose the reliability of erosion assessments using freely available data such as the combination of MODIS images (250m) and SRTM DEMs (90m).

6 CONCLUSION AND RECOMMENDATION

6.1 Conclusion

The following conclusions can be drawn from this study:

The effect of spatial aggregation of ASTER image (average-based aggregation) on land use/cover classification was a significant decrease in accuracy and kappa coefficient especially in 250m resolution. By decreasing the spatial resolution, land use/cover classes were considerably converted to each other. Two factors can aggravate the effect of resolution on classification; first, patch size and fragmentation of land use/cover classes and second, spectral characteristics of the dominant class in different bands. The smaller patch size and more fragmentation of land use/cover classes, the higher conversion of land use/cover classes to each other. Spectral values closer to mean spectral value in different bands cause more conversion of non-dominant classes to dominant class. According to the results, ASTER or Landsat images can be used to obtain an accurate land use/cover map in the study area.

Majority-based aggregation of land use/cover also caused a considerable decrease in accuracy and kappa coefficient of classification results especially in 250m resolution. By decreasing the spatial resolution, land use/cover classes were considerably converted to the dominant class, since in majority-based aggregation only one factor can affect the conversion rate; patch size and fragmentation of land use/cover classes.

There was an upward trend in the RMSE and RRMSE of slope maps in coarser resolutions. Indeed by changing DEM resolution, the slopes and the distribution of slopes have changed within the watershed; the average slope, standard deviation, and maximum slope values reduced as DEM resolution became coarser, in other words the topographic features of the watershed were smoothed.

Although by using satellite images in coarser resolutions soil erosion was slightly overestimated, the spatial pattern of soil erosion in coarser resolutions even in 250m resolution approximately coincided with the finest resolution. These results revealed that the RMMF model is not sensitive to the land use/cover factor, so it is feasible to use freely available MODIS images with 250m resolution in erosion assessment.

Namchun watershed is a mountainous area with more than 60% steep slope ($>20^\circ$), nevertheless the spatial pattern of soil erosion by using DEM in coarser resolutions even in 90m conformed very well to the finest resolution. This implies that it may not be necessary to produce costly, fine resolution DEMs to assess soil erosion at regional scale, available SRTM could be an appropriate choice with acceptable results.

6.2 Limitations

The main limitation of the study was the availability of data for running the model. The used climate data could not realistically represent the spatial variability of the rainfall in the study area.

Most of the input parameters for running the model were obtained from the literature or previous MSc thesis that might affect soil erosion assessment. Another limitation for running the model; the land use/cover parameters were only specified for five land use/cover classes, while different vegetation types have different protective effects against soil erosion.

Although, the Spectral Angle Mapper (SAM) algorithm assumes reflectance data as input image for classification, but in the study the radiance data was used to classify satellite images.

Due to the lack of control erosion plots in the study area, quantitative validation of the annual soil loss prediction was not possible.

This study was carried out without any fieldwork, so the reliability of the results depends on the quality of provided data.

6.3 Recommendations

Most of the input parameters for running the RMMF model were obtained from literature. Therefore, to increase the reliability of results more field measurements are suggested.

To improve the classification results, it is recommended to use reflectance data for Spectral Angle Mapper (SAM) algorithm. Another recommendation is to consider more than one image for classification to extract more appropriate training points.

Although there was no erosion data available for qualitative soil assessment, but field measurements are necessary to validate the erosion results in different resolutions comprehensively.

REFERENCES

- Allan, R., Förstner, U. & Salomons, W., 2007. *Climate and Land Degradation*. Berlin, Heidelberg: Springer-Verlag.
- Amare Kassa, S., 2007. *Modelling runoff and soil erosion using the revised MMF model : a case study in Namchun watershed, Thailand*. M.Sc. Enschede: ITC.
- Atkinson, P.M., and Curran, P.J., 1995. Defining an optimal size of support for remote sensing investigations. *IEEE Transactions on Geoscience and Remote Sensing*, 33, pp.768–776.
- Bamutaze, Y., 2003. *Comparative study of soil erosion modelling in Lom Kao - Phetchabun, Thailand*. M.Sc. Enschede: ITC.
- Bennett, J.P., 1974. Concepts of mathematical modelling of sediment yield. *Water Resources Research*, 10, pp.485–492.
- Beven, K., 1995. Linking parameters across scales: Subgrid parameterizations and scale-dependent hydrological models. *Hydrological Processes*, 9(5–6), pp.507–525.
- Bishop, Y., Fienberg, S. & Holland, P., 1975. *Discrete Multivariate Analysis Theory and Practice*. Massachusetts: MIT Press.
- Boardman, J.W., 1992. *SIPS User's Guide Spectral Image Processing System*. Version 1.2. Boulder: Center for the Study of Earth from Space.
- Bocco, G., Palacio, J.L., Valenzuela, C.R., 1991. Gully erosion modelling using GIS and geomorphological knowledge. *ITC Journal*, (3), pp.253– 261.
- Bocco, G., Valenzuela, C.R., 1993. Integrating satellite remote sensing and Geographic Information Systems technologies in gully erosion research. *Remote Sensing Reviews*, pp.7233– 7240.
- Bolstad, P.V., Stowe, T., 1994. An evaluation of DEM accuracy: elevation, slope, and aspect. *Photogrammetric Engineering & Remote Sensing*, 60, pp.1327–1332.
- Bowles, D.S. & O'Connell, P.E., 1991. *Recent Advances in the Modelling of Hydrological Systems*. Dordrecht: Kluwer Academic. Ch. 20.
- Chang, K.T., Tsai, B.W., 1991. The effect of DEM resolution on slope and aspect mapping. *Cartography and Geographic Information Systems*, 18, pp.69–77.
- Congalton, R., Oderwald, R., Mead, R., 1983. Assessing Landsat classification accuracy using discrete multivariate statistical techniques. *Photogrammetric Engineering and Remote Sensing*, 49(12), pp.1671-1678.
- De Roo, A.P.J., 1996. *Soil erosion assessment using GIS*. Geographical information systems in hydrology, Kluwer, Boston, pp.339–356.
- DeGroot, M.H., 1980. *Probability and Statistics*. 2nd ed. Addison-Wesley.
- De Vente, J., Poesen, J., 2005. Predicting soil erosion and sediment yield at the basin scale: scale issues and semi-quantitative models. *Earth-Science Reviews*, 71(1–2), pp.95–125.
- De Vente, J., Poesen, J., Govers, G., Boix-Fayos, C., 2009. The implications of data selection for regional erosion and sediment yield modelling. *Earth Surface Processes and Landforms*, 34, 1994–2007.
- Eswaran, H., Lal, R., Reich, P.F., 2001. Land degradation: an overview. Bridges, E.M., Hannam, I.D., Oldeman, L.R., Penning de Vries, F.W.T., Scherr, S.J., Sombatpanit, S. (Eds.), *Response to Land Degradation*. Science Publishers Inc, Enfield, NH, USA, pp.20– 35.
- Fahsi, A., 1989. *The effect of spatial resolution of digital elevation model data on map characteristics*. M.Sc. Boise: University of Idaho.

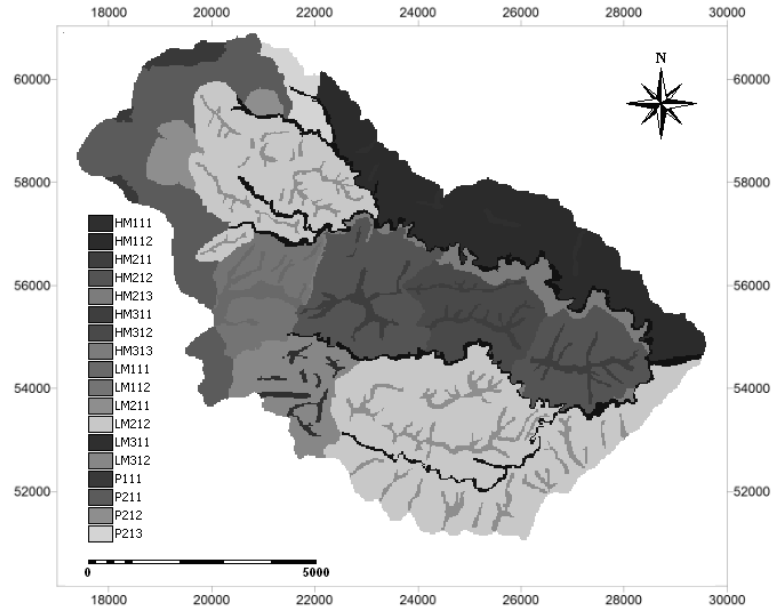
- FAO, 1994. Land degradation in South Asia: it's severity, causes and effects upon the people. World Soil Resources Reports: FAO; 78. FAO, Rome.
- Fenstermaker, L., 1991. A proposed approach for national to global scale error assessments. Proceedings GIS/LIS '91, ASPRS, ACSM, AAG, AM/FM International and URISA. 1, pp. 293-300.
- Florinsky, I.V., 1998. Accuracy of local topographic variables derived from digital elevation models. International Journal of Geographical Information Systems, 12, pp.47-61.
- Forshaw, M.R.B., Haskell, A., Miller, P.F., Stanley, D.J., Townshend, J.R.G., 1983. Spatial resolution of remotely sensed imagery: a review paper. International Journal of Remote Sensing, 4, pp.497-520.
- Gao, J., 1998. Impact of sampling intervals on the reliability of topographic variables mapped from grid DEMs at a micro-scale. International Journal of Geographical Information Systems, 12, pp.875-890.
- Gerrard, A.J.W., Robinson, D.A., 1971. Variability in slope measurement: a discussion of the effects of different recording intervals and micro relief in slope studies. Transactions, Institute of British Geographers, 54, pp.45-54.
- Henderson-Sellers, A., Pitman, A.J., 1992. Land-surface schemes for future climate models: specification, aggregation and heterogeneity. Journal of Geophysical Research, 97, pp.2687-2696.
- Jensen, J.R., 1986. Introductory Digital Image Processing. Prentice-Hall, Englewood Cliffs, New Jersey.
- Jenson, S.K., Domingue, J.O., 1988. Extracting topographic structure from digital elevation data for geographic information system analysis. Photogrammetric Engineering and Remote Sensing, 54, pp.1593-1600.
- Jetten, V., de Roo, A., Favis-Mortlock, D., 1999. Evaluation of field-scale and catchment-scale soil erosion models. CATENA, 37(3-4), pp.521-541.
- Jetten, V., Govers, G., and Hessel, R., 2003. Erosion models: quality of spatial predictions. John Wiley & Sons, 17, pp.887-900.
- Ju, J., Gopal, S., Kolaczyk, E.D., 2005. On the choice of spatial and categorical scale in remote sensing land cover classification. Remote Sensing of Environment, 96, pp.62-77.
- Justice, C.O., Markham, B.L., Townshend, J.R.G., Kennard, R.L., 1989. Spatial degradation of satellite data. International Journal of Remote Sensing, 10, pp.1539-1561.
- King, C., Delpont, G., 1993. Spatial assessment of erosion: contribution of remote sensing, a review. Remote Sensing Reviews 7, pp.223- 232.
- King, R.C., Baker, M.E., Whigham, D.F., Weller, D.E., Jordan, T.E., Kazyak, P.F., Hurd, M.K., 2005. Spatial considerations for linking watershed land cover to ecological indicators in streams. Ecological Applications, 15(1), pp.137-153.
- Kienzle, S., 2004. The effect of DEM raster resolution on first order, second order and compound terrain derivatives. Transactions in GIS, 8, pp.83-111.
- Kruse, F.A., Lefkoff, A.B., Boardman, J.B., Heidebrecht, K.B., Shapiro, A.T., Barloon, P.J., Goetz, A.F.H., 1993. The Spectral Image Processing System (SIPS) - Interactive Visualization and Analysis of Imaging spectrometer Data. Remote Sensing of the Environment, 44, pp.145-163.
- Kumar, A.B., Dwivedi, R.S., Tiwari, K.N., 1996. The effects of image scale on delineation of eroded lands using remote sensing data. International Journal of Remote Sensing, 17(11), pp.2135-2143.

- Kuriakose, S.L., van Beek, L.P.H., van, Westen, C.J., 2009. Parameterizing a physically based shallow landslide model in a data poor region. *Earth Surface Processes and Landforms*, 34(6), pp.867–881.
- Lal, R.e., 1994. *Soil erosion: research methods*. Delray Beach, Ankeny: St. Lucie Press; Soil and Water Conservation Society.
- Lal, R.e., 1998. *Methods for assessment of soil degradation*. Advances in soil science, series: 14. Boca Raton: CRC Press.
- Lal, R.e., 2001. Soil degradation by erosion. *Land Degradation & Development*, 12(6), pp.519 – 539.
- Langran, K.J., 1983. Potential for monitoring soil erosion features and soil erosion modelling components from remotely sensed data. *Proceedings of IGARSS'83*. IEEE, San Francisco, CA, pp.2.1– 2.4.
- Loch, R.J., 2000. Effects of vegetation cover on runoff and erosion under simulated rain and overland flow on a rehabilitated site on the Meandu Mine, Tarong. *Australian Journal of Soil Research* 38(2), pp.299 - 312.
- Macmillan, R.A., Martin, T.C., Earle, T.J., McNabb, D.H., 2003. Automated analysis and classification of landforms using high-resolution digital elevation data: application and issues. *Canadian Journal of Remote Sensing*, 29, pp.592–606.
- Marceau, D.J., Howarth, P.J., Gratton, D.J., 1994a. Remote Sensing and the Measurement of Geographical Entities in a Forested Environment. 1. The Scale and Spatial Aggregation Problem. *Remote Sensing Environment*, 49, pp.93-104.
- Marceau, D.J., Howarth, P.J., Gratton, D.J., 1994b. Remote sensing and the measurement of geographical entities in a forest environment. 2: The optimal spatial resolution. *Remote Sensing of Environment*, 49, pp.105–117.
- Margate, D.E., Shrestha, D.P., 2001. The Use of Hyperspectral Data in Identifying “DESERT-LIKE” Soil Surface Features in Tabernas Area, Southeast Spain. *The 22nd Asian Conference on Remote Sensing*. Singapore 5-9 November 2001. CRISP, SISV, AARS.
- Mayaux, P., Lambin, E.F., 1995. Estimation of tropical forest area from coarse spatial resolution data: a two-step correction function for proportional errors due to spatial aggregation. *Remote Sensing of Environment*, 53, pp.1–15.
- Merritt, W.S., Letcher, R.A., Jakeman, A.J., 2003. A review of erosion and sediment transport models. *Environmental Modelling & Software*, 18(8-9), pp.761-799.
- Molnar, D.K., Julien, P.Y., 2000. Grid size effects on surface runoff modeling. *Journal of Hydrological Engineering*, 5(1), pp.8–16.
- Moody, A., Woodcock, C.E., 1994. Scale-dependent errors in the estimation of landcover proportions: implications for global land-cover datasets. *Photogrammetric Engineering and Remote Sensing*, 60, pp.585–594.
- Moody, A., Woodcock, C.E., 1995. The influence of scale and the spatial characteristics of landscapes on land-cover mapping using remote sensing. *Landscape Ecology*, 10(6) pp.363-379.
- Morgan, R.P.C., 1995. *Soil Erosion And Conservation*. 2nd edn, Malaysia: Longman.
- Morgan, R.P.C., 2001. A simple approach to soil loss prediction: a revised Morgan-Morgan-Finney model. *Catena* 44, pp.305-322.
- Morgan, R.P.C., 2005. *Soil erosion and conservation*. Harlow: Longman.
- Nelson, M.D., McRoberts, R.E., Holden, G.R., Bauer, M.E., 2009. Effects of satellite image spatial aggregation and resolution on estimates of forest land area. *International Journal of Remote Sensing*, 30(8), pp.1913-1940.
- Patanakanog, B., Shrestha, D.P., Saengthongpinit, C., Sapet, A., Farshad, A., 2004. Land use change and land degradation: a case study in Nam Chun subwatershed in Thailand. *Proceedings of the*

- 25th Asian conference on remote sensing. Chiang Mai, Thailand November 22-26, 2004. Geo-Informatics and Space Technology Development Agency (GISTDA), pp.1384-1389.
- Pax-Lenny, M., Woodcock, C.E., 1997, The effects of spatial resolution on the ability to monitor the status of agricultural lands. *Remote Sensing of Environment*, 61, pp.210–220.
- Prachansri, S., 2007. Analysis of soil and land cover parameters for flood hazard assessment: a case study of the Nam Chun watershed, Phetchabun, Thailand. M.Sc. Enschede: ITC.
- Qu, J.J., Gao, W., Kafatos, M., Murphy, R.E. & Salomonson, V.V., 2006. *Earth science satellite remote sensing: Data, computational processing, and tools*. Beijing: Springer-Verlag.
- Quattrochi, D.A. & Goodchild, M.A., 1997. *Scale in remote sensing and GIS*. Boca Raton: CRC Press.
- Quinn, P., Beven, K., Chevallier, P., Planchon, O., 1991. The prediction of hillslope flow paths for distributed hydrological modelling using digital terrain models. *Hydrological Processes*, 5(1), pp.59–79.
- Renschler, C.S., Harbor, J., 2002. Soil erosion assessment tools from point to regional scales – the role of geomorphologists in land management research and implementation. *Geomorphology* 47(2–4), pp.189–209.
- Richards, J.A., 1999. *Remote Sensing Digital Image Analysis*. Berlin: Springer-Verlag.
- Rojas, R., Velleux, M., Julien, P.Y., ASCE, M., Johnson, B.E., 2008. Grid Scale Effects on Watershed Soil Erosion Models. *Journal of Hydrologic Engineering*, 13(9), pp.793-802.
- Rosenfield, G., Fitzpatrick-Lins, K., 1986. A coefficient of agreement as a measure of thematic classification accuracy. *Photogrammetric Engineering and Remote Sensing*, 52(2), pp.223-227.
- Saengthongpinit, C., 2004. Soil erosion assessment using revised MMF equations with special reference to terrain parameter(s): a case study in Nam Chun sub - watershed, Lomsak district. Thailand. M.Sc. Enschede: ITC.
- Sapkota, R., 2008. Modelling Runoff and Erosion in Numchun Watershed, Thailand. M.Sc.Thesis. M.Sc. Enschede: ITC.
- Sasowski, K.C., Petersen, G.W., Evans, B.M., 1992. Accuracy of SPOT digital elevation model and derivatives: utility for Alaska's north slope. *Photogrammetric Engineering & Remote Sensing Photogramm*, 58, pp.815–824.
- Shanti, K., 2003. *Remote Sensing and GIS in watershed area management*. Institute of Environmental Management, ESPS/DANIDA.
- Siakeu, J., Oguchi, T., 2000. Soil erosion analysis and modelling: a review. *Transactions of the Japanese Geomorphological Union* 21(4), pp.413–429.
- Shrestha, D.P., 1997. Soil erosion modelling. *ILWIS 2.1 for Windows: Applications Guide*, Chapter 24 (pp. 323-341). Enschede: ITC.
- Shrestha, D.P., Zink, J.A., 2001. Land use classification in Mountainous areas: integration of image processing, digital elevation data and field knowledge (application to Nepal). *International Journal of Applied Earth Observation and Geoinformation*, 3(1), pp.78-85.
- Singh, R., Phadke, V.S., 2006. Assessing soil loss by water erosion in Jamni River Basin, Bundelkhand region, India, adopting universal soil loss equation using GIS. *Current Science* 90(10), pp.1431-1435.
- Solomon, H., 2005. GIS based surface runoff modeling and analysis of contributing factors: a case study of Nam Chun watershed, Thailand. M.Sc. Enschede: ITC.
- Suriyaprasit, M., 2008. Digital terrain and image processing for assessing erosion prone areas. M.Sc. Enschede: ITC.
- Swain, P.H. & Davis, S.M., 1978. *Remote Sensing: The Quantitative Approach*. New York: McGraw-Hill.

- Townshend, J.R.G., Justice, C.O., 1988. Selecting the spatial resolution of satellite sensors required for global monitoring of land transformations. *International Journal of Remote Sensing*, 9, pp.187–236.
- Thicken, A.H., Lucke, A., Diekkruger, B., Richter, O., 1999. Scaling input data by GIS for hydrological modeling. *Hydrological Processes*, 13, pp.611–630.
- Turner, M.G., O’neill, R.V., Gardner, R.H., Milne, B.T., 1989. Effects of changing spatial scale on the analysis of landscape pattern. *Landscape Ecology*, 3, pp.153–162.
- Usery, E.L., Finn, M.P., Scheidt, D.J., Ruhl, S., Beard, T., Bearden, M., 2004. Geospatial data resampling and resolution effects on watershed modeling: A case study using the agricultural non-point source pollution model. *Journal of Geographical Systems*, 6, pp.289–306.
- Van Rompaey, A.J.J., Govers, G., 2002. Data quality and model complexity for regional scale soil erosion prediction. *Geomorphology* 16 (7), 663– 680.
- Vigiak, O., Okoba, B.O., Sterk, G., Groenenberg, S., 2005. Modelling catchment-scale erosion patterns in the East African Highlands. *Earth Surface Processes and Landforms*, 30, pp.183–196.
- Vrieling, A., 2006. Satellite remote sensing for water erosion assessment, a review. *Catena*, 65, pp.2–18.
- Wang, M., Hjelmfelt, A.T., Garbrecht, J., 2000. DEM aggregation for watershed modeling. *Journal of the American Water Resources Association*, 36(3), pp.579–584.
- Wheater, H.S., Jakeman, A.J., Beven, K.J., 1993. Progress and directions in rainfall-runoff modelling. In: Jakeman, A.J., Beck, M.B., McAleer, M.J. (Eds.), *Modelling Change in Environmental Systems*. John Wiley and Sons, Chichester, pp.101–132.
- Wilson J.P. & Gallant J.C., 2000. *Terrain Analysis, Principles and Applications*. New York: John Wiley.
- Wischmeier, W.H. & Smith, D.D., 1978. Predicting rainfall erosion losses. *USDA Agricultural Research Service Handbook* 537.
- Wolock, D.M., Price, C.V., 1994. Effects of digital elevation model map scale and data resolution on a topography-based watershed model. *Water Resource Research*, 30(11), pp.3041–3052.
- Yu, Z., 1997. Grid-spacing effect on watershed hydrologic simulations. *Hydrological Science Technology*, 13(1–4), pp.75–85.
- Zhang, W., Montgomery, D. R., 1994. Digital elevation model grid size, landscape representation, and hydrologic simulations. *Water Resource Research*, 30(4), pp.1019–1028.
- Zhang, J.X., Chang, K.T., Qiong, WU, J., 2008. Effects of DEM resolution and source on soil erosion modelling: a case study using the WEPP model. *International Journal of Geographical Information Science*, 22(8), pp.925–942.

APPENDIX I – MODEL INPUTS



Appendix 1: Geopedological soil map of Namchun watershed (Solomon, 2005).

Appendix 2: Description of the soil legend

Landscape	Relief	Lithology	Landform	Soils	Map unit	Area (Ha)
Plateau (P)	Cuesta (P1)	Sand Stone (P11)	Undifferentiated		(P111)	72
	Escarpment (P2)	Sand Stone (P21)	Scarp	Typic Haplustalts	(P211)	730
			Talus		(P212)	136
			Undulating Slope Complex		(P213)	100
High Mountain (HM)	Ridge (HM1)	Andesite (HM11)	Summit		(HM111)	34
			Slope Complex	Ultic Haplustalts	(HM112)	900
	Ridge (HM2)	Andesitic Tuff (HM21)	Summit	Lithic Haplustolls	(HM211)	112
			Middle Slope	Ultic Haplustalts	(HM212)	800
			Foot Slope	Ultic Haplustalts	(HM213)	94
	Erosional Glacis (HM3)	Andesitic and Rhyolitic Tuff (HM31)	Summit	Lithic Haplustalts	(HM311)	52
			Middle Slope	Typic Paleustalts	(HM312)	325
			Foot Slope	Lithic Haplustalts	(HM313)	68
Low Mountain (LM)	High Ridges (LM2)	Andesitic Tuff (LM21)	Summit	Ultic Haplustalts	(LM211)	271
			Middle Slope	Ultic Haplustalts	(LM212)	1,968
	Moderately High Ridges (LM1)	Andesitic and Rhyolitic Tuff (LM11)	Summit	Typic Haplustalts	(LM111)	80
			Middle Slope	Ultic Haplustalts	(LM112)	286
	Low Ridges (LM3)	Andesitic and Rhyolitic Tuff (LM31)	Summit	Typic Dystrustepts	(LM311)	45
			Middle Slope	Ultic Haplustalts	(LM312)	308
Valley (V)		Alluvial Colluvial	Side slope/bottom complex	Fluvents and Haplumbrepts	(V111)	8

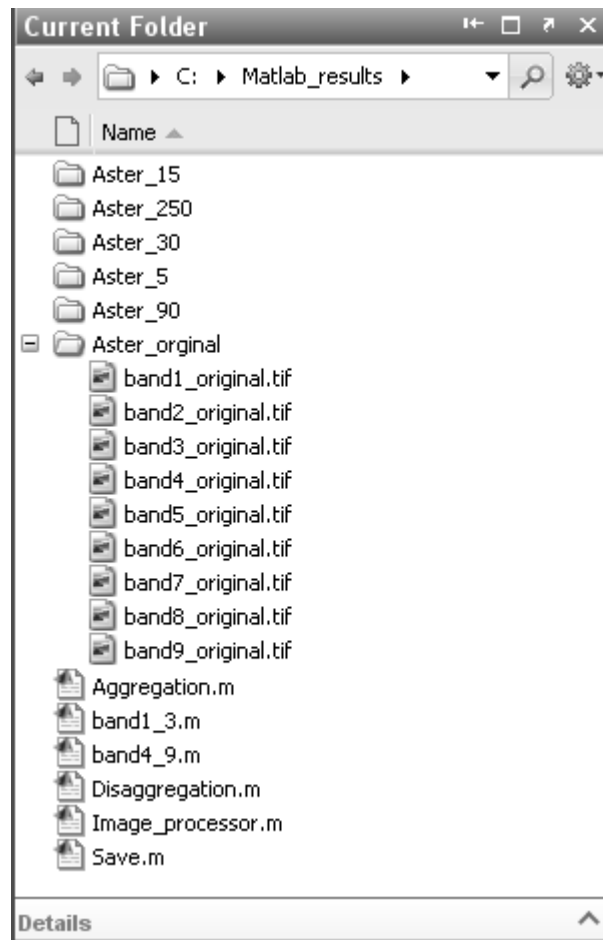
Appendix 3: Soil Parameters (Sapkota, 2008).

Class	MS	BD	K	COH
HM111	0.25	1.3	0.70	10.0
HM112	0.25	1.3	0.21	10.5
HM211	0.25	1.3	0.73	7.7
HM212	0.25	1.3	0.61	9.6
HM213	0.25	1.3	0.47	10.6
HM311	0.25	1.3	0.70	3.0
HM312	0.25	1.3	0.44	10.3
HM313	0.25	1.3	0.66	10.0
LM111	0.25	1.3	0.33	11.0
LM112	0.25	1.3	0.54	10.5
LM211	0.25	1.3	0.75	6.5
LM212	0.25	1.3	0.67	8.0
LM311	0.25	1.3	0.50	10.0
LM312	0.25	1.3	0.14	11.7
P111	0.25	1.3	0.28	11.0
P211	0.25	1.3	0.29	9.8
P212	0.25	1.3	0.50	10.0
P213	0.25	1.3	0.50	10.0

Appendix 4: Land use parameters in the RMMF model (Sapkota, 2008)

Land cover	A	E_t/E_0	C	CC	GC	PH	EHD
Forest	0.250	0.900	0.002	0.820	0.910	19.400	0.200
Degraded Forest	0.250	0.800	0.010	0.350	0.500	14.950	0.160
Agriculture	0.250	0.500	0.200	0.490	0.370	1.800	0.080
Grassland	0.350	0.650	0.080	0.930	0.950	1.500	0.100
Orchard	0.200	0.700	0.050	0.310	0.500	7.300	0.080

APPENDIX II – MATLAB CODES



Appendix 5: C:\Matlab code organization

After creating all folders like Appendix 5, open the “Image_processor.m” file and run the model.

Appendix 6: MATLAB Codes; 1. Aggregation.m 2. Band1_3.m 3. Band4_9.m 4. Disaggregation.m 5.

Image_processor.m 6. Save.m

```
%Aggregation.m *****
aux1=round(row_lu/n);
aux2=round(col_lu/n);
band = zeros(aux1,aux2,'single');
for i=1:round(row_lu/n)-1
    for j=1:round(col_lu/n)-1
        if (i==1) && (j==1)
            band(i,j)=mean(mean(band5((1):(i*n),(1):(j*n))));
        elseif (i==1) && (j>1)
            band(i,j)=mean(mean(band5((1):(i*n),((j-1)*n+1):(j*n))));
        elseif (i>1) && (j==1)
            band(i,j)=mean(mean(band5(((i-1)*n+1):(i*n),(1):(j*n))));
        else
            band(i,j)=mean(mean(band5(((i-1)*n+1):(i*n),((j-1)*n+1):(j*n))));
        end
    end
end
end
```

```
%Aggregation.m *****

%Band1_3.m *****
%Disaggregate bands 1 to 3 from 15 to 5
[row_lu,col_lu]=size(band);
n=3;
Disaggregation
band5=a;
%Save bands 1 to 3 in resolutions 5m and 15m
counter=1;
Save
counter=2;
Save
%Aggregate bands 1 to 3 to 30m resolution
[row_lu,col_lu]=size(band5);
n=6;
Aggregation
%Disaggregate bands 1 to 3 to 5m resolution
[row_lu,col_lu]=size(band);
Disaggregation
%Save bands 1 to 3 in resolution 30m
Save
%Aggregate bands 1 to 3 to 90m resolution
[row_lu,col_lu]=size(band5);
n=18;
Aggregation
%Disaggregate bands 1 to 3 to 5m resolution
[row_lu,col_lu]=size(band);
Disaggregation
%Save bands 1 to 3 in resolution 90m
Save
%Aggregate bands 1 to 3 to 250m resolution
[row_lu,col_lu]=size(band5);
n=50;
Aggregation
%Disaggregate bands 1 to 3 to 5m resolution
[row_lu,col_lu]=size(band);
Disaggregation
%Save bands 1 to 3 in resolution 250m
Save
%Band1_3.m *****

%Band4_9.m *****
%Disaggregate bands 4 to 9 from 30 to 5
[row_lu,col_lu]=size(band);
n=6;
Disaggregation
band5=a;
%Save bands 4 to 9 in resolutions 5m, 15m and 30m
counter=1;
Save
counter=2;
Save
counter=3;
Save
%Aggregate bands 4 to 9 to 90m resolution
[row_lu,col_lu]=size(band5);
n=18;
Aggregation
%Disaggregate bands 4 to 9 to 5m resolution
```

```

[row_lu,col_lu]=size(band);
Disaggregation
%Save bands 1 to 3 in resolution 90m
Save
%Aggregate bands 4 to 9 to 250m resolution
[row_lu,col_lu]=size(band5);
n=50;
Aggregation
%Disaggregate bands 4 to 9 to 5m resolution
[row_lu,col_lu]=size(band);
Disaggregation
%Save bands 4 to 9 in resolution 250m
Save
%Band4_9.m *****

%Disaggregate.m *****
i1=round(row_lu);
j1=round(col_lu);
aux1=round(row_lu*n);
aux2=round(col_lu*n);
a = zeros(aux1,aux2,'single');
for i1=1:row_lu
    for j1=1:col_lu
        for i=((i1-1)*(n)+1):(i1*n)
            for j=((j1-1)*(n)+1):(j1*n)
                a(i,j)= band(i1,j1);
            end
        end
    end
end
ascii=a;
%Disaggregate.m *****

%Image_processor.m *****
clc
clear all
close all
format short
for l=1:9
    %*****
    if (l==1)
        band=imread('D:\Matlab_results\ASTER_original\band1_original.tif');
        band1_3
    elseif (l==2)
        band=imread('D:\Matlab_results\ASTER_original\band2_original.tif');
        band1_3
    elseif (l==3)
        band=imread('D:\Matlab_results\ASTER_original\band3_original.tif');
        band1_3
    elseif (l==4)
        band=imread('D:\Matlab_results\ASTER_original\band4_original.tif');
        band4_9
    elseif (l==5)
        band=imread('D:\Matlab_results\ASTER_original\band5_original.tif');
        band4_9
    elseif (l==6)
        band=imread('D:\Matlab_results\ASTER_original\band6_original.tif');
        band4_9
    elseif (l==7)
        band=imread('D:\Matlab_results\ASTER_original\band7_original.tif');

```

```
        band4_9
    elseif (l==8)
        band=imread('D:\Matlab_results\ASTER_original\band8_original.tif');
        band4_9
    elseif (l==9)
        band=imread('D:\Matlab_results\ASTER_original\band9_original.tif');
        band4_9
    end
    %*****
end
%Image_processor.m *****

%Save.m *****
if (l==1) && (n==3)
    if (counter==1)
        FileName='D:\Matlab_results\ASTER_5\band1_5.asc';
    elseif (counter==2)
        FileName='D:\Matlab_results\ASTER_15\band1_15.asc';
    end
elseif (l==1) && (n==6)
    FileName='D:\Matlab_results\ASTER_30\band1_30.asc';
elseif (l==1) && (n==18)
    FileName='D:\Matlab_results\ASTER_90\band1_90.asc';
elseif (l==1) && (n==50)
    FileName='D:\Matlab_results\ASTER_250\band1_250.asc';
    %*****
elseif (l==2) && (n==3)
    if (counter==1)
        FileName='D:\Matlab_results\ASTER_5\band2_5.asc';
    elseif (counter==2)
        FileName='D:\Matlab_results\ASTER_15\band2_15.asc';
    end
elseif (l==2) && (n==6)
    FileName='D:\Matlab_results\ASTER_30\band2_30.asc';
elseif (l==2) && (n==18)
    FileName='D:\Matlab_results\ASTER_90\band2_90.asc';
elseif (l==2) && (n==50)
    FileName='D:\Matlab_results\ASTER_250\band2_250.asc';
    %*****
elseif (l==3) && (n==3)
    if (counter==1)
        FileName='D:\Matlab_results\ASTER_5\band3_5.asc';
    elseif (counter==2)
        FileName='D:\Matlab_results\ASTER_15\band3_15.asc';
    end
elseif (l==3) && (n==6)
    FileName='D:\Matlab_results\ASTER_30\band3_30.asc';
elseif (l==3) && (n==18)
    FileName='D:\Matlab_results\ASTER_90\band3_90.asc';
elseif (l==3) && (n==50)
    FileName='D:\Matlab_results\ASTER_250\band3_250.asc';
    %*****
elseif (l==4) && (n==6)
    if (counter==1)
        FileName='D:\Matlab_results\ASTER_5\band4_5.asc';
    elseif (counter==2)
        FileName='D:\Matlab_results\ASTER_15\band4_15.asc';
    elseif (counter==3)
        FileName='D:\Matlab_results\ASTER_30\band4_30.asc';
    end
elseif (l==4) && (n==18)
```

```
FileName='D:\Matlab_results\ASTER_90\band4_90.asc';
elseif (l==4) && (n==50)
    FileName='D:\Matlab_results\ASTER_250\band4_250.asc';
    %*****
elseif (l==5) && (n==6)
    if (counter==1)
        FileName='D:\Matlab_results\ASTER_5\band5_5.asc';
    elseif (counter==2)
        FileName='D:\Matlab_results\ASTER_15\band5_15.asc';
    elseif (counter==3)
        FileName='D:\Matlab_results\ASTER_30\band5_30.asc';
    end
elseif (l==5) && (n==18)
    FileName='D:\Matlab_results\ASTER_90\band5_90.asc';
elseif (l==5) && (n==50)
    FileName='D:\Matlab_results\ASTER_250\band5_250.asc';
    %*****
elseif (l==6) && (n==6)
    if (counter==1)
        FileName='D:\Matlab_results\ASTER_5\band6_5.asc';
    elseif (counter==2)
        FileName='D:\Matlab_results\ASTER_15\band6_15.asc';
    elseif (counter==3)
        FileName='D:\Matlab_results\ASTER_30\band6_30.asc';
    end
elseif (l==6) && (n==18)
    FileName='D:\Matlab_results\ASTER_90\band6_90.asc';
elseif (l==6) && (n==50)
    FileName='D:\Matlab_results\ASTER_250\band6_250.asc';
    %*****
elseif (l==7) && (n==6)
    if (counter==1)
        FileName='D:\Matlab_results\ASTER_5\band7_5.asc';
    elseif (counter==2)
        FileName='D:\Matlab_results\ASTER_15\band7_15.asc';
    elseif (counter==3)
        FileName='D:\Matlab_results\ASTER_30\band7_30.asc';
    end
elseif (l==7) && (n==18)
    FileName='D:\Matlab_results\ASTER_90\band7_90.asc';
elseif (l==7) && (n==50)
    FileName='D:\Matlab_results\ASTER_250\band7_250.asc';
    %*****
elseif (l==8) && (n==6)
    if (counter==1)
        FileName='D:\Matlab_results\ASTER_5\band8_5.asc';
    elseif (counter==2)
        FileName='D:\Matlab_results\ASTER_15\band8_15.asc';
    elseif (counter==3)
        FileName='D:\Matlab_results\ASTER_30\band8_30.asc';
    end
elseif (l==8) && (n==18)
    FileName='D:\Matlab_results\ASTER_90\band8_90.asc';
elseif (l==8) && (n==50)
    FileName='D:\Matlab_results\ASTER_250\band8_250.asc';
    %*****
elseif (l==9) && (n==6)
    if (counter==1)
        FileName='D:\Matlab_results\ASTER_5\band9_5.asc';
    elseif (counter==2)
        FileName='D:\Matlab_results\ASTER_15\band9_15.asc';
    elseif (counter==3)
        FileName='D:\Matlab_results\ASTER_30\band9_30.asc';
```

```

end
elseif (l==9) &&(n==18)
    FileName='D:\Matlab_results\ASTER_90\band9_90.asc';
elseif (l==9) &&(n==50)
    FileName='D:\Matlab_results\ASTER_250\band9_250.asc';
end
%*****
fid=fopen(FileName,'w');
if (n==3)
    fprintf(fid,'ncols 2643          \n'); % Number of columns
    fprintf(fid,'nrows 2253         \n'); % Number of lines
elseif (n==6)
    fprintf(fid,'ncols 2646          \n'); % Number of columns
    fprintf(fid,'nrows 2256         \n'); % Number of lines
elseif (n==18)
    fprintf(fid,'ncols 2646          \n'); % Number of columns
    fprintf(fid,'nrows 2250         \n'); % Number of lines
elseif (n==50)
    fprintf(fid,'ncols 2650          \n'); % Number of columns
    fprintf(fid,'nrows 2250         \n'); % Number of lines
end
if (l<4)
    fprintf(fid,'xulcorner 716751.5   \n'); % x upper left
    fprintf(fid,'yulcorner 1861251.5 \n'); % y upper left
else
    fprintf(fid,'xulcorner 716744.0   \n'); % x upper left
    fprintf(fid,'yulcorner 1861259.0 \n'); % y upper left
end
fprintf(fid,'cellsize 5              \n'); % resolution
fprintf(fid,'NODATA_value 0         \n'); % No data available
for i=1:row_lu*n
    for j=1:col_lu*n
        fprintf(fid,'%f ', ascii(i,j));
    end
    fprintf(fid,'\n');
end
end
%Save.m *****

```

APPENDIX III – FIELD DATA VALIDATION POINTS

No.	UTM-X	UTM-Y	Land use/cover	No.	UTM-X	UTM-Y	Land use/cover
1	722984	1856578	Agriculture	49	727379	1853488	Bare
2	722996	1856605	Agriculture	50	727364	1853488	Bare
3	723004	1856572	Agriculture	51	727348	1853503	Bare
4	721966	1855683	Agriculture	52	727394	1853503	Bare
5	728102	1853655	Agriculture	53	727350	1853533	Bare
6	725294	1855813	Agriculture	54	724658	1855737	Bare
7	721825	1853307	Agriculture	55	724724	1855727	Bare
8	727424	1853474	Agriculture	56	724634	1855661	Bare
9	727439	1853489	Agriculture	57	724590	1855602	Bare
10	725452	1856096	Agriculture	58	724575	1855633	Bare
11	725373	1856085	Agriculture	59	724603	1855604	Bare
12	725342	1856122	Agriculture	60	724618	1855618	Bare
13	725332	1856086	Agriculture	61	724631	1855708	Bare
14	720084	1856091	Agriculture	62	724854	1855484	Bare
15	718844	1856459	Agriculture	63	724892	1855452	Bare
16	718828	1856445	Agriculture	64	724916	1855576	Bare
17	721469	1853232	Agriculture	65	725171	1855628	Bare
18	726139	1855953	Agriculture	66	725235	1855574	Bare
19	726030	1856127	Agriculture	67	724538	1854950	Bare
20	724667	1855994	Agriculture	68	724520	1854967	Bare
21	724665	1855970	Agriculture	69	724535	1854954	Bare
22	725136	1855982	Agriculture	70	724580	1854938	Bare
23	725135	1855966	Agriculture	71	724700	1855029	Bare
24	725427	1856115	Agriculture	72	724638	1854830	Bare
25	725414	1856093	Agriculture	73	725768	1856049	Degraded Forest
26	725528	1856054	Agriculture	74	725788	1856057	Degraded Forest
27	725369	1856133	Agriculture	75	725488	1855718	Degraded Forest
28	717984	1859554	Agriculture	76	725495	1855746	Degraded Forest
29	718079	1859494	Agriculture	77	725381	1856393	Degraded Forest
30	718134	1859614	Agriculture	78	725346	1856421	Degraded Forest
31	725176	1855825	Bare	79	726417	1855581	Degraded Forest
32	725250	1855773	Bare	80	726435	1855494	Degraded Forest
33	725249	1855723	Bare	81	726394	1855538	Degraded Forest
34	724738	1855800	Bare	82	726411	1855601	Degraded Forest
35	724743	1855769	Bare	83	726374	1855565	Degraded Forest
36	725170	1855964	Bare	84	722881	1856665	Degraded Forest
37	725204	1855934	Bare	85	726734	1855438	Degraded Forest
38	725219	1855934	Bare	86	726692	1855363	Degraded Forest
39	720196	1853932	Bare	87	726657	1855345	Degraded Forest
40	720184	1853923	Bare	88	726583	1855449	Degraded Forest
41	720185	1853932	Bare	89	726324	1855490	Degraded Forest
42	727405	1853503	Bare	90	726356	1855488	Degraded Forest
43	727394	1853519	Bare	91	726379	1855499	Degraded Forest
44	727379	1853534	Bare	92	726353	1855645	Degraded Forest
45	727379	1853518	Bare	93	723228	1856554	Degraded Forest
46	727364	1853519	Bare	94	724181	1856531	Degraded Forest
47	727347	1853519	Bare	95	725430	1855693	Degraded Forest
48	727364	1853504	Bare	96	726189	1855477	Degraded Forest

Effect of spatial resolution on erosion assessment in Namchun watershed, Thailand

No.	UTM-X	UTM-Y	Land use/cover	No.	UTM-X	UTM-Y	Land use/cover
97	726192	1855424	Degraded Forest	145	723069	1851949	Forest
98	723958	1856458	Degraded Forest	146	723084	1851919	Forest
99	724500	1856355	Degraded Forest	147	723129	1851954	Forest
100	724629	1855844	Degraded Forest	148	722994	1851874	Forest
101	724602	1855837	Degraded Forest	149	722964	1851874	Forest
102	724548	1855816	Degraded Forest	150	722859	1851799	Forest
103	724524	1855827	Degraded Forest	151	721722	1853103	Grassland
104	724871	1856167	Degraded Forest	152	721707	1853107	Grassland
105	724876	1856196	Degraded Forest	153	721724	1853088	Grassland
106	724904	1856160	Degraded Forest	154	721454	1853252	Grassland
107	724909	1856187	Degraded Forest	155	721476	1853242	Grassland
108	721751	1856736	Degraded Forest	156	721751	1856736	Grassland
109	721773	1856765	Degraded Forest	157	721785	1856734	Grassland
110	727964	1853398	Degraded Forest	158	721773	1856765	Grassland
111	727672	1853214	Degraded Forest	159	721790	1856704	Grassland
112	724739	1855858	Degraded Forest	160	724309	1856697	Grassland
113	722870	1855686	Forest	161	726099	1855964	Grassland
114	726180	1855978	Forest	162	721593	1853281	Grassland
115	724062	1856304	Forest	163	721619	1853242	Grassland
116	724062	1856288	Forest	164	722100	1853953	Grassland
117	724108	1856773	Forest	165	722095	1853941	Grassland
118	724078	1856672	Forest	166	722085	1853945	Grassland
119	725504	1855706	Forest	167	724192	1856510	Grassland
120	720229	1856060	Forest	168	724205	1856480	Grassland
121	722787	1856634	Forest	169	722924	1856608	Grassland
122	727252	1856197	Forest	170	725369	1856133	Grassland
123	718796	1856301	Forest	171	724673	1856045	Grassland
124	720549	1860244	Forest	172	725859	1856794	Grassland
125	718104	1860214	Forest	173	725919	1856809	Grassland
126	718049	1860184	Forest	174	725904	1856839	Grassland
127	718014	1860159	Forest	175	725949	1856839	Grassland
128	720567	1860314	Forest	176	725969	1855924	Grassland
129	720534	1860304	Forest	177	724686	1856019	Grassland
130	720574	1860229	Forest	178	725594	1855919	Grassland
131	720594	1860369	Forest	179	725393	1856003	Grassland
132	717714	1858534	Forest	180	726090	1856029	Grassland
133	717744	1858594	Forest	181	725609	1855948	Grassland
134	720144	1859524	Forest	182	722094	1858924	Grassland
135	718179	1860094	Forest	183	721989	1858834	Grassland
136	718074	1860114	Forest	184	726819	1853809	Grassland
137	718299	1860169	Forest	185	725590	1855987	Orchard
138	718194	1860069	Forest	186	725594	1855968	Orchard
139	720474	1860514	Forest	187	725594	1855934	Orchard
140	720394	1860559	Forest	188	725607	1855934	Orchard
141	720444	1860124	Forest	189	725623	1855946	Orchard
142	720804	1860109	Forest	190	725602	1855910	Orchard
143	721749	1853369	Forest	191	725611	1855861	Orchard
144	723039	1852034	Forest	192	725450	1856009	Orchard

Effect of spatial resolution on erosion assessment in Namchun watershed, Thailand

No.	UTM-X	UTM-Y	Land use/cover	No.	UTM-X	UTM-Y	Land use/cover
193	725489	1856052	Orchard	209	726460	1855536	Orchard
194	721269	1853403	Orchard	210	721574	1853254	Orchard
195	721274	1853430	Orchard	211	724170	1856550	Orchard
196	721500	1853683	Orchard	212	725104	1855972	Orchard
197	721469	1853713	Orchard	213	721811	1856726	Orchard
198	721479	1853685	Orchard	214	727544	1853663	Orchard
199	724747	1855855	Orchard	215	726134	1856404	Orchard
200	725150	1855959	Orchard	216	726129	1856389	Orchard
201	725846	1856036	Orchard	217	725889	1856824	Orchard
202	720127	1856077	Orchard	218	725909	1856794	Orchard
203	718828	1856461	Orchard	219	720127	1856111	Orchard
204	718836	1856509	Orchard	220	720127	1856077	Orchard
205	726412	1855704	Orchard	221	718799	1856445	Orchard
206	726266	1855476	Orchard	222	725664	1856089	Orchard
207	726379	1855369	Orchard	223	725739	1856074	Orchard
208	726406	1855416	Orchard				

The coordinate systems: WGS84 UTM zone 47

Appendix 7: Signatures value of SAM classification in each band (Radiance)

ASTER Bands	Agriculture	Bare	Deg. Forest	Forest	Grassland	Orchard
Band 1	48.90	48.77	40.91	43.60	45.47	46.47
Band 2	31.53	34.88	22.55	23.46	28.90	30.06
Band 3	80.40	55.11	61.07	88.99	67.21	62.73
Band 4	12.15	10.60	8.56	9.70	10.36	10.66
Band 5	2.32	2.34	1.81	1.85	2.12	2.21
Band 6	2.24	2.22	1.60	1.69	1.99	2.07
Band 7	1.87	1.89	1.37	1.44	1.68	1.75
Band 8	1.13	1.16	0.81	0.83	1.01	1.07
Band 9	0.72	0.75	0.60	0.61	0.68	0.70

Appendix 8: Crop calendar for Phetchabun Province in 2007

Crop type	Jan	Feb	March	Apr	May	June	July	Aug	Sep	Oct	Nov	Dec	Remark
Maize	←→	↔	↔	↔	↔	↔	↔	↔				↔	
Millet, Sorghum					↔			↔	↔	↔	↔	↔	
Soil bean	←→	↔	↔					↔	↔	↔	↔	↔	
Bean	←→	↔	↔					↔	↔	↔	↔	↔	
Cassava	←→	↔	↔	↔				↔	↔	↔	↔	↔	
Sugar can	←→	↔	↔	↔	↔	↔	↔	↔	↔	↔	↔	↔	
Cabbage	↔	↔	↔	↔	↔	↔	↔	↔				↔	
Chili, Egg plant	↔				↔	↔	↔	↔	↔	↔	↔	↔	
Corn	↔				↔		↔	↔	↔	↔	↔	↔	
Ginger							↔	↔	↔	↔	↔	↔	
Lettuce	↔	↔					↔	↔	↔	↔	↔	↔	
pumpkin	←→	↔	↔	↔							↔	↔	
Seasonal-cultivating rice					↔	↔	↔	↔	↔	↔	↔	↔	
Irrigation-al-cultivating rice	←→	↔	↔	↔				↔	↔	↔	↔	↔	

Where:

- ←→ = the whole period of vegetations and crops growing
- ↔ = starting the planting period (young plants)
- ↔ = the crops and vegetations grow up
- ↔ = the harvesting period of crops and vegetations

Source: Provincial agriculture department of Phetchabun Province, Thailand.

APPENDIX IV – EFFECT OF SIMULATED SATELLITE DATA RESOLUTION ON CLASSIFICATION

Appendix 9: Covered area by different land use classes in different resolutions

Land use/cover	5m	30m	90m	250m
Agriculture	36%	37%	42%	47%
Bare	6%	5%	4%	2%
Degraded Forest	26%	26%	26%	25%
Forest	11%	10%	7%	4%
Grassland	10%	11%	10%	14%
Orchard	11%	10%	11%	8%

Appendix 10: Confusion matrix in 30m resolution

Class	Agriculture	Bare	Deg. Forest	Forest	Grassland	Orchard	Total
Agriculture	752683	79	98679	88450	46791	3442	990124
Bare Soil	118	122051	381	0	1073	18050	141673
Degraded Forest	94422	567	542877	2305	33603	21222	694996
Forest	65074	0	1289	210773	0	0	277136
Grassland	41656	1866	31886	86	151528	60692	287714
Orchard	3496	33536	13274	9	40247	179131	269693
Total	957449	158099	688386	301623	273242	282537	2661336
Kappa Coefficient	0.63	0.85	0.70	0.73	0.47	0.62	0.65
Overall Accuracy							73.61%

Appendix 11: Confusion matrix in 90m resolution

Class	Agriculture	Bare	Deg. Forest	Forest	Grassland	Orchard	Total
Agriculture	669694	3309	158801	165232	87081	29354	1113471
Bare Soil	1979	77864	2163	81	3448	15089	100624
Degraded Forest	137569	6856	448983	13825	45583	47304	700120
Forest	68378	30	5429	120274	738	206	195055
Grassland	57048	10752	43870	1464	84149	70149	267432
Orchard	22781	59288	29140	747	52243	120435	284634
Total	957449	158099	688386	301623	273242	282537	2661336
Kappa Coefficient	0.38	0.76	0.52	0.57	0.24	0.35	0.43
Overall Accuracy							57.17%

Appendix 12: Confusion matrix in 250m resolution

Class	Agriculture	Bare	Deg. Forest	Forest	Grassland	Orchard	Total
Agriculture	638302	9632	222725	219974	102399	52358	1245390
Bare Soil	4115	42796	3401	398	4035	8832	63577
Degraded Forest	160479	17942	361964	23774	47901	56053	668113
Forest	40362	33	4552	49662	1501	457	96567
Grassland	85477	27440	70427	6122	83804	97805	371075
Orchard	28714	60256	25317	1693	33602	67032	216614
Total	957449	158099	688386	301623	273242	282537	2661336
Kappa Coefficient	0.24	0.65	0.38	0.45	0.14	0.23	0.28
Overall Accuracy							46.73%

Appendix 13: Separability Matrix of signatures (least to most)

Class one	Class two	Separability
Grassland	Orchard	1.21625214
Degraded Forest	Grassland	1.40872185
Agriculture	Grassland	1.45574481
Bare	Orchard	1.67187127
Degraded Forest	Orchard	1.67835488
Agriculture	Forest	1.69379711
Agriculture	Degraded Forest	1.73461707
Agriculture	Orchard	1.74444159
Degraded Forest	Forest	1.84956349
Forest	Grassland	1.87910070
Bare	Grassland	1.93170449
Bare	Degraded Forest	1.96453148
Agriculture	Bare	1.96806397
Forest	Orchard	1.97271433
Bare	Forest	1.99682875

Appendix 14: User's accuracy

Class	30m	90m	250m
Agriculture	76%	60%	51%
Bare Soil	86%	77%	67%
Degraded Forest	78%	64%	54%
Forest	76%	62%	51%
Grassland	53%	31%	23%
Orchard	66%	42%	31%

Appendix 15: Producer's accuracy

Class	30m	90m	250m
Agriculture	79%	70%	67%
Bare Soil	77%	49%	27%
Degraded Forest	79%	65%	53%
Forest	70%	40%	16%
Grassland	55%	31%	31%
Orchard	63%	43%	24%

APPENDIX V – EFFECT OF MAJORITY-BASES AGGREGATION ON LAND USE/COVER

Appendix 16: Covered area by different land use/cover classes in different resolutions

Land use/cover	5m	15m	30m	90m	250m
Agriculture	36%	37%	39%	43%	53%
Bare	6%	6%	6%	6%	7%
Degraded Forest	26%	26%	27%	29%	31%
Forest	11%	11%	10%	9%	6%
Grassland	10%	10%	9%	6%	3%
Orchard	11%	10%	10%	10%	10%

Appendix 17: Confusion matrix in 15m resolution

Class	Agriculture	Bare	Deg. Forest	Forest	Grassland	Orchard	Total
Agriculture	799229	1109	75719	64116	39375	9156	988704
Bare Soil	1003	135916	1895	16	3395	18335	160560
Degraded Forest	71199	1827	575507	6311	23841	19925	698610
Forest	51027	25	4792	230769	289	126	287028
Grassland	27542	2528	16972	305	176169	30974	254490
Orchard	7449	16694	13501	106	30173	204021	271944
Total	957449	158099	688386	301623	273242	282537	2661336
Kappa Coefficient	0.70	0.84	0.76	0.78	0.66	0.72	0.73
Overall Accuracy							79.72%

Appendix 18: Confusion matrix in 30m resolution

Class	Agriculture	Bare	Deg. Forest	Forest	Grassland	Orchard	Total
Agriculture	757862	2136	100928	89271	55050	15185	1020432
Bare Soil	2053	127946	3207	92	5266	23946	162510
Degraded Forest	89794	3194	541021	9166	31359	29248	703782
Forest	62533	49	6749	202547	564	252	272694
Grassland	33946	2664	19260	361	141259	35586	233076
Orchard	11261	22110	17221	186	39744	178320	268842
Total	957449	158099	688386	301623	273242	282537	2661336
Kappa Coefficient	0.60	0.77	0.69	0.71	0.56	0.62	0.65
Overall Accuracy							73.23%

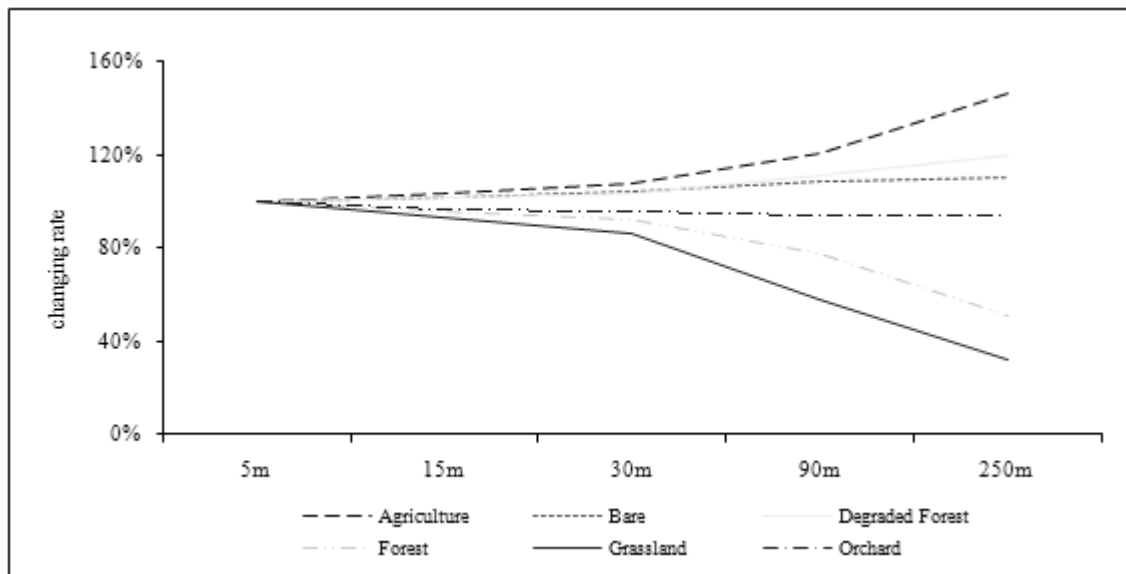
Appendix 19: Confusion matrix in 90m resolution

Class	Agriculture	Bare	Deg. Forest	Forest	Grassland	Orchard	Total
Agriculture	681844	9324	144784	141735	93982	42783	1114452
Bare Soil	9111	103760	9085	652	10973	30525	164106
Degraded Forest	139038	12316	476907	22645	47422	51768	750096
Forest	72195	444	12561	134493	2074	947	222714
Grassland	31011	3811	16313	766	68707	31252	151860
Orchard	24250	28444	28736	1332	50084	125262	258108
Total	957449	158099	688386	301623	273242	282537	2661336
Kappa Coefficient	0.39	0.61	0.51	0.55	0.39	0.42	0.46
Overall Accuracy							59.78%

Effect of spatial resolution on erosion assessment in Namchun watershed, Thailand

Appendix 20: Confusion matrix in 250m resolution

Class	Agriculture	Bare	Deg. Forest	Forest	Grassland	Orchard	Total
Agriculture	659996	23228	205107	187508	124267	75356	1275462
Bare Soil	15707	75774	12932	1555	13006	28334	147308
Degraded Forest	175062	24584	415258	40512	57021	69481	781918
Forest	49600	41	12565	67488	1902	962	132558
Grassland	17511	3205	11165	1370	27444	17731	78426
Orchard	39573	31267	31359	3190	49602	90673	245664
Total	957449	158099	688386	301623	273242	282537	2661336
Kappa Coefficient	0.25	0.48	0.37	0.45	0.28	0.29	0.32
Overall Accuracy							50.22%



Appendix 21: Changing rate of land use/cover classes

Appendix 22: User's accuracy

Class	15m	30m	90m	250m
Agriculture	81%	74%	61%	52%
Bare Soil	85%	79%	63%	51%
Degraded Forest	82%	77%	64%	53%
Forest	80%	74%	60%	51%
Grassland	69%	61%	45%	35%
Orchard	75%	66%	49%	37%

Appendix 23: Producer's accuracy

Class	15m	30m	90m	250m
Agriculture	83%	79%	71%	69%
Bare Soil	86%	81%	66%	48%
Degraded Forest	84%	79%	69%	60%
Forest	77%	67%	45%	22%
Grassland	64%	52%	25%	10%
Orchard	72%	63%	44%	32%

APPENDIX VI – EFFECT OF SIMULATED SATELLITE DATA RESOLUTION ON EROSION

Appendix 24: Confusion matrix in 30m resolution

Erosion Class	Very Slight	Slight	Moderate	Severe	Very Severe	Total
Very Slight	1131914	45551	108161	62896	11251	1359773
Slight	32858	130248	6548	10078	4144	183876
Moderate	113179	3711	383865	354	1711	502820
Severe	78910	7328	314	307288	98	393938
Very Severe	12111	6363	1156	172	74159	93961
Total	1368972	193201	500044	380788	91363	2534368
Kappa Coefficient	0.64	0.68	0.71	0.74	0.78	0.69
Overall Accuracy						80.00%

Appendix 25: Confusion matrix in 90m resolution

Erosion Class	Very Slight	Slight	Moderate	Severe	Very Severe	Total
Very Slight	953940	67473	164880	80268	15633	1282194
Slight	50553	88140	8293	21023	2396	170405
Moderate	194293	6057	321365	638	3964	526317
Severe	147444	18328	550	278486	97	444905
Very Severe	22742	13203	4956	373	69273	110547
Total	1368972	193201	500044	380788	91363	2534368
Kappa Coefficient	0.44	0.48	0.51	0.56	0.61	0.50
Overall Accuracy						67.52%

Appendix 26: Confusion matrix in 250m resolution

Erosion Class	Very Slight	Slight	Moderate	Severe	Very Severe	Total
Very Slight	830365	85252	198122	85136	13958	1212833
Slight	48183	58728	9904	21473	3807	142095
Moderate	252146	6284	282255	1011	5616	547312
Severe	207188	27635	2931	271960	424	510138
Very Severe	31089	15302	6832	1208	67558	121989
Total	1368971	193201	500044	380788	91363	2534367
Kappa Coefficient	0.31	0.36	0.40	0.45	0.54	0.39
Overall Accuracy						59.62%

Appendix 27: Average erosion of land use/cover classes in different resolutions

Land use/cover	5m	15m	30m	90m	250m
Agriculture	2.47	2.47	2.49	2.56	2.53
Degraded Forest	0.13	0.13	0.13	0.12	0.12
Forest	0.04	0.04	0.04	0.05	0.04
Grassland	0.28	0.28	0.28	0.25	0.24
Orchard	0.48	0.48	0.47	0.47	0.45

Appendix 28: Fraction of erosion classes in each resolution

Erosion Class	5m	15m	30m	90m	250m
Very Slight	54%	54%	54%	51%	48%
Slight	8%	8%	7%	7%	6%
Moderate	20%	20%	20%	21%	22%
Severe	15%	15%	16%	18%	20%
Very Severe	4%	4%	4%	4%	5%

Appendix 29: User's accuracy

Class	30m	90m	250m
Very Slight	83%	74%	68%
Slight	71%	52%	41%
Moderate	76%	61%	52%
Severe	78%	63%	53%
Very Severe	79%	63%	55%

Appendix 30: Producer's accuracy

Class	30m	90m	250m
Very Slight	83%	70%	61%
Slight	67%	46%	30%
Moderate	77%	64%	56%
Severe	81%	73%	71%
Very Severe	81%	76%	74%

APPENDIX VII – EFFECT OF DEM RESOLUTION ON SLOPE MAP

Appendix 31: Confusion matrix in 15m resolution

Class	0-7	7-15	15-20	20-25	>25	Total
0-7	160476	47849	4541	1872	1668	216406
7-15	46880	251388	110173	33229	16727	458397
15-20	8186	68619	142636	118937	93145	431523
20-25	9495	27953	94585	102232	127157	361422
>25	4733	31301	83370	198949	857123	1175476
Total	229770	427110	435305	455219	1095820	2643224
Kappa Coefficient	0.72	0.46	0.20	0.13	0.54	0.41
Overall Accuracy						57.27%

Appendix 32: Confusion matrix in 30m resolution

Class	0-7	7-15	15-20	20-25	>25	Total
0-7	120006	47411	12200	7556	9855	197028
7-15	79552	198702	118322	71770	80346	548692
15-20	15210	79934	100188	92901	129145	417378
20-25	10051	64715	103651	102099	158266	438782
>25	4951	36348	100944	180893	718208	1041344
Total	229770	427110	435305	455219	1095820	2643224
Kappa Coefficient	0.57	0.24	0.09	0.07	0.47	0.28
Overall Accuracy						46.88%

Appendix 33: Confusion matrix in 90m resolution

Class	0-7	7-15	15-20	20-25	>25	Total
0-7	106500	99705	64829	50645	85248	406927
7-15	79027	149245	126694	110842	198568	664376
15-20	22838	71762	80965	82139	166045	423749
20-25	13615	55346	72626	83258	190223	415068
>25	7790	51052	90191	128335	455736	733104
Total	229770	427110	435305	455219	1095820	2643224
Kappa Coefficient	0.19	0.08	0.03	0.03	0.35	0.14
Overall Accuracy						33.13%

Appendix 34: Confusion matrix in 250m resolution

Class	0-7	7-15	15-20	20-25	>25	Total
0-7	106626	141975	114545	104171	222241	689558
7-15	87258	155231	159794	162698	331832	896813
15-20	21141	68972	83090	92406	217365	482974
20-25	10264	32460	39518	44564	112691	239497
>25	4481	28472	38358	51380	211691	334382
Total	229770	427110	435305	455219	1095820	2643224
Kappa Coefficient	0.07	0.01	0.01	0.02	0.37	0.06
Overall Accuracy						22.75%

Appendix 35: Effect of resolution on slope map

Slope Class	5m	15m	30m	90m	250m
0-7	9%	8%	7%	15%	26%
7-15	16%	17%	21%	25%	34%
15-20	16%	16%	16%	16%	18%
20-25	17%	14%	17%	16%	9%
>25	41%	44%	39%	28%	13%

APPENDIX VIII – EFFECT OF DEM RESOLUTION ON EROSION

Appendix 36: Confusion matrix in 15m resolution

Class	Very Slight	Slight	Moderate	Severe	Very Severe	Total
Very Slight	1316453	40177	3338	301	26	1360295
Slight	41010	121741	34592	1149	62	198554
Moderate	9481	28388	360988	78221	1265	478343
Severe	1694	2525	98888	274886	20794	398787
Very Severe	331	370	2238	26231	69216	98386
Total	1368969	193201	500044	380788	91363	2534365
Kappa Coefficient	0.93	0.58	0.69	0.63	0.69	0.76
Overall Accuracy						84.57%

Appendix 37: Confusion matrix in 30m resolution

Class	Very Slight	Slight	Moderate	Severe	Very Severe	Total
Very Slight	1307393	51785	7518	1121	78	1367895
Slight	44666	98569	47462	6260	268	197225
Moderate	14778	39868	335995	109336	4472	504449
Severe	1731	2632	106259	237667	24485	372774
Very Severe	401	347	2810	26404	62060	92022
Total	1368969	193201	500044	380788	91363	2534365
Kappa Coefficient	0.90	0.46	0.58	0.57	0.66	0.70
Overall Accuracy						80.56%

Appendix 38: Confusion matrix in 90m resolution

Class	Very Slight	Slight	Moderate	Severe	Very Severe	Total
Very Slight	1314290	81583	48239	14386	744	1459242
Slight	37938	70232	80171	23064	1339	212744
Moderate	14475	37267	281550	154892	10900	499084
Severe	2036	3895	86369	166674	26316	285290
Very Severe	233	224	3715	21772	52064	78008
Total	1368972	193201	500044	380788	91363	2534368
Kappa Coefficient	0.78	0.27	0.46	0.51	0.65	0.59
Overall Accuracy						74.37%

Appendix 39: Confusion matrix in 250m resolution

Class	Very Slight	Slight	Moderate	Severe	Very Severe	Total
Very Slight	1328609	114038	91359	44345	3313	1581664
Slight	25327	44611	112421	58470	4671	245500
Moderate	14099	32258	254568	190774	18120	509819
Severe	660	2092	38665	76244	25907	143568
Very Severe	166	202	3031	10955	39352	53706
Total	1368861	193201	500044	380788	91363	2534257
Kappa Coefficient	0.65	0.11	0.38	0.45	0.72	0.49
Overall Accuracy						68.79%

Appendix 40: Average erosion of land use/cover classes in different resolutions

Land use/cover	5m	15m	30m	90m	250m
Agriculture	2.47	2.52	2.44	2.14	1.63
Degraded Forest	0.13	0.14	0.13	0.11	0.08
Forest	0.04	0.05	0.04	0.04	0.03
Grassland	0.28	0.29	0.28	0.24	0.18
Orchard	0.48	0.52	0.50	0.40	0.30

Appendix 41: Fraction of erosion classes in each resolution

Class	5m	15m	30m	90m	250m
Very Slight	54%	54%	54%	58%	62%
Slight	8%	8%	8%	8%	10%
Moderate	20%	19%	20%	20%	20%
Severe	15%	16%	15%	11%	6%
Very Severe	4%	4%	4%	3%	2%

Appendix 42: Changing rate of average erosion of land use/cover classes in different resolutions

Land use/cover	5m	15m	30m	90m	250m
Agriculture	100%	102%	99%	87%	66%
Degraded Forest	100%	107%	103%	84%	61%
Forest	100%	114%	109%	93%	66%
Grassland	100%	102%	99%	84%	64%
Orchard	100%	107%	103%	83%	61%

Appendix 43: User's accuracy

Class	15m	30m	90m	250m
Very Slight	97%	96%	90%	84%
Slight	61%	50%	33%	18%
Moderate	75%	67%	56%	50%
Severe	69%	64%	58%	53%
Very Severe	70%	67%	67%	73%

Appendix 44: Producer's accuracy

Class	15m	30m	90m	250m
Very Slight	96%	96%	96%	97%
Slight	63%	51%	36%	23%
Moderate	72%	67%	56%	51%
Severe	72%	62%	44%	20%
Very Severe	76%	68%	57%	43%